NBS TECHNICAL NOTE 615

WR15 Thermal Noise Standard

NATIONAL BUREAU OF STANDARDS

The National Bureau of Standards[1] was established by an act of Congress March 3, 1901. The Bureau's overall goal is to strengthen and advance the Nation's science and technology and facilitate their effective application for public benefit. To this end, the Bureau conducts research and provides: (1) a basis for the Nation's physical measurement system, (2) scientific and technological services for industry and government, (3) a technical basis for equity in trade, and (4) technical services to promote public safety. The Bureau consists of the Institute for Basic Standards, the Institute for Materials Research, the Institute for Applied Technology, the Center for Computer Sciences and Technology, and the Office for Information Programs.

THE INSTITUTE FOR BASIC STANDARDS provides the central basis within the United States of a complete and consistent system of physical measurement; coordinates that system with measurement systems of other nations; and furnishes essential services leading to accurate and uniform physical measurements throughout the Nation's scientific community, industry, and commerce. The Institute consists of a Center for Radiation Research, an Office of Measurement Services and the following divisions:

Applied Mathematics—Electricity—Heat—Mechanics—Optical Physics—Linac Radiation[2]—Nuclear Radiation[2]—Applied Radiation[2]—Quantum Electronics[3]—Electromagnetics[3]—Time and Frequency[3]—Laboratory Astrophysics[3]—Cryogenics[3].

THE INSTITUTE FOR MATERIALS RESEARCH conducts materials research leading to improved methods of measurement, standards, and data on the properties of well-characterized materials needed by industry, commerce, educational institutions, and Government; provides advisory and research services to other Government agencies; and develops, produces, and distributes standard reference materials. The Institute consists of the Office of Standard Reference Materials and the following divisions:

Analytical Chemistry—Polymers—Metallurgy—Inorganic Materials—Reactor Radiation—Physical Chemistry.

THE INSTITUTE FOR APPLIED TECHNOLOGY provides technical services to promote the use of available technology and to facilitate technological innovation in industry and Government; cooperates with public and private organizations leading to the development of technological standards (including mandatory safety standards), codes and methods of test; and provides technical advice and services to Government agencies upon request. The Institute also monitors NBS engineering standards activities and provides liaison between NBS and national and international engineering standards bodies. The Institute consists of the following technical divisions and offices:

Engineering Standards Services—Weights and Measures—Flammable Fabrics—Invention and Innovation—Vehicle Systems Research—Product Evaluation Technology—Building Research—Electronic Technology—Technical Analysis—Measurement Engineering.

THE CENTER FOR COMPUTER SCIENCES AND TECHNOLOGY conducts research and provides technical services designed to aid Government agencies in improving cost effectiveness in the conduct of their programs through the selection, acquisition, and effective utilization of automatic data processing equipment; and serves as the principal focus within the executive branch for the development of Federal standards for automatic data processing equipment, techniques, and computer languages. The Center consists of the following offices and divisions:

Information Processing Standards—Computer Information—Computer Services—Systems Development—Information Processing Technology.

THE OFFICE FOR INFORMATION PROGRAMS promotes optimum dissemination and accessibility of scientific information generated within NBS and other agencies of the Federal Government; promotes the development of the National Standard Reference Data System and a system of information analysis centers dealing with the broader aspects of the National Measurement System; provides appropriate services to ensure that the NBS staff has optimum accessibility to the scientific information of the world, and directs the public information activities of the Bureau. The Office consists of the following organizational units:

Office of Standard Reference Data—Office of Technical Information and Publications—Library—Office of Public Information—Office of International Relations.

---

[1] Headquarters and Laboratories at Gaithersburg, Maryland, unless otherwise noted; mailing address Washington, D.C. 20234.
[2] Part of the Center for Radiation Research.
[3] Located at Boulder, Colorado 80302.

UNITED STATES DEPARTMENT OF COMMERCE
Peter G. Peterson, Secretary
U.S. NATIONAL BUREAU OF STANDARDS • Lewis M. Branscomb, Director

NBS TECHNICAL NOTE 615

ISSUED MARCH 1972

Nat. Bur. Stand. (U.S.), Tech Note 615, 154 pages
CODEN: NBTNA

WR15 Thermal Noise Standard

W. C. Daywitt, W. J. Foote, and E. Campbell

Electromagnetics Division
Institute for Basic Standards
National Bureau of Standards
Boulder, Colorado 80302

NBS Technical Notes are designed to supplement the Bureau's regular publications program. They provide a means for making available scientific data that are of transient or limited interest. Technical Notes may be listed or referred to in the open literature.

For sale by the Superintendent of Documents, U.S. Government Printing Office, Washington, D.C. 20402
(Order by SD Catalog No. C13.46:615), Price $1.25

ERRATA

Page No.	Line No.	Erratum
17	15	"Silicon" to "Silicon carbide"
	16	"Silicon" to "Silicon carbide"
	last	"beryllium" to "beryllia"
21	7	"varified" to "verified"
31	last	"Si" to "SiC"
32	7,12,25	"Si" to "SiC"
33	2,6,9,10 12,14,20	"Si" to "SiC"

1.

2.

3.

4.

CONTENTS

CONTENTS (Continued)

CONTENTS (Continued)

APPENDICES

CONTENTS (Continued)

WR15 THERMAL NOISE STANDARD

W. C. Daywitt, W. J. Foote, and E. Campbell

ABSTRACT

This note describes the design and construction of a WR15 thermal noise power standard. The standard is designed to operate around the Silver Point Temperature (963.19°C) with a noise temperature output accurate to approximately ± 2 K.

Complete details of the theory, design, construction, and performance tests are given.

Key Words: Noise; Thermal noise standard; Millimeter wave; Error analysis; Nyquist's theorem.

1. INTRODUCTION

This note describes the analysis, design, construction, and performance tests of the NBS WR15 Thermal Noise Power Standard. This standard consists of a 0.148" x 0.074" I.D. rectangular waveguide that is terminated by a well matched load. The load and waveguide are heated to approximately 962°C in a specially designed oven. The noise temperature output of the standard is approximately 1235 K and is known to an accuracy of approximately ± 2 K. A sample of the output temperature T as a function of frequency is shown in figure 1.1.

The description of the standard is divided into three parts: The internal oven components; the external oven

components; and the auxiliary components. The internal components include the high temperature resistive generator or termination, the inconel heat distributor and heating coils, the high temperature platinum 10% rhodium waveguide, and the thermocouples. The external oven components include the oven casing and the cooling coils. The auxiliary components include the control rack containing the oven temperature monitor and controlling circuits, and the recirculating cooling system. Photographs of the total system are shown in figures 1.2, and 1.3.

Before the design and construction were begun, a thorough error analysis of the proposed standard's noise temperature output was performed to determine the necessary design specifications for holding the error to approximately ± 2 K. This error analysis along with the noise output calculation were computerized and used to determine the final error estimate.

The rest of the report is divided into three sections, each with a number of subsections. Where necessary they are liberally augmented by appendices to avoid destroying continuity, and a large amount of cross-referencing to avoid excessive repetition. The figures and drawings are labled alphanumerically, where the number or letter before the decimal point indicates in which section or appendix the principle discussion of the figure is to be found.

The discussion of noise power output and error calculations for the standard are contained in section 2. The discussion of important design specifications resulting from these calculations is found there also. Section 3 contains a description of, and the design and construction details for the standard. Measurement results and observations taken during the course of construction and final testing of the standard are found in section 4, as are the performance tests supporting the output and error calculations.

In many cases detail drawings of an item under discussion are not presented and the reader is hereby referred to the main assembly drawing (drawing #1). However, detail drawings are available upon request.

Most of the fabrication was done in the Shops Division (282) and measurements in the Electromagnetics Division (272) of the Institute for Basic Standards of the National Bureau of Standards, Boulder Laboratories.

Throughout the text SS stands for subsection, ap for appendix, and ( ) for an equation. For example, the equation for ΔT is to be found both in SS 2.1 as (2.2), and in ap A as (A.2).

A proposed standard must undergo rigorous NBS internal review before acceptance as a national standard. This review requires complete documentation of all work associated with theory, design, construction, and evaluation of the proposed

standard. Therefore, since this note was drafted for such documentation, and since it is intended for metrologists with interests similar to the authors', a number of items are contained herein which ordinarily would be omitted from a document intended for more general distribution.

2. ANALYSIS

The average thermal noise power output of a standard is described by the noise temperature T [1] which is the thermal noise power P per unit bandwidth available at its output connector divided by Boltzmann's Constant k. That is

$$T \equiv \frac{P}{k}.$$

In the standard, T is a calculated quantity [2] against which the noise temperature of another noise source can be compared. This calculated noise temperature depends upon a number of parameters of the physical source, and the corresponding error, δT, in T is the result of uncertainties in these parameters.

This section deals with the calculation of T and δT and the resulting design specifications. In particular, SS 2.1 covers the details of calculating T, and SS 2.2 with those of δT. Subsection 2.3 discusses the design specifications.

2.1. Noise Temperature Output

A schematic drawing of a heated thermal noise source is

shown in figure 2.1. The impedance Z terminates a transmission line used to convey the noise power from the impedance to an accessible output port. The impedance and part of the line is maintained at an elevated temperature by an appropriately designed oven. The available output power P is the sum of two effects; the noise power generated by Z and attenuated by the line, and the noise power generated by the line itself. The calculation of P or T requires the line to be uniform and reflectionless, and is the subject of this subsection.

An equivalent circuit model of figure 2.1 is shown in figure 2.2. T_m represents the measured temperature of the impedance Z terminating the end of the line at x = 0. T_x is the measured temperature distribution along the line from x = 0 to the output connector at x = ℓ. α_x is the available power ratio [1] for the length of line from x to x = ℓ, and a_x is the attenuation per unit length (dB/length) of the line at x. T is the output noise temperature and is the result of the attenuated noise $\alpha_o T_m$ of the impedance and the noise contributed by the line. T can be written as the sum of the impedance temperature T_m and a correction temperature ΔT which accounts for the total effect of the line.

$$T = T_m + \Delta T \tag{2.1}$$

A convenient expression for the correction is given by (ap A)

$$\Delta T = (T_o - T_m)(1-\alpha_o) + \int_o^{\ell} T_x'(1-\alpha_x)dx \tag{2.2}$$

where T_o is $T_{x=0}$, α_o is $\alpha_{x=0}$, and T_x' is the temperature gradient along the waveguide. In terms of the decibel attenuation A_x of the line from x to $x = \ell$ (ap A)

$$\alpha_x = 10^{-A_x/10} - \frac{2|\Gamma_\ell|^2}{1 - |\Gamma_\ell|^2} \operatorname{Sinh}(A_x/10 \log e) \tag{2.3}$$

where

$$A_x \equiv \int_x^{\ell} a_z \, dz. \tag{2.4}$$

The last term in (2.3) is both a function of the line loss A_x and the standard's reflection coefficient Γ_ℓ. A_x and Γ_ℓ are usually small, making the last term small and resulting in a noise temperature T that is independent of the reflection coefficient. A rough estimate of the size of the uncertainty in ΔT when this last term is neglected is given by

$$2(\overline{T}-T_m) \; |\Gamma_\ell|^2 \; (0.23\Delta) \tag{2.5}$$

where $\overline{T}$ is the average temperature of that portion of the T_x curve from the high temperature fall off to $x = \ell$, and Δ is the attenuation in dB of that same region.

The attenuation per unit length is given by

$$a_x = c\rho_x^{\frac{1}{2}} \qquad (2.6)$$

where c is a constant that is a function of the frequency and the geometry of the line, and ρ_x is the resistivity of the line material. The variation of this resistivity with temperature for an alloy of 90% platinum – 10% rhodium (Pt – 10 Rh) is shown in figure 2.3.

The attenuation per unit length can be treated in either of two ways; it can in general be measured as a function of temperature, or calculated from (2.6) in certain instances. Measurement data for a_x as a function of temperature is difficult to obtain and generally unavailable. Therefore a_x is calculated from (2.6). Justification for this decision is to be found in SS 4.1.4.

The WR15 noise standard employs a Pt – 10 Rh waveguide (SS 3.1.2) of inner dimensions 0.148" x 0.074", with a terminating element whose reflection coefficient is not greater than 0.006 (SS 3.1.1). A computer program (ap D) has been written for the calculation of ΔT (fig. 1.1) and its associated error (fig. D.1.), neglecting the second term in (2.3) (ap A). In order to perform this calculation, the computer requires the waveguide temperature distribution x versus T (fig. 2.5), the resistivity dependence upon the temperature

$(\rho^{\frac{1}{2}} = A_o + A_1 t + A_2 t^2 + A_3 t^3)$, the operating frequency F in GHz, the transverse waveguide dimensions A and B, and the termination temperature T_m. For the sample temperature distribution (SS 4.4.2) shown in figure 2.5, where the termination temperature is 962.0°C (1235.2 K), the computed correction temperature ΔT and its error are

$$\Delta T = -26.3 \text{ K}$$

and

$$\delta\Delta T = \pm 1.5 \pm 0.9 = \pm 2.4 \text{ K},$$

0.9 K being added due to uncertainties in the temperature distribution (SS 4.4.2). The variation of $\delta\Delta T$ with frequency for the sample data in figure 2.5 is shown in figure 2.4. ΔT as a function of frequency is found in figure 1.1.

2.2. Error Analysis

The total maximum uncertainty, or error, δT in the output noise temperature can be written as (ap C)

$$\delta T = (\delta T)_{T_m} + (\delta T)_{T_o} + (\delta T)_{\ell} + (\delta T)_o + (\delta T)_{\rho} + (\delta T)_c + (\delta T)_g + (\delta T)_1 + (\delta T)_w + (\delta T)_A \qquad (2.7)$$

where

$(\delta T)_{T_m}$ ≡ the uncertainty in T caused by the uncertainty δT_m in T_m (SS 4.4.1).

$(\delta T)_{T_o}$ ≡ the uncertainty in T caused by the uncertainty in T_o.

$(\delta T)_{\ell}$ ≡ the uncertainty in T caused by the uncertainty in the position of the output connector at $x = \ell$. Since the reference position is taken at the output connector, $(\delta T)_{\ell} = 0$.

$(\delta T)_{o}$ ≡ the uncertainty in T caused by the uncertainty in the position (x=o) of the termination.

$(\delta T)_{\rho}$ ≡ the uncertainty in T caused by the uncertainty in ρ.

$(\delta T)_{c}$ ≡ the uncertainty in T caused by the uncertainty in c.

$(\delta T)_{g}$ ≡ the uncertainty in T caused by the uncertainty in the temperature gradient T_x' along the waveguide.

$(\delta T)_{1}$ ≡ the uncertainty in T caused by neglecting the second term in (2.3).

$(\delta T)_{W}$ ≡ the uncertainty in T (ap C) caused by different wall gradients (SS 4.4.4).

$(\delta T)_{A}$ ≡ the uncertainty in T (ap I) caused by air attenuation in the waveguide.

$(\delta T)_{g}$ can be estimated in either of two ways as pointed out in ap C. The second method is employed here as explained in SS 4.4.2.

Using the sample temperature distribution in figure 2.5, the results of the error calculation for the WR15 standard (figure D.1.) are tabulated below along with their computer output designations where applicable.

Parameter Uncertainty (With Computer Designation)	Corresponding Uncertainty in T	Percent of Total Uncertainty
δT_m (DTM) = 0.4 K	0.342	14.2
δT_{T_o} (DTO) = 0.5 K	0.0724	3.0
δT_ℓ (DDB) = 0	0	0
δT_o (DDO) = 1/4"	0	0
δT_ρ (DR) = 10%	0.0234	1.0
δT_c (DC) = 2.46%	0.637	26.3
$(\delta T)_g$ (See SS 4.4.2)	0.92	38.1
$(\delta T)_w$ (See ap C)	0.36	14.9
$(\delta T)_A$ (See ap I)	0.05	2.1
$(\delta T)_1$ (See ap A)	0.01	0.4
Error (Total Uncertainty)	2.41 K	

The value for $(\delta T)_g$ was obtained from the three computer correction calculations ΔT shown in figure 2.6, as the difference between the first and second or second and third ΔT's. The curve in figure 2.5 is the curve C in figure 4.7, from which the correction temperature ΔT (Delta T in the computer

output) for the standard's output noise temperature is calculated. Thus the noise temperature output is

$$T = T_m + \Delta T \pm \delta T$$

$$= 1235.2 - 26.3 \pm 2.4$$

$$= 1208.9 \pm 2.4. \qquad (2.8)$$

The calculations leading to (2.8) were carried out for the operating frequency of 55 GHz. Figure 2.4 shows this error as a function of frequency for the band from 55 GHz to 65 GHz.

2.3. Critical Design Specifications

Before a final design for the WR15 standard was chosen, a number of error calculations similar to the calculation in SS 2.2 were performed on different assumed temperature distributions. One important characteristic of the temperature distribution can be seen in figure 4.7. With the separate parameter uncertainties being held constant, the three distributions shown in the figure each produce an error $\delta\Delta T$ as shown. It is obvious from the figure the farthest right produces the least error. Thus the temperature transition region, that region where the temperature distribution falls from a value near the termination temperature T_m to a value near the output connector temperature T_o,

should be kept as near the output connector as possible if the output error is to be reduced to a minimum. This consideration is given considerable weight in the present design (SS 3.1).

Another uncertainty, $(\delta T)_c$, which is negligible at lower frequencies (e.g., WR62, 90, and 284), contributes a large portion of the error in WR15. Most of this uncertainty (ap C) comes from dimensional tolerances (SS 3.1.2) and shows that the transverse dimensions of the waveguide must be held to as tight a tolerance as possible.

The next largest uncertainty in T comes from the measurement of the termination temperature T_m. The uncertainty, δT_m in T_m (SS 4.4.1) comes from the uncertainty in the temperature gradient across the termination, and the calibration uncertainty of the thermocouple used in the measurement.

The other sources of uncertainty are seen to be insignificant when compared to these first three discussed. The details of their origin may be found in ap C.

3. DESCRIPTION AND DESIGN

A block diagram for the operation of the WR15 noise standard is shown in figure 3.1. The termination and waveguide are placed in an oven that feeds information in the form of thermocouple EMF's to a potentiometer for temperature measurement, and to the heating control circuits. The EMF's

fed to the control circuits can, at will, be measured by the potentiometer. This measurement allows the heating coil temperatures to be adjusted to insure that a predetermined temperature distribution can be repeated (SS 4.4.3). The outputs from the circuit control transformers that supply currents to three heating coils in the oven, allowing the temperature gradient within the oven to be held constant. A separate temperature controlled (22°C ± 0.05°C) water cooling system keeps the output connector of the standard at room temperature and cools the oven casing.

These components can be located in figures 1.2 and 1.3. The cylindrical object that has been placed on the table is the oven with the output connector at its left end as shown in figure 1.2, and with the thermocouples and ice baths evident in figure 1.3. The clear plastic tubing conducts water to the water cooled output flange, through coils inside the cylindrical casing to the rear oven cooling plate, then back to the recirculating cooler at the bottom right of the photographs. The oven sits on an oven carriage that can ride in the same rail on which the comparison radiometer is mounted. The carriage has four adjustments that allow the output connector of the standard to be precisely mated to the radiometer input connector. The thermocouples which monitor the coil temperatures and those used to measure the termination temperature are inserted through the rear cooling plate (fig. 1.3).

They are connected in the ice baths to thermocouple grade, Teflon* coated copper wire leads. The ice baths are contained in the silvered vacuum bottles and ride on a platform that is connected to the oven carriage. The copper leads conduct the thermocouple EMF's to the measurement and control rack at the left in the figures. These leads are contained in a small plastic tube that enters the rack just under and to the left of the rack desk. The short looped piece of larger plastic tubing attached to the rack allows the thermocouple leads to be held without kinking. These leads then enter a terminal strip contained in the aluminum shell just under the rack desk. The EMF's from three of the leads, from the thermocouples monitoring the coil temperatures, are balanced against three internally generated EMF's and are then amplified by the three amplifiers located in the lower half of the rack. The amplified outputs are then conducted to the three control circuits at the bottom interior of the rack. The three dials at the bottom of the rack adjust the three internally generated EMF's. The resulting coil currents are conducted through three fused ammeters and out through the cord at the bottom of the rack into the rear of the oven (fig. 1.3) to the oven heating coils. The precision potentiometer

*Certain commercial materials are identified in this paper in order to adequately specify the experimental procedure. In no case does such identification imply recommendation or endorsement by the National Bureau of Standards, nor does it imply that the material identified is necessarily the best available for the purpose.

used to measure the EMF's is located at the top of the rack. The current source for the potentiometer is located inside the rack. The null detector used with the potentiometer, and the switch used to connect the individual leads to the potentiometer, are located just above the rack desk.

The details of the design and construction of these components are contained in the following subsections. SS 3.1 contains the details of the internal oven components, including the waveguide termination, the waveguide, the heat distributor, heating coils, sleeve, and the thermocouples. A description of the thermocouple ice baths is also given in this subsection. SS 3.2 contains the details of the external oven components, including the oven casing, the support spider from which the internal components are suspended, the cooling coils, and the carriage. SS 3.3 contains the details of the auxiliary components consisting of the temperature measurement system, the heating control system, and the water cooling system.

3.1. Internal Oven Components

Drawing #1 shows the oven assembly and carriage. The oven assembly itself (items 25 through 41) shows the internal oven components (items 26, 32, 33, 34, 40, and 41) suspended in the center of the oven casing (items 24, 31, 35) by the supporting spiders (item 36) which are bolted to

the oven end plates (items 29 and 35). The internal components shown include the resistive termination (item 41), the high temperature waveguide (item 26), the inconel heat distributor (item 32) with three sets of bifilar wound heating coils, and the locking rings (item 42) which hold the heat distributor together and support it in the heat distributor sleeve (item 33). Not shown in the drawing is the insulation packed between the coils and the sleeve, at both ends of the heat distributor, and just inside the cooling coils (item 30) leaving an air gap between this insulation and the insulation around the sleeve. Two of the thermocouple grooves in the heat distributor are shown.

When in operation, the front coil (left in the drawing) is used to keep the front end of the heat distributor as near as possible to the termination temperature (SS 2.3); the center coil is used to set the termination temperature; and the back coil is used to compensate for heat loss from the rear of the oven.

3.1.1. High Temperature Resistive Generator

The high temperature termination (resistive generator) from which most of the standard's noise power output originates is designed for high RF loss, high thermal conductivity, and a low reflection coefficient. To insure that the termination material had sufficient loss from 55 to 65 GHz, the losses of

a number of materials were measured (SS 4.1.2) in this band. From this data the length of termination needed could be estimated to be great enough to completely terminate the waveguide, and to provide a low reflection coefficient.

A low reflection coefficient (SS 4.1.3) was achieved by cutting the termination material at an angle to its length resulting in a face length (ap F) of 0.75". The length of material needed turned out to be 0.28" (ap G) resulting in a minimum termination length of approximately 1". It is over this 1" length that the termination temperature T_m is determined (SS 4.4.1). The final overall length chosen was 2.3" (drawing #2).

To achieve a high thermal conductivity at high temperatures, the material chosen was a homogeneous mixture of beryllium oxide and 40% silicon, the beryllium oxide providing the high thermal conductivity and the silicon the high RF loss. Figure 3.2 shows a table of thermal conductivities for a number of materials.

The final design, shown in drawing #2, has a cutting angle of 23.4° corresponding to vertical and horizontal face angles of 10° and 24° respectively. The cutting angle is used by the manufacture in fabricating the termination, which could not be done "in-house" because of the toxic nature of beryllium [3]. The edges of the termination have a 0.006"

chamfer to allow good thermal contact with the waveguide walls. A 0.5" groove is provided at the end of the termination to allow a hollow ceramic (Al_2O_3) rod to be attached (Al_2O_3 cement). The rod is used to position the termination longitudinally in the waveguide and to provide a means for inserting a thermocouple into the back of the termination. After cementing, the load and rod are cured at 1100°C in a laboratory furnace.

3.1.2. High Temperature Waveguide

The high temperature (962°C) waveguide provides a low loss transmission path from the high temperature termination to the output connector of the noise source. To allow the use of (2.6) (SS 2.1) in calculating the noise output, the inside waveguide dimensions must be precisely known (to calculate c accurately), and the waveguide resistivity as a function of temperature known to calculate $\rho_x^{\frac{1}{2}}$.

The dimensions of the waveguide are 8 3/8" x 0.228" (± .001) x 0.154" (± .001) with corner bend radii less than 0.031" outside; by 0.148" x 0.074" (± .001) with corner bend radii less than 0.006" inside. The dimensional tolerances can produce a reflection as large as 0.01 (ap H and SS 4.1.3) from the waveguide when compared to a perfect waveguide.

The length of the waveguide, although not critical, was chosen long enough to protrude out of the heat distributor and into the cooler region of the insulating felt at the rear end of the oven. This was done to avoid contamination of the inside of the waveguide by heat distributor.

An alloy of 90% platinum and 10% rhodium was chosen for the waveguide material because it has proven to follow (2.6) quite well (SS 4.1.4) in the past. Other important reasons for choosing this material were [2]: 1) its nonmagnetic character avoids uncertainties associated with the Curie Point suffered by magnetic materials; 2) it has a high resistance to oxidation and corrosion; 3) it has a high melting point (fig. 3.3); 4) it is not too soft for repeated high temperature use; 5) it is fairly workable; and 6) there is a large amount of resistivity data available for platinum 10% rhodium [4]. Some care must be taken to reduce the free silicon content around the waveguide in the high temperature region of the oven. This silicon can combine with the platinum in the waveguide and the standard thermocouples to form a eutectic that melts around 800°C [5].

For the length of line from the termination to the output connector, atmospheric attenuation (fig. 3.4) in the waveguide produces a completely negligible effect on the output noise temperature (ap I).

3.1.3. Heat Distributor Assembly

The heat distributor assembly consists of the heat distributor (item 32 in drawing #1), the heating coils, the heat distributor sleeve (item 33), the locking rings (item 34), and the insulation surrounding the sleeve and both ends of the heat distributor, and between the coils and the inside of the sleeve.

The heat distributor is approximately 2 1/4" in diameter and is constructed in two halves (fig. 3.5) with four flanges to separate and contain the heating coils. By studying the photograph, six thermocouple grooves and the main waveguide groove can be discerned. A radial bifilar coil is wound into the front end section (right end in the photograph). The distributor is fabricated from inconel "601," a high temperature alloy compound of approximately 76.0% Ni, 0.04% C, 0.20% Mn, 7.20% Fe, 0.007% S, 0.20% Si, 0.10% Cu, and 15.8% Cr [6]. The thermal properties of this material for comparison with other materials can be found in figure 3.2.

Boron nitride [7] is another material that was considered for the heat distributor. This material has a very high thermal conductivity at 1000°C (fig. 3.2) and is very machinable. Figures 3.6 and 3.7 show a finished boron nitrade distributor. The center and back coils are wound directly on the distributor (fig. 3.7). In tests with this material it was found that when heated to 1000°C a sticky substance,

possibly boric oxide [7], was formed that became a "glass" at room temperature. This flaw prevented its use in the noise standard. Some work with the material was done in a nitrogen atmosphere with the same results, but was not conclusive. Experimentation with the material was discontinued as soon as the high stability of the inconel "601" distributor at elevated temperatures was varified.

Drawing #3 shows the dimensions of the heat distributor and the placement of the thermocouple grooves. By referring to the bottom profile the three separate heating coils, which are all bifilar wound, may be located. The back (left hand) coil is wound from left to right and back. The center coil is wound from right to left and back, and the front coil is wound from inside to outside along the radial groove provided. The coils are an #18 gauge (0.040" diameter) resistance wire on which are strung alumina (Al_2O_3) fish spine beads (0.11" O.D. x 0.056" I.D. x 0.110" length) to prevent shorting. The wire is an alloy of 5.5% Al, 22% Cr, 0.5% Co, and 72% Fe with a resistance to oxidation considerably greater than the nichrome wire used in previous NBS noise standards.

The inconel sleeve which contains the distributor and coils is shown in figure 3.8 on the left of the photograph. Also shown are the inconel locking rings which hold the two halves of the distributor together and support

them in the sleeve. The assembled heat distributor with the waveguide and eight thermocouple grooves are shown at the right. Figure 3.9 shows the whole assembly, including the sleeve, locking rings, and heating distributor from the front. The front and center heating coil leads are brought through two of the front slots while the rear heating coil lead is brought through a slot in the rear of the assembly.

Three forms of zirconium oxide insulation [7] were used in the standard, a 0.15" felt, a cloth, and a yarn. The insulating characteristics of this material are indicated in figure 3.10 and in SS 4.2.1.

3.1.4. Thermocouples

The detailed locations of the thermocouple grooves are given in drawing #3. Figure 3.11 shows a schematic diagram of the location of the tips of the thermocouples. The dots represent the points at which the temperature of the heat distributor is sampled by the thermocouple junction. The three control thermocouples B, C, and F are located in close contact to the back, center, and front heating coils respectively, and are connected to three separate servo-control circuits that maintain the coils at given temperatures. S_2 and S_3 are calibrated standard thermocouples

in contact with the waveguide and can be positioned anywhere along the dotted line to be just above and below the termination. The thermocouples are used, in conjunction with a third (S_1) inserted in the rear of the termination, to determine the average termination temperature (SS 3.1.1). The other thermocouple grooves shown in drawing #3 turned out to be unnecessary and are not used.

The thermocouples are constructed by fusing two dissimilar metal leads together and running the two leads through a double bore ceramic tube. The junction resulting from fusing generates the EMF which indicates the temperature. The ends of the leads are soldered to thermocouple grade copper wire leads and are immersed in a non-conducting liquid which is cooled in an ice bath to 0°C. The copper leads then convey the resultant EMF to a suitable measuring instrument.

The standard thermocouples S_1, S_2, and S_3 employ a reference grade, 0.010" diameter platinum wire and a platinum – 10% rhodium wire for the two leads. The ceramic tube is a high purity (99.8%) alumina (Al_2O_3) tube with 0.047" ± 0.003 O.D., and 0.014" bores. The table in figure 3.2 shows some of the properties of the alumina and figure 3.12 shows a graph for the EMF output versus temperature for the platinum 10% rhodium thermocouple. The leads are cut to 36" lengths and sent to NBS-Gaithersburg where they are fused together at

one end, annealed, and calibrated (fig. 3.13) according to Schedule 221.112Z found in the NBS Special Publication 250. After the thermocouple has been calibrated, it is returned with a calibration report (fig. 3.13), inserted into a double bore ceramic rod, and soldered to the copper leads. Extreme care must be exercised in handling the thermocouple [5] after it has been calibrated.

The control thermocouples B, C, and F are constructed from 0.005" diameter Platinel #7674 and #5330 wire leads in a similar fashion to the standard thermocouples. The rod has a 0.031" ± 0.003 O.D. with 0.007" bores. This thermocouple has a high output as a function of temperature (fig. 3.13) and a longer life, making it more suitable for control purposes.

3.2. External Oven Components

The oven casing (drawing #1) is constructed from a welded aluminum cylinder of 5.75" diameter onto which two brass end plates are bolted. The rear plate supports the rear support spider, the rear guide plate, and waterjacket. The output (front) end plate supports a support spider, and contains a concentric 2.5" diameter hole into which is bolted the water cooled flange of the high temperature waveguide.

The support spiders are constructed so that (ap J) as the heat distributor sleeve expands on heating, the ends of the sleeve in contact with the tapered spiders remain in

contact, keeping the sleeve and heat distributor concentric with the oven casing, thus preventing damage to the waveguide.

A 3/16" helical copper cooling coil is inserted just inside and in contact with the cylindrical oven casing. This coil protrudes through slots at both ends of the casing where it is connected to the lower adaptors of the end plates. When in operation, coolant flows in the front top adaptor, through the coil, and out the back top adaptor of the rear end plate to maintain the oven casing at room temperature. The platinum-rhodium waveguide is soft soldered into the front water cooling flange, protruding enough to allow a WR15 flange to be attached. The composition of the solder used is 95% Tin - 5% Silver. A cylindrical jacket of insulation is located inside the I.D. of the cooling coil with an air gap between this insulation and the insulation surrounding the heat distributor sleeve.

The oven carriage is designed for single-handed adjustment of the oven position while mating the output waveguide flange to the flange of a radiometer. The plastic wheels of the carriage are designed to run in the same rail to which the radiometer is attached.

3.3. Auxiliary Components

Figure 3.1 shows the three auxiliary systems used in the standard; the temperature measurement system (fig. 3.14), the heating control system (fig. 3.15), and the water cooling system. These systems are described in this section.

3.3.1. Temperature Measurement System

The ice bath, used as a 0°C reference junction where the thermocouple leads are soldered to copper leads, consists of a 440 cc. vacuum insulated bottle filled with distilled water and ice (made from distilled water) in equilibrium at 0°C. Glass test tubes prepared from 1/4" tubing contain the soldered junctions and are immersed in the ice baths. Before the junctions are inserted into the test tubes, each tube is partially filled with a fluorochemical liquid to reduce temperature gradients along the leads and junctions.

The thermocouple grade, teflon coated copper leads conduct the EMF's from the bath to the terminal board. Approximately 13' of this wire is used for each lead (ap L).

The terminal board is housed in a metal shell to encourage a uniform temperature distribution along the junction terminals, thus minimizing the effects of thermal EMF's (SS 4.3.1) generated at the contacts of the copper leads and brass terminals of the terminal board.

The switch is a commercially available, low thermal-EMF switch that connects one switch output lead to any of the thermocouple input leads.

The potentiometer used to measure the EMF's is a commercially available high precision laboratory potentiometer, with a limit of error on the 9.1 mV range equal to 0.1°C when used with a constant current standardizing supply.

The brass lugs used on the leads between the switch and potentiometer, and between the potentiometer and the null detector were gold flashed to resist oxidation and minimize contact EMF's.

3.3.2. Heating Control System

A diagram of the heating control system is shown in figure 3.15. Both the oven and rack are gounded to the line ground. The current in the three heating coils are servo controlled to maintain known and small temperature gradients in the oven. The heating control is obtained by sampling the coil temperatures and maintaining them at a desired temperature via control circuits that are mechanically coupled to the current control transformers through drive motors. The maximum current settings of these control transformers are limited by the current limiting transformers to obtain maximum control sensitivity and to prevent the oven from overheating during warmup. The control transformers are commercially available 7.5 amp units,

three of whose shafts have been modified for coupling to servo control drive motors.

A diagram showing how the servo drive voltage is obtained, and how the coil temperatures are measured, is given in figure 3.16. The thermocouple EMF on the upper terminal of the board can be measured by the potentiometer to obtain the coil temperature. For control purposes, this EMF is opposed by an offset voltage set to a value corresponding to the desired coil temperature. The resulting correction voltage is amplified and fed to the control circuits.

A diagram showing the operation of the control circuits (ap M) is given in figure 3.17. A non-zero correction voltage changes the width of a square wave which is then compared to the width of a reference square wave by an "AND" gate. The resulting output signal actuates the transformer drive motors which adjust the transformers to control the coil currents.

The oven is brought up to temperature by the following procedure: 1) the limiting transformers are set to a value that will limit the maximum current available to the control transformers to a value that will not operate the coil fuses or burn out the coils; and 2) as the correction voltage approaches zero, as evidenced by the needle indicators on the amplifiers coming on scale, the limiting transformers are separately adjusted upwards in current to provide just enough

current to maintain the heating coils at temperature with zero correction voltage, or when the needle indicators read zero. Once up to temperature the heating controls need no further adjustment.

3.3.3. Cooling System

The oven casing is cooled by circulating distilled water through the end plates and the cooling coil. The coolant is supplied from a constant temperature (± 0.05°C) bath and recirculated to the bath.

A manifold was constructed that allows the water pressure drop across the oven to be adjusted (fig. 1.2). A thermometer is provided in the manifold to monitor the water temperature entering the front cooling plate of the oven, and two pressure gauges allow the pressure drop across the manifold to be checked.

4. MEASUREMENTS AND OBSERVATIONS

This section contains measurement reports and observations made during the course of the design, construction, and testing of the noise standard. In addition, a few brief descriptions of measurement procedures and critical comments are given. For ease in locating specific data the section is subdivided into six subsections. Subsection 4.1 covers the measurements made on the internal oven components.

SS 4.2 and SS 4.3 cover the rest of the oven and auxiliary components.

Subsection 4.4, entitled "System Performance," contains the main measurement documentation supporting the conclusions drawn in previous subsections (SS 2.1 and 2.2) concerning the standard's output and accuracy.

Subsection 4.5 contains a potpourri of measurement data, some more important than others, that was accumulated during work on the standard. Much of the data is only tangentially related to the noise standard, but could be of use for future work and is therefore recorded here for later convenience.

Subsection 4.6 contains critical comments on the standard's construction, which although not incorporated in the present standard, could be put to profitable use later.

The various data appear under brief descriptive headings in a roughly descending order of importance.

4.1. Internal Oven Components

4.1.1. Thermocouple Accuracy

The thermocouples used to determine the termination temperature T_m were constructed (SS 3.1.4.) from 0.010" diameter thermocouple wire that was calibrated at NBS-Gaithersburg to an accuracy of ± 3 microvolts at the fixed points (fig. 3.13), and to an accuracy of ± 5 microvolts elsewhere in the range from 0°C to 1100°C. The termination temperature is held close to the silver point (961.93°C) to take advantage of the smaller ± 3 microvolt uncertainty in the calibration data. This amounts to a 0.27°C uncertainty at that temperature.

In measuring the thermocouple EMF with the laboratory potentiometer the measurement uncertainty is estimated to be (SS 3.3.1) 0.1°C. Thus, the total uncertainty in the measurement of a temperature around the silver point with a calibrated thermocouple is 0.37°C.

4.1.2. Lossy Termination Materials

The approximate attenuation per unit length of three materials was measured at 55.8 GHz. These measurements were performed to assure that the load material chosen (60% BeO-40% Si) for the high temperature termination

(SS 3.1.1.) would have adequate loss prior to its being fabricated, and to obtain some feeling for the loss characteristics of other load materials. The results were:

Silicon Carbide:	96 dB/inch
Polyiron:	69 dB/inch
High Loss Plastic:	126 dB/inch

The BeO-Si termination should therefore have a loss of approximately 40% of a similar Silicon Carbide load, or approximately 92 dB/inch.

4.1.3. Reflection Coefficient of the Termination and Waveguide

Three reflection coefficient measurements of the BeO-Si terminations (SS 3.1.1.) were performed; two swept and one fixed frequency measurement of the termination by itself, and a swept frequency measurement of the termination-high-temperature waveguide combination. The output traces of the three swept measurements are shown in figures 4.1, 4.2, and 4.3. The first figure shows a conventional swept measurement [8] where the labels for the return loss calibration lines appear at the left. The top set of lines contains a calibration line and two lines made by commercial terminations. The second set shows a calibration line and a line made by another commercial termination. The bottom set contains four calibration lines and a line made by the BeO-Si termination.

Figure 4.2 shows a Holloway-Somlo (H-S) swept reflectometer measurement [8] of the BeO-Si terminations using two calibrating reflections whose coefficients are 0.024 and 0.001 (at most) respectively. The top trace is a frequency calibration trace. The next set of traces consists of the 0.024 reflection and the BeO-Si termination which is seen, by comparing the vertical magnitude of the lines, to have a reflection coefficient of 0.006 or less. The third set shows the BeO-Si termination compared to the 0.001 termination. Comparison of these magnitudes shows the BeO-Si reflection coefficient to be about 0.008. The bottom trace is from the BeO-Si termination again, shifted slightly in the H-S reflectometer input waveguide lead.

The two sets of traces in figure 4.3 show the BeO-Si termination-high temperature waveguide combination compared to a 0.024 reflection, and to a 0.048 reflection in the H-S reflectometer. These traces indicate that the combination has a reflection coefficient of approximately 0.012 (c.f. aps G and H).

The reflection coefficient of three BeO-Si terminations were measured in a tuned reflectometer [8] at 59.4 GHz. The results, including measurement uncertainties, show that the reflection coefficients of all three terminations fall in the range from 0.002 to 0.006.

4.1.4. High-Temperature Waveguide Loss

The attenuation per unit length of the high-temperature waveguide (SS 3.1.2) was measured [9] at 59.4 GHz and 22°C. The average result of five measurements shows this loss to be 0.023 dB/inch with an uncertainty no greater than 20%.

4.1.5. Thermocouple Insertion Distance

The thermocouple used in the temperature distribution measurement of the high-temperature waveguide is inserted by holding the thermocouple stationary and moving the oven along the support rail by rotating the plastic wheels of the oven carriage. If need be, the oven can be positioned to within a few tenths of 0.001" by this technique. A typical measurement setup is shown in figure 4.4. The thermocouple is being inserted into the waveguide from the left. Once the zero distance setting is established by positioning the point of contact between the thermocouple bead and the waveguide at the flange reference plane, the apparent insertion distance of the thermocouple into the waveguide can be measured by the steel scale on the rail or the dial indicator secured to the rail at the right in the picture. By setting the pointer attached to the oven carriage to a given mark on the scale, the apparent insertion distance can be measured to an accuracy approximately 0.005". By using the dial indicator at the right, this distance accuracy is approximately 0.002".

The actual insertion distance is obtained from the apparent distance by adding to the apparent distance a correction accounting for the expansion of the thermocouple rod upon heating as it is inserted into the waveguide. This correction is calculated (ap E) from knowledge of the distribution curve (fig. 2.5) and the expansion characteristics [10] of the Al_2O_3 rod (fig. 4.5). The accuracy of this calculation is estimated to be 0.0005".

4.1.6. Inconel Heating Test

Before deciding to use inconel 601 for the heat distributor, a piece with nominal dimensions 4 x 1 x 3/16 inches was maintained at 1100°C for 34 hours. Before heating, one end of the piece was measured to be 0.197" and the other end to be 0.204" in thickness. After heating, the piece was remeasured and found to have the same dimensions to within the measurement accuracy (0.0005"), and was found to have no measurable warp caused by the heating.

Observation of the final heat distributor after many hours of use shows it not to have oxidized further than the initial oxidation acquired upon first heating.

4.1.7. Heating Coil Resistances

The heating coil resistances were measured at 22°C (room temperature) and 1000°C. At room temperature the coil resistances, front to back, are 3.3, 22, and 10 ohms respectively. When heated to 1000°C, these same coil resistances increased to 3.8, 24, and 11 ohms respectively.

These resistances appear not to have changed over 3 months intermittent usage (SS 4.1.7).

4.2. External Oven Components

4.2.1. Zirconium Oxide Insulation

A 3/4" cylinder of boron nitride was heated to 1000°C by a heating coil wrapped tightly around it. The combination was insulated by a 0.15" thick zirconium oxide felt wrapping, and suspended in air during heating. The temperature drop from the inside to the outside of the insulation was measured to be 700°C.

4.3. Auxiliary Components

4.3.1. Residual Thermal EMF

The residual EMF generated in the contacts of the terminal board, the thermocouple switch, and the potentiometer

(fig. 3.14) reduce the accuracy of the temperature measurements. This EMF was measured by tying together a pair of the copper leads in the ice bath and measuring the EMF appearing at the potentiometer. This EMF was less than 0.1 microvolt, corresponding to an error of 0.009°C at the Silver Point Temperature (961.93°C) where the high-temperature termination is maintained.

4.3.2. Copper Lead Resistance and Resulting Measurement Error

The resistance of the copper leads between the thermocouple leads in the ice junction and the measuring apparatus (fig. 3.14) was measured to be 1.5 ohms, or approximately 0.1 ohms per foot for the total length of 13'. The error in a temperature measurement caused by this resistance and a slight unbalance at the null detector is estimated (ap L) to be no greater than 0.002°C.

4.3.3. Water Temperature Control and Measurement

The temperature of the water coolant entering the oven casing at the waveguide flange is held at approximately 22°C to ± 0.05°C. The estimated error in the measurement of this temperature by the manifold thermometer (SS 3.3.3, fig. 1.2) is ± 2°C.

4.4. System Performance

4.4.1. The Termination Temperature

The temperature of the high-temperature termination is determined by measuring the EMF of thermocouple S_1 (SS 3.3.1). The error in this measurement is no greater than 3 microvolts or 0.27°C (SS 4.1.1) when operating near the Silver Point (fig. 3.13). A measurement of the temperature in the waveguide just in front of the termination, and under the waveguide just below the termination, revealed these temperatures to be the same as the termination temperature to within at most 0.1°C. Therefore the determination of the termination temperature by thermocouple S_1 is uncertain to no greater than 0.4°C (0.27°C + 0.1°C).

4.4.2. Determination of the Waveguide Temperature Distribution

The presence of the thermocouple rod inside the waveguide disturbs the waveguide temperature distribution at both ends and in the temperature transition region. Therefore, the normal (unperturbed) distribution cannot be measured directly in these regions. Instead, an area is located between two perturbed distributions in which the normal distribution must lie.

This area is established in the following way. If the high-temperature termination is removed from inside the waveguide, two perturbed temperature distributions can be measured (fig. 4.6); one by inserting the thermocouple into the waveguide from the back end of the oven, and one by inserting the thermocouple from the front. In the first measurement, heat is conducted by the thermocouple rod from the heat distributor region of the waveguide into the temperature transition region as the thermocouple enters this region, giving a higher than normal temperature indication. In the second measurement, as the thermocouple enters the transition region from the front, heat is conducted via the rod away from the transition region giving a lower indication than is normal. It is clear that the normal distribution must lie in an area somewhere between the two perturbed distributions. Since the predominant heat transfer in the transition region is along the waveguide, the distribution in this region should be nearly linear. This is seen to be the case from curves A and B in figure 4.7.

The area in which the normal distribution must lie can be reduced further, as shown by the following argument. The two perturbed distributions from figure 4.6 are expanded in

figure 4.7 in the transition region as curves A and B. In the water cooled region the normal curve is closer to curve B since the distribution is less perturbed in this region when measured from the front than when measured from the back of the oven. Similarly, the normal distribution is closer to curve A in the heat distributor region. Thus the normal distribution lies between the unlabeled curve (which is halfway between curves A and B in the water cooled and heat distributor regions) and curve B in the water cooled region, and between the unlabeled curve and curve A in the heat distributor region. Then if the partial curves in the water cooled and heat distributor regions are joined linearly as shown in figure 4.7, it is clear that the normal curve will lie in the shaded area bordered by the resulting two curves.

The solid curve C which is vertically halfway between the bordering curves is then taken to be the normal distribution, and the correction temperature ΔT (SS 2.1) is calculated from it. This correction temperature is -26.34°C in the figure. The uncertainty in this correction (SS 2.2), $(\delta T)_g$, is taken to be one-half of the difference between the correction temperatures as calculated from the bordering curves, since the normal curve cannot lie outside these curves. From the figure, this uncertainty is 0.92°C.

The foregoing procedure is valid provided that the curves A and B remain substantially unchanged when the termination is reinserted into the waveguide. This is seen to be the case in figure 4.8 which shows two distribution measurements from the front just before and after the termination was inserted.

The difference between curves A and B is plotted in figure 4.9 for the average coil temperature needed to maintain the termination at 962°C. This curve can be used to predict curve A around the transition region from curve B, obviating the need to remove the termination from the waveguide if it can be shown that the differential curve is relatively independent of the average coil temperature. That this is the case is seen in figure 4.10 which shows the three differential curves for three different average coil temperatures to be closely the same. The dates on which the differential curves were taken indicate the stability and repeatability of the oven characteristics.

4.4.3. Temperature Measurement Repeatability

The ability to repeat a temperature measurement at a specified point in the waveguide is very important if one is to have confidence in the temperature distribution measurements. In order to do this in the temperature transition

region, one must be able to reposition the thermocouple in the waveguide (SS 4.1.5) quite accurately. For example, a 0.001" error in repositioning the thermocouple in the transition region causes a 1°C change in the temperature measurement.

In order to check the repeatability, a set of temperature measurements were performed at three points (0", 0.8", 1.3") in the waveguide. The table in figure 4.11 shows the results of these tests. The time in hours measured from the beginning of the first measurement along with the temperature-distance sensitivity around the various points are also given in the table. The results indicate that the measurement of a temperature at a given point in the waveguide, even in the highest gradient region of the temperature distribution, should be repeatable to 2°C. This result is consistent with the fact that the thermocouple can be repositioned to within 0.002" anywhere along the waveguide interior.

4.4.4. Wall Temperature Distributions

The temperature distributions along the four walls inside the waveguide differ from each other in the temperature transition region. Figure 4.12 shows this effect, where the difference between the temperature of each wall and the average temperature of the four walls is plotted as a function of distance into the waveguide from the output

flange. These differences are accurate to 2°C, showing that the wall temperatures are closely the same outside the 0.3" to 1.6" length of waveguide. The error caused by these different temperature distributions is discussed in SS 2.2 and ap C.

4.5. Additional Measurements

4.5.1. Oven Power Consumption

The power consumed by the oven when operating at 962°C was measured to be

Front Coil	7.2 A x 30.7 V	=	221 Watts
Center Coil	2.1 A x 51.3 V	=	108 Watts
Back Coil	3.85 A x 44.8 V	=	172 Watts
	Total		501 Watts

By measuring the temperature rise (22°C → 30°C) and flow-rate (811 mℓ/min) of the oven casing coolant, the heat removed from the oven is calculated to be 453 Watts.

4.5.2. Laboratory Environment

The temperature and relative humidity of the laboratory in which most of the measurements described in this report were carried out were 69°F and 40%, respectively. A recording of the variation of these quantities over a seven-day period appears in figure 4.13.

4.6. Possible Improvements

The following comments are recorded here for future use. They involve both suggestions for improvement of the present WR15 noise standard, and comments that may prove useful in later work.

4.6.1. Thermocouple Grooves

The thermocouple grooves in the inconel heat distributor were machined with a milling cutter, leaving a circular runout of the cutter radius at the end of the groove. This circular runout prevents the thermocouple from making repeatable contact when the thermocouple is removed and reinserted. The design of the groove for the front coil thermocouple also prevents this thermocouple from making repeatable contact with the front coil. This non-repeatability prevents changing the control thermocouples without remeasuring the gradient to be sure it hasn't changed. This problem can be remedied by milling off the radius in grooves B and C (fig. 3.11 and drawing #3), and plugging the hole in groove F leaving a thin wall between the thermocouple bead and the front coil.

4.6.2. Isolation Between Heating Coils

The ability to shape the temperature distribution down the waveguide depends on the amount of thermal isolation between the regions heated by the front, center, and back heating coils. In the present design of the heat distributor this isolation is not great enough to allow much control over the position of the high temperature fall off between the water cooled and heat distributor regions (fig. 2.5). For accuracy reasons (SS 2.3) it is beneficial to push this high-temperature fall-off to as close to the output flange as possible.

One possible means of effecting greater thermal isolation is to cut annular spaces between the front, center, and back coil regions.

4.6.3. Diameter of the Heat Distributor

The diameter of the heat distributor was chosen intuitively, the smoothing of heating irregularities along the central heating coil being the main factor in the choice. Time permitting, some experimentation may show that a smaller diameter is quite feasible.

4.6.4. Different Wall Temperature Distributions

By examining the wall temperature differential curves in figure 4.12, one is led to the conclusion that the different distributions are caused by varying contact between the waveguide and insulation in the transition region (fig. 2.5), and between the waveguide and heat distributor at the end of the heat distributor. At present this effect is not important, amounting to only 2.9% of the total error in the calculated output temperature (SS 2.2).

5. ACKNOWLEDGMENTS

The success of this project is due in part to the efforts of the following people: R. D. Hunter, M. Kanda, A. C. Newell, M. P. Weidman, and B. C. Yates of the Electromagnetics Division for many V-band measurements and consultations; P. F. Biddle, W. F. Decker, R. J. Fischer, H. H. Garing, P. G. Karas, V. Lecinski, W. E. McNaney, K. C. Nuss, A. Padilla, and to D. L. Smith of the Shops Division; Sharon C. Foote of the Electromagnetics Division for the excellent job of typing; and to D. B. Miner of Audio Visual Aids.

Thanks are also due to Dave Sawyer for making up the conductivity tables.

6. REFERENCES

[1] Miller, C. K. S., W. C. Daywitt, and M. G. Arthur, "Noise Standards, Measurements, and Receiver Noise Definitions," Proc. IEEE, 55, pp. 865-877, June 1967.

[2] Wells, J. S., W. C. Daywitt and C. K. S. Miller, "Measurement of Effective Temperature of Microwave Noise Sources," IEEE Trans. on I & M, IM-13, pp. 17-28, March 1964.

[3] Ferreira, L. E., "Recommended Practices for Safe Handling of Beryllium Oxide Ceramics," Symposium on Materials and Electron Device Processing, Special Technical Publication No. 300, American Society for Testing and Materials, 1961.

[4] Vines, R. F. and E. M. Wise, "The Platinum Metals and Their Alloys," The International Nickel Company, Inc., New York 5, N. Y.

[5] Zysk, E. D., "Platinum Metal Thermocouples," Temperature, Its Measurement and Control in Science and Industry, 3, Part 2, Reinhold Publishing Corp., 1962.

[6] "Nickel and Nickel-Base Alloys -- Their Use in the Design of Corrosion-Resistant Machinery and Equipment," Technical Bulletin T-13, The International Nickel Company, Inc. "Properties of Some Metals and Alloys," The International Nickel Company, Inc.

[7] Kohl, W. H., Handbook of Material and Techniques for Vacuum Devices, Reinhold Publishing Corporation, New York, 1967.

[8] Newell, A. C., Private Communication, National Bureau of Standards, Boulder Laboratories. Hollway, D. L. and P. I. Somlo, "A High Resolution Swept-Frequency Reflectometer," IEEE Trans. MTT, MTT-17, No. 4, April 1969. Anson, W. J., "A Guide to the Use of the Modified Reflectometer Technique of VSWR Measurement," NBS Report 6095, April 1960.

[9] Weidman, M. P., Private Communication, National Bureau of Standards, Boulder Laboratories.

[10] Alumina and Beryllia Properties Handbook, Bulletin 952, Coors Porcelain Company, July 1969.

[11] Kerns, D. M. and R. W. Beatty, Basic Theory of Waveguide Junctions and Introductory Microwave Network Analysis, Pergamon Press, Long Island City, New York, 1967.

[12] Yates, B. C., Private Communication, National Bureau of Standards, Boulder Laboratories.

[13] Kerns, D. M. and W. T. Grandy, Jr., "Perturbation Theorems for Waveguide Junctions, with Applications," Program and Digest of the 1962 PGMTT National Symposium, Boulder, Colorado 80302.

[14] Haus, H. A. and R. B. Adler, Circuit Theory of Linear Noisy Networks, The Technology Press of the Massachusetts Institute of Technology and John Wiley and Sons, New York, 1959.

[15] Wait, D. F., "Thermal Noise from a Passive Linear Multiport," IEEE Trans. MTT, MTT-16, No. 9, p. 687, September 1968.

[16] Sees, J. E., "Fundamentals in Noise Source Calibration at Microwave Frequencies," U.S. Naval Research Lab., Report 5051, January 1958.

[17] Stelzreid, C. T., "Temperature Calibration of Microwave Thermal Noise Sources," IEEE Trans. MTT (Correspondence), MTT-13, p. 128, January 1965.

[18] Kerns, D. M. and R. W. Hedberg, "Propagation Constant in Rectangular Waveguide of Finite Conductivity," Journal of Applied Physics, 25, p. 1550, 1954.

7. FIGURES

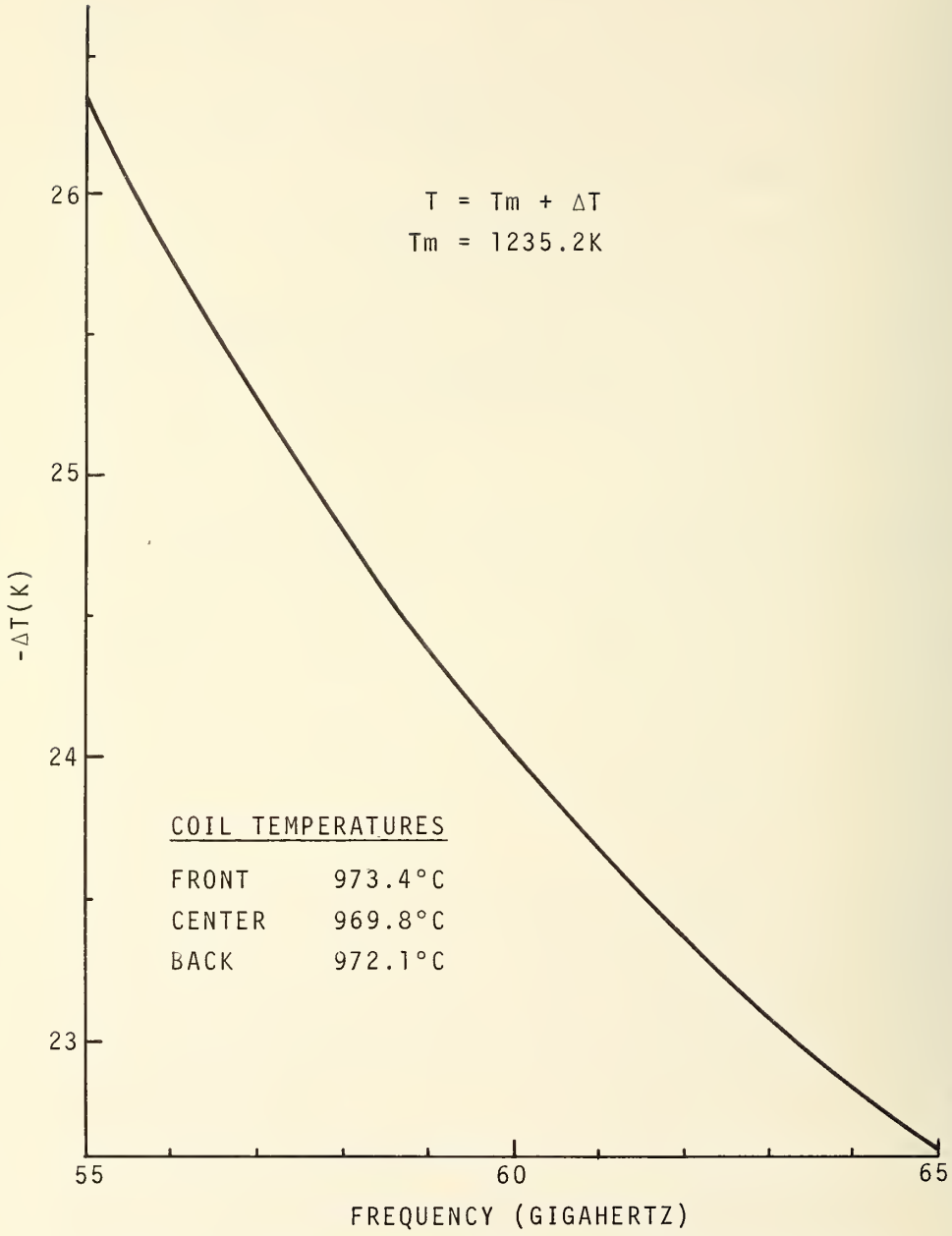

Figure 1.1. Output Noise Temperature Versus Operating Frequency.

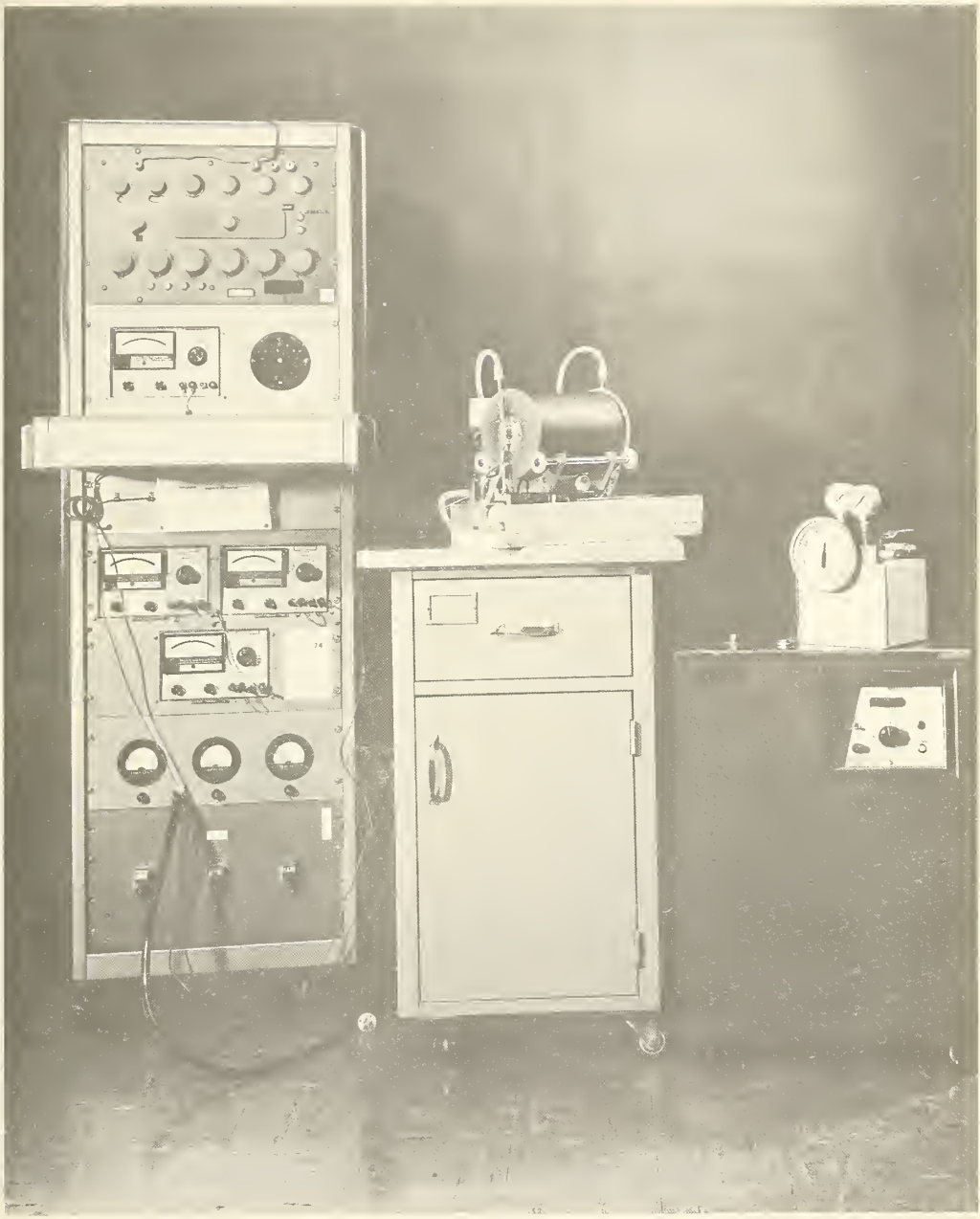

Figure 1.2. Photograph of the WR15 Noise Standard Showing the Output Flange.

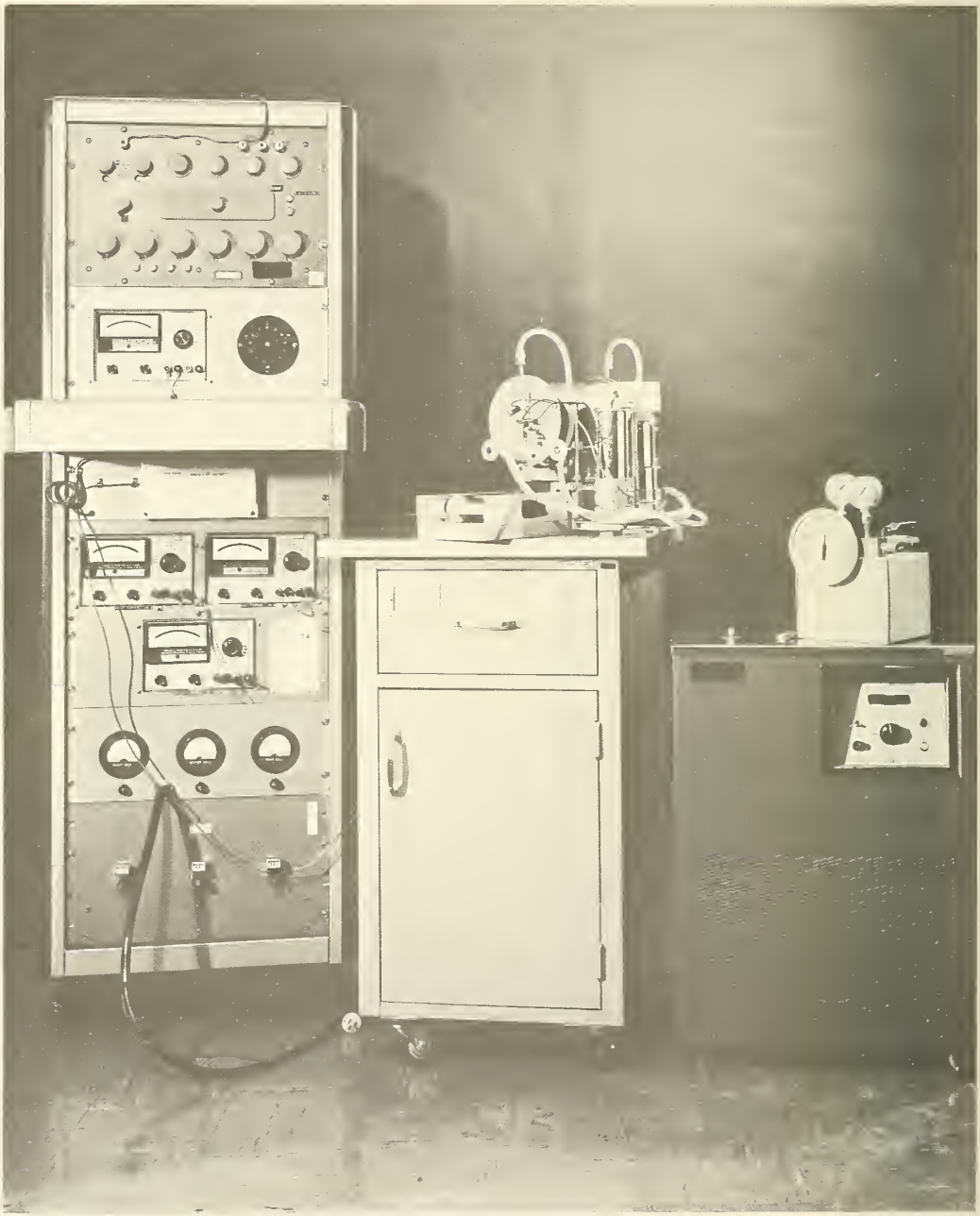

Figure 1.3. Photograph of the WR15 Noise Standard Showing Thermocouples and Ice Junctions.

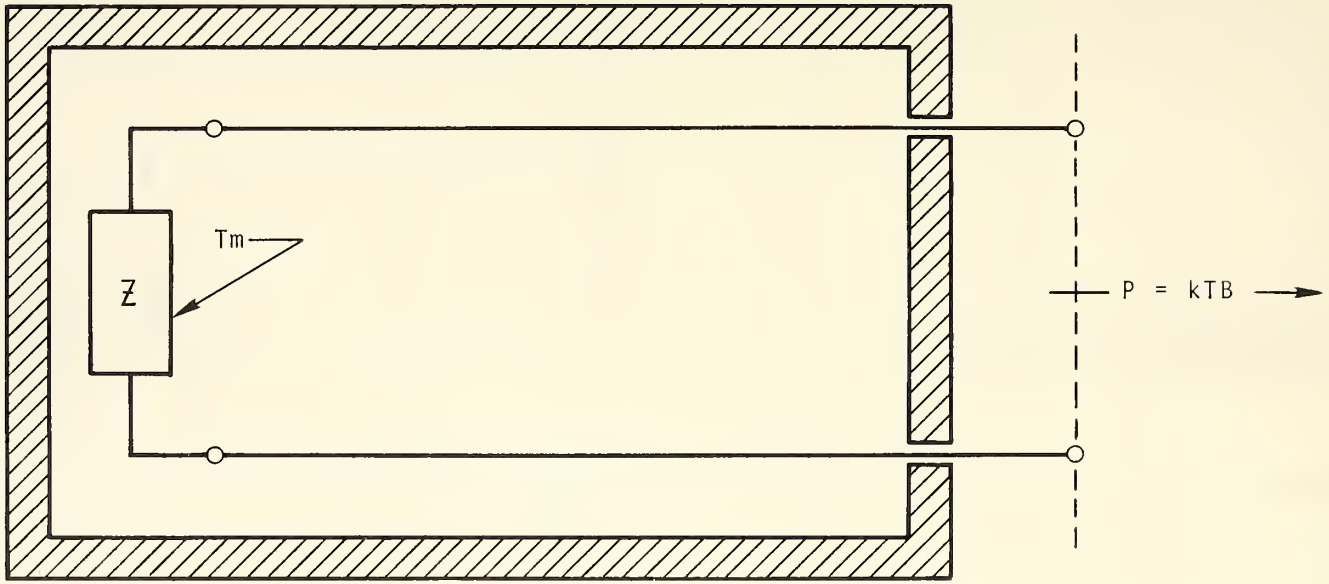

Figure 2.1. Schematic for a Thermal Noise Source.

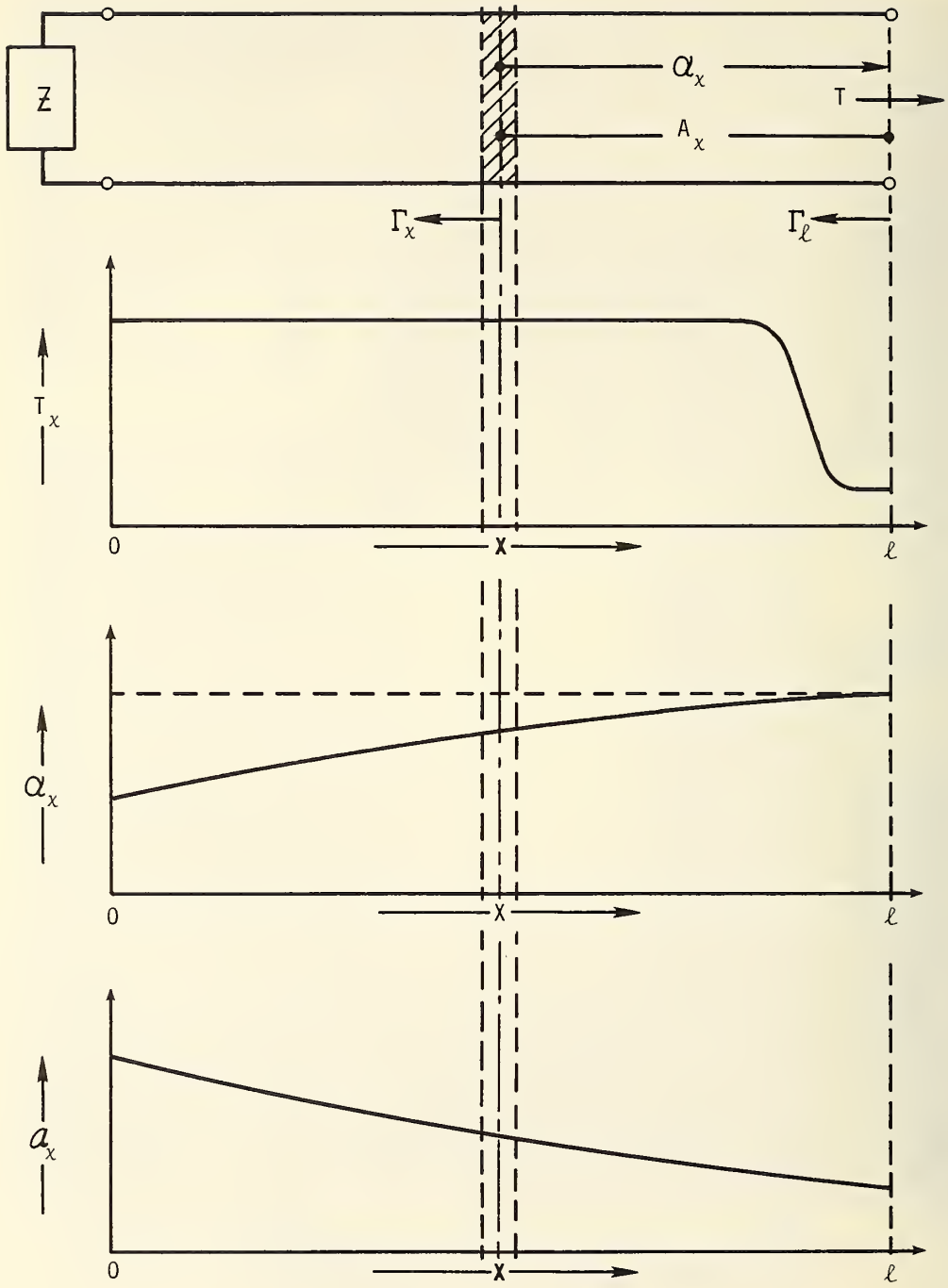

Figure 2.2. Equivalent Circuit of a Thermal Noise Source.

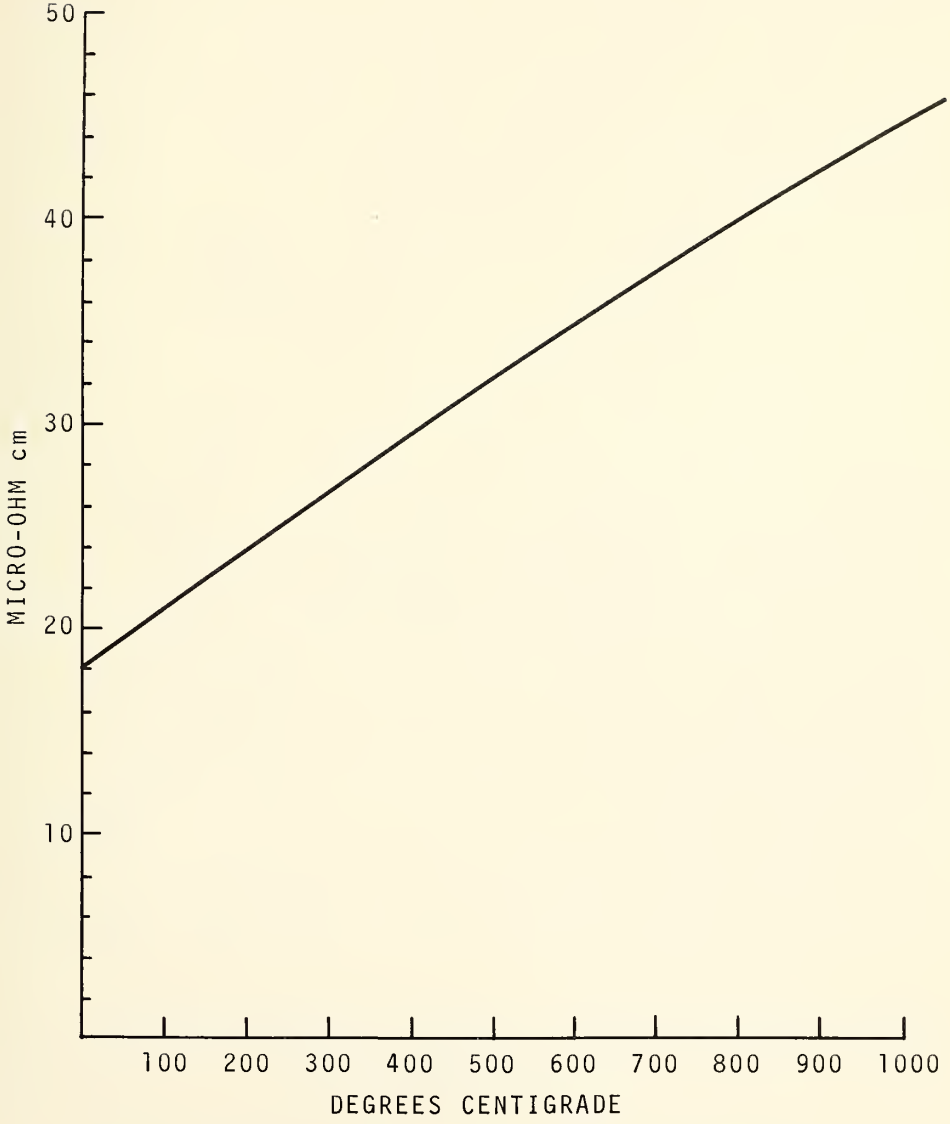

Figure 2.3. Line Resistivity Versus Temperature.

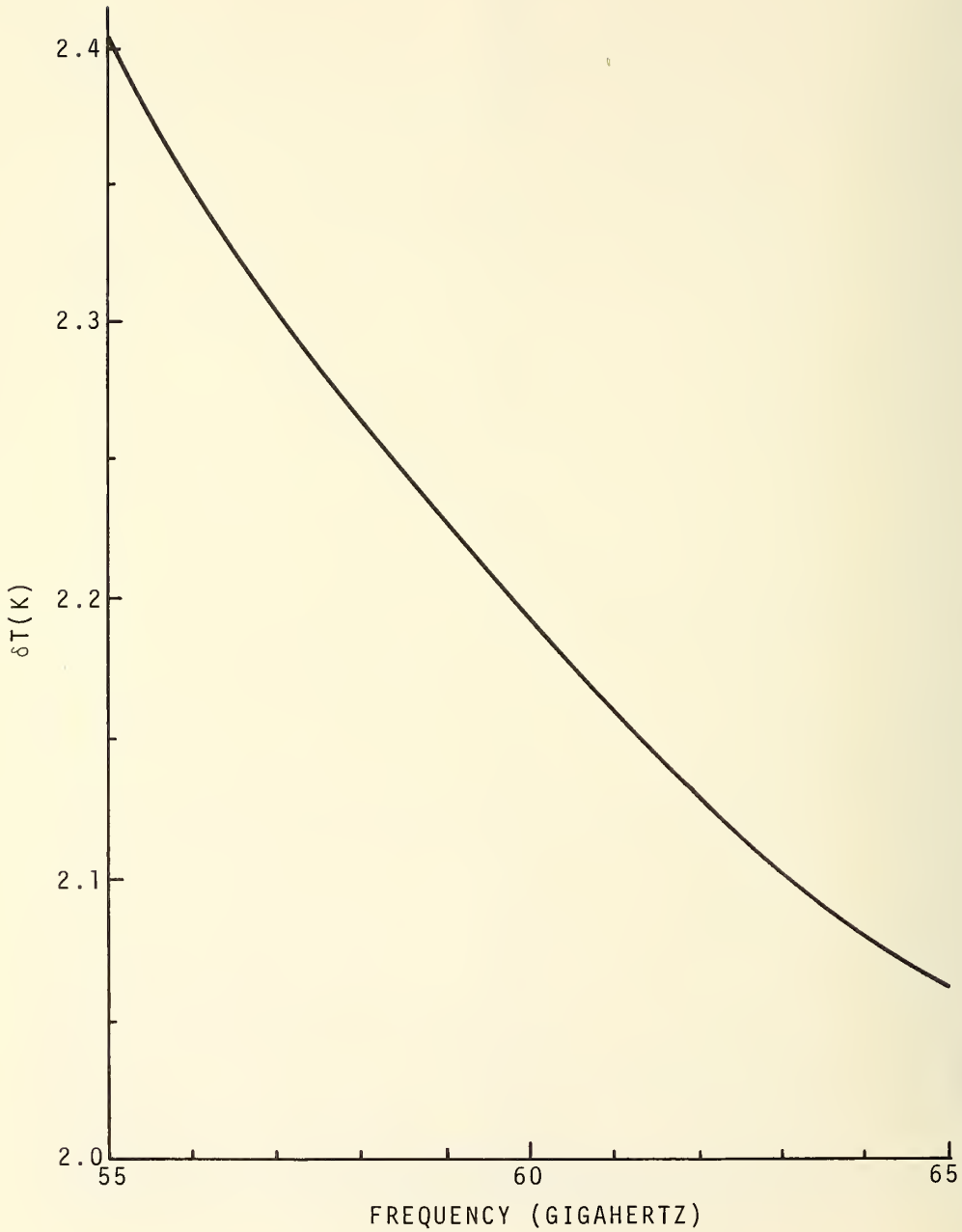

Figure 2.4. Output Error Versus Operating Frequency.

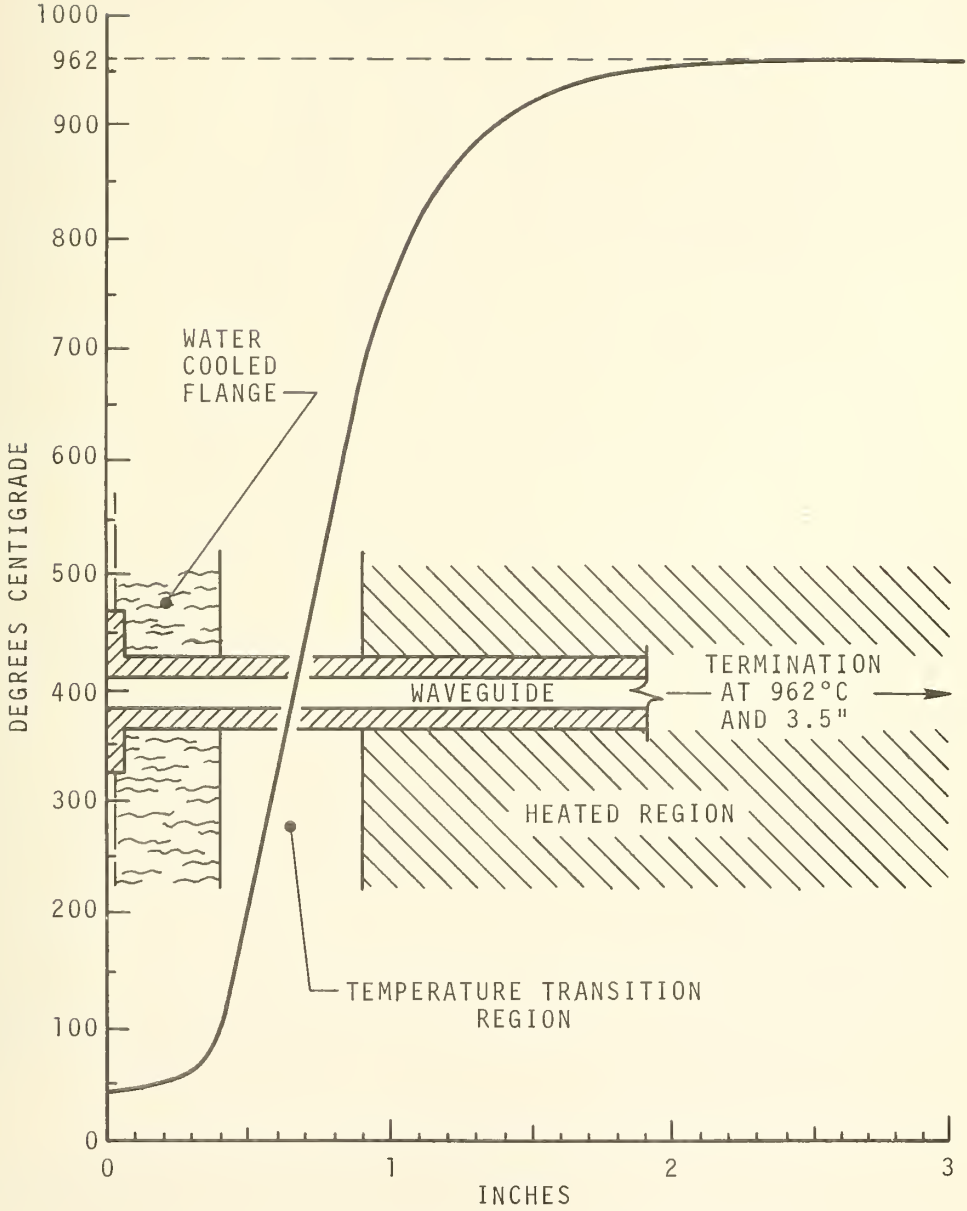

Figure 2.5. Sample Temperature Distribution for Calculations.

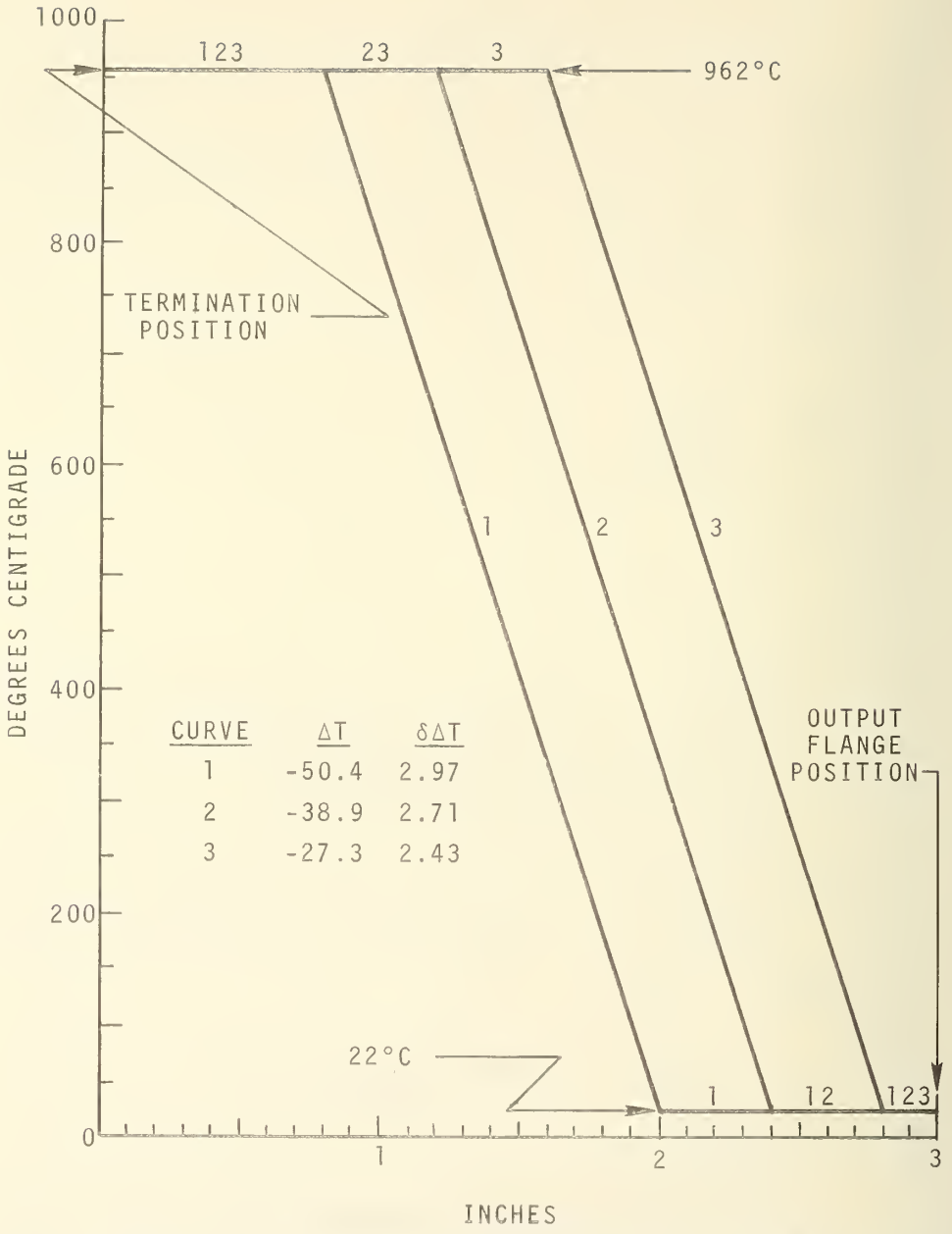

Figure 2.6. The Effect of the Temperature Transition Region on the Output Error.

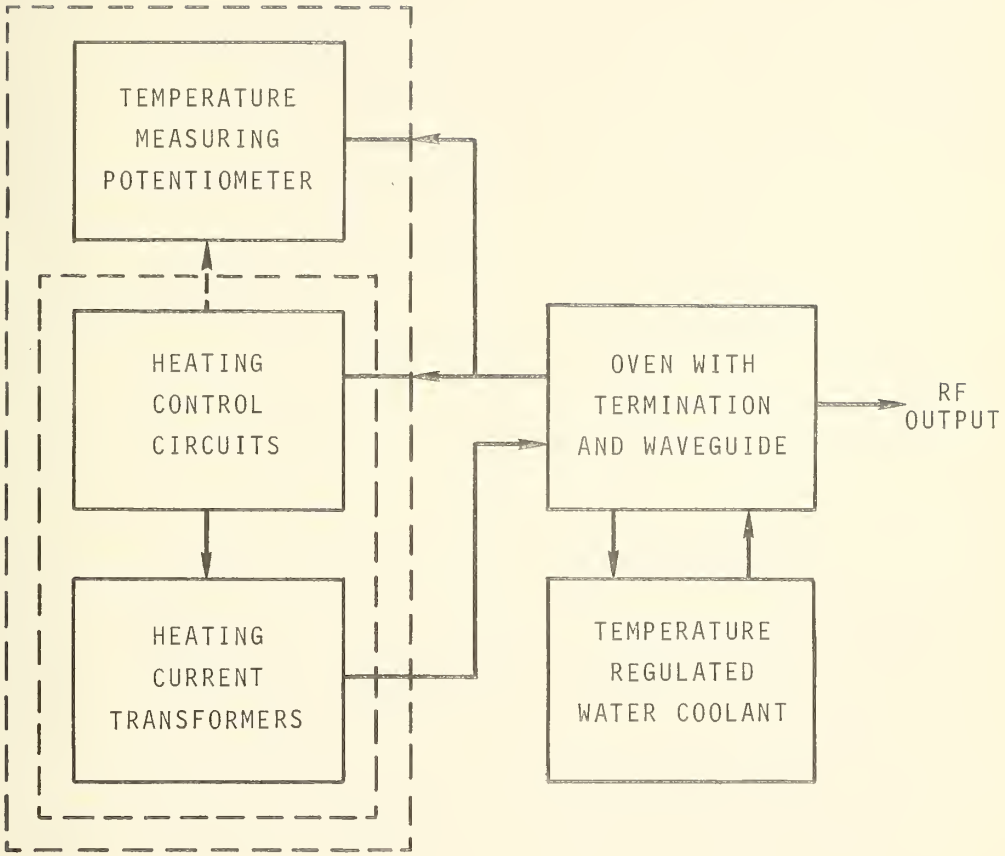

Figure 3.1. Block Diagram of the Standard's Operation.

Material	Thermal Conductivity (~ 20°C) Watts / Cm °C	Thermal Conductivity (~ 20°C) Normalized to Silver	Coefficient of Linear Thermal Expansion (20°C to 500°C nominally) 10^{-6}/°C
Air	0.00024	5.7×10^{-5}	-
Aluminum	2.2	0.52	24
Alumina	0.29	0.069	6.7
Beryllium Oxide	2.2	0.52	6.4
Boron Nitride (Parallel)	0.61	0.14	0
Boron Nitride (Perpendicular)	0.40	0.095	0
Brass	1.2	0.29	20
Carbon Steel	0.45	0.11	18
Copper	3.9	0.93	16
Glass	0.0079	0.0019	9
Gold	3.0	0.71	14
Inconel	0.15	0.036	12
Lead	0.35	0.083	29
Nickel	0.92	0.22	13
Platinum	0.69	0.16	8.9
403 Stainless Steel	0.25	0.060	6
Silver	4.2	1	20
Zirconium Oxide Felt	0.00079	0.00019	-

Figure 3.2. A Table of Thermal Conductivities and Thermal Expansion Coefficients.

Material	Melting Temperature in ^{o}C	Electrical Resistivity ($20^{o}C$) in $\mu\Omega$ - cm
Gold	1063	2.4
Iridium	2454	7
Osmium	2700	60
Palladium	1549	11
Platinum	1773	10
Rhodium	1966	5
Silver	961	1.6

Figure 3.3. Table of Some Properties of Some of the Noble Metals.

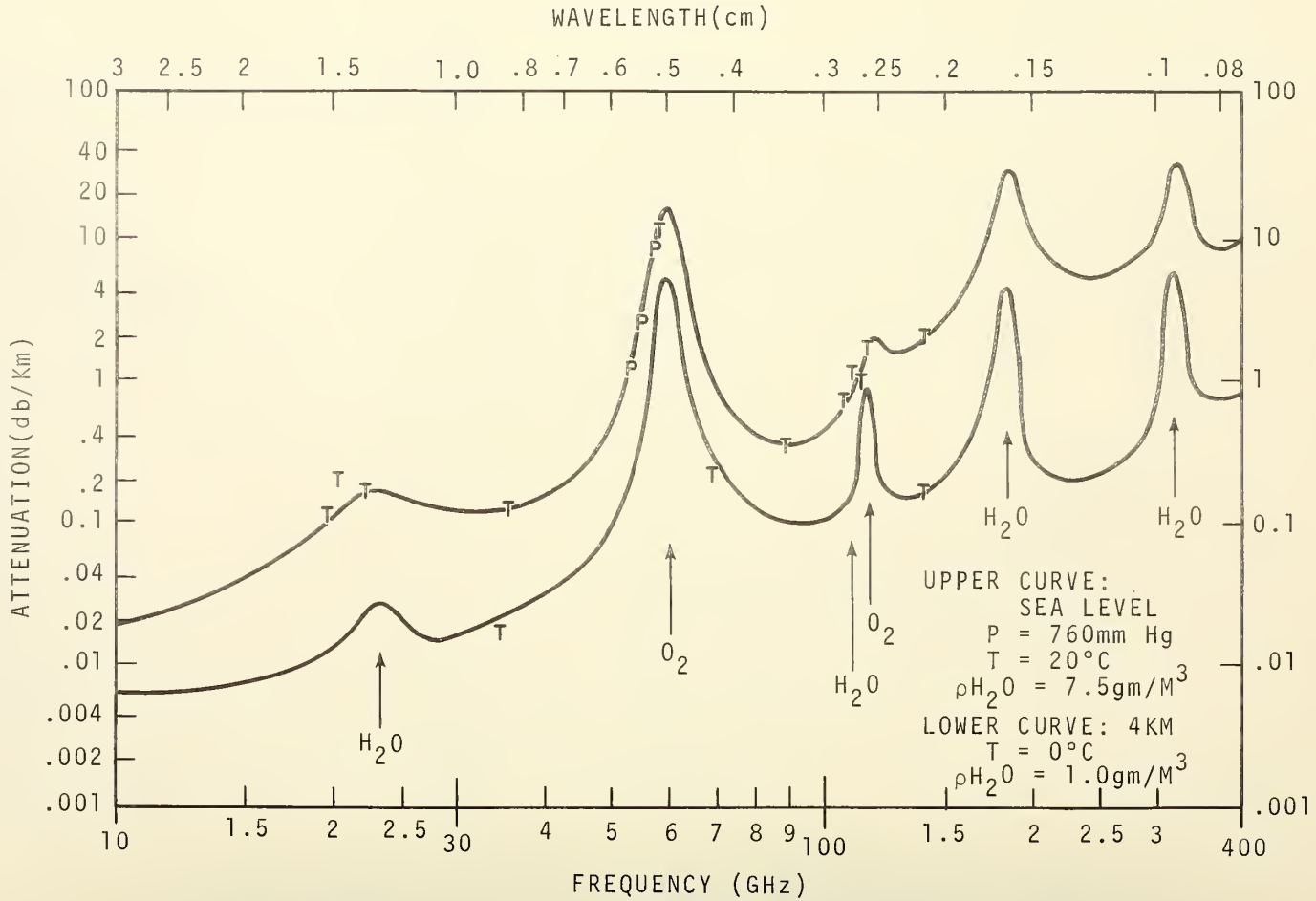

Figure 3.4. Atmospheric Attenuation Versus Frequency (Courtesy Microwave Journal).

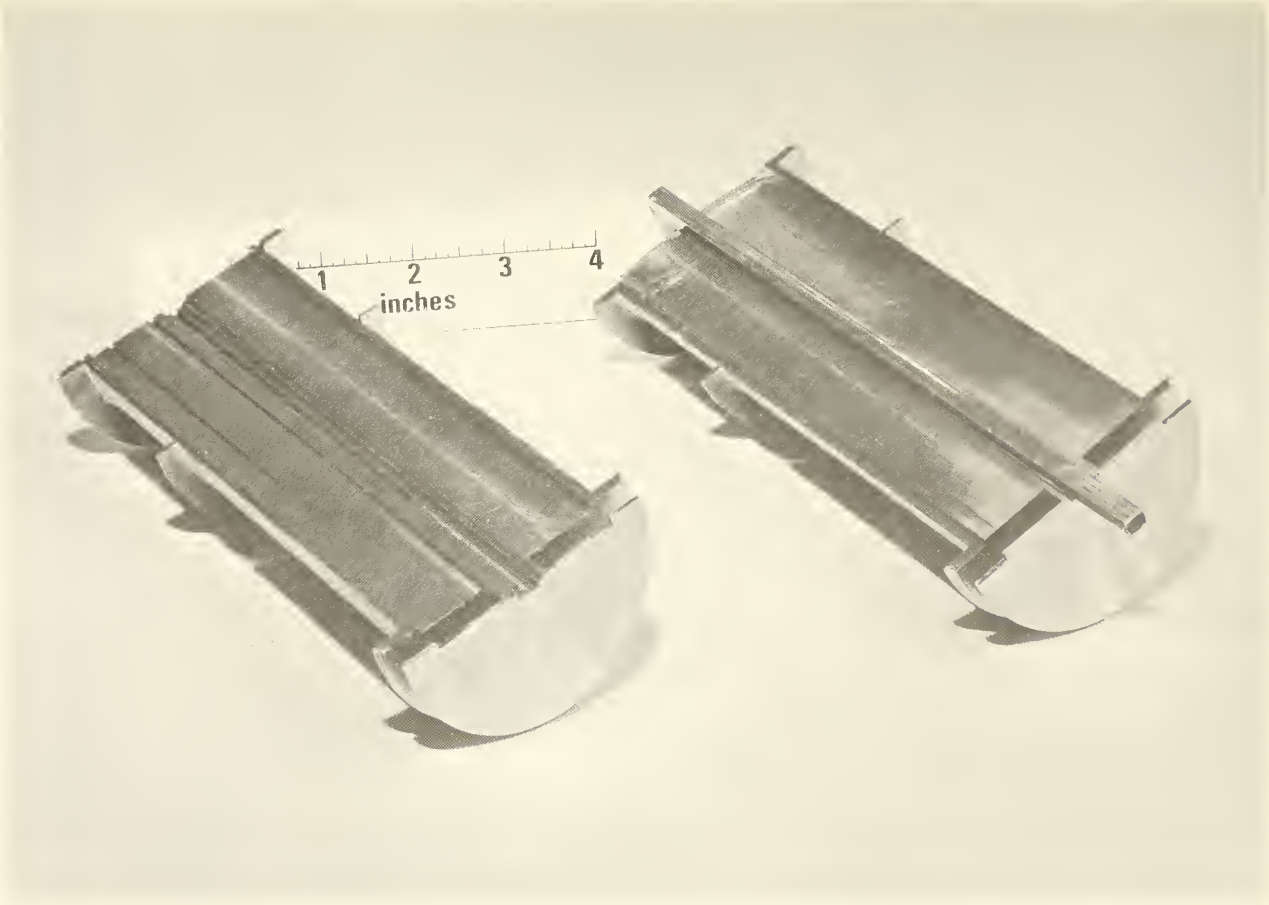

Figure 3.5. Photograph of the Inconel "601" Heat Distributor.

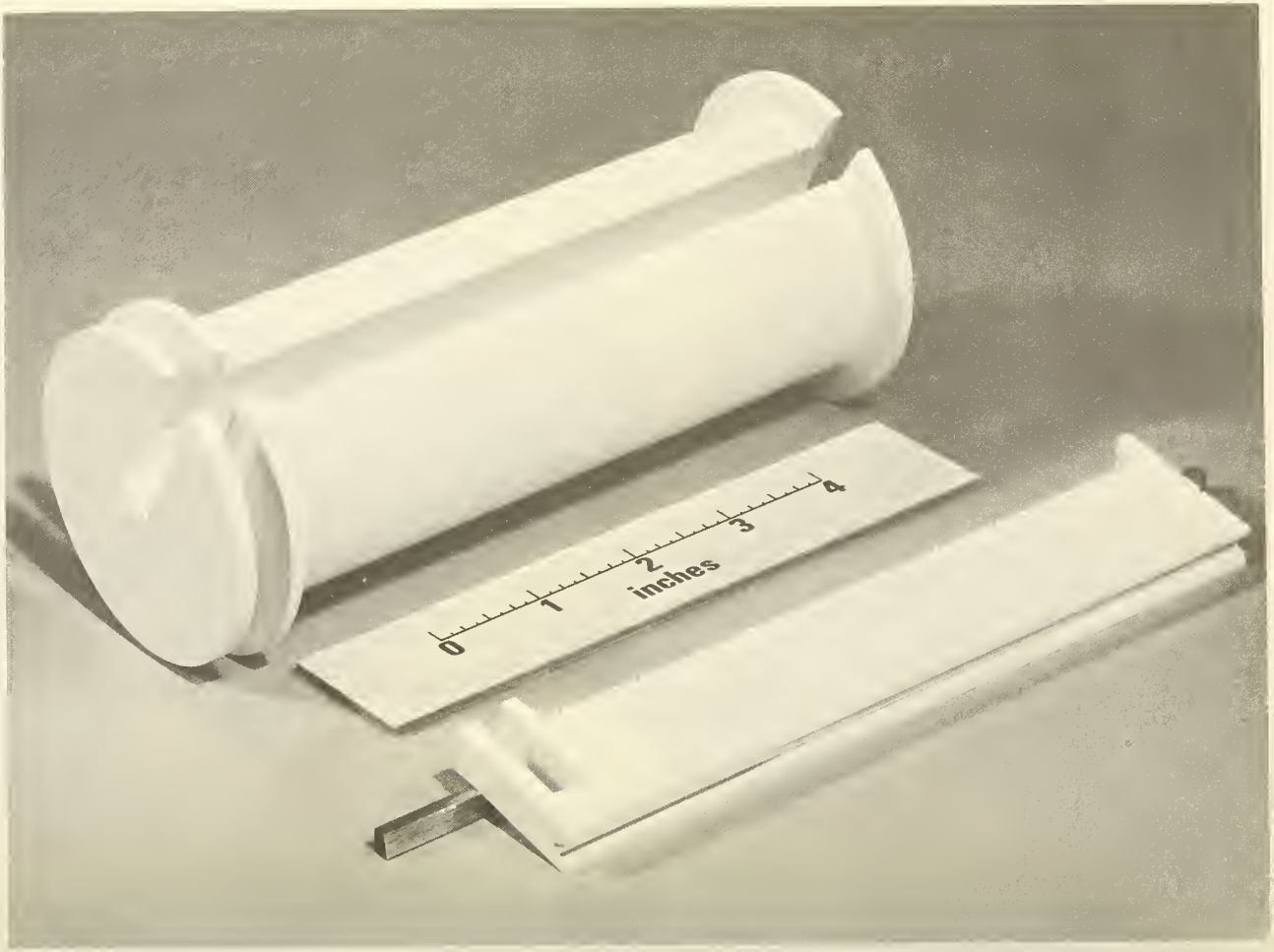

Figure 3.6. Exploded View of the Boron Nitride Heat Distributor.

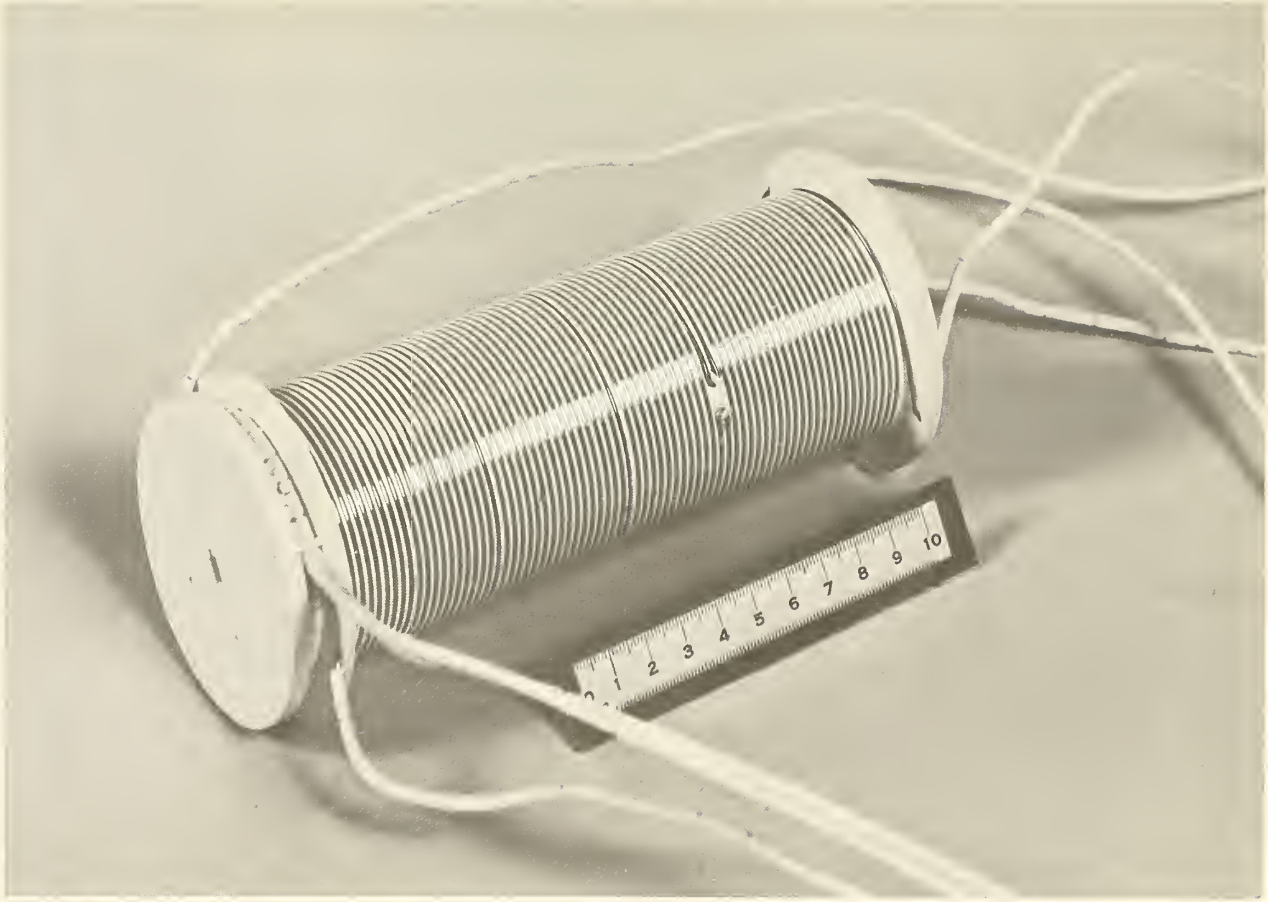

Figure 3.7. Photograph of the Assembled Boron Nitride Heat Distributor.

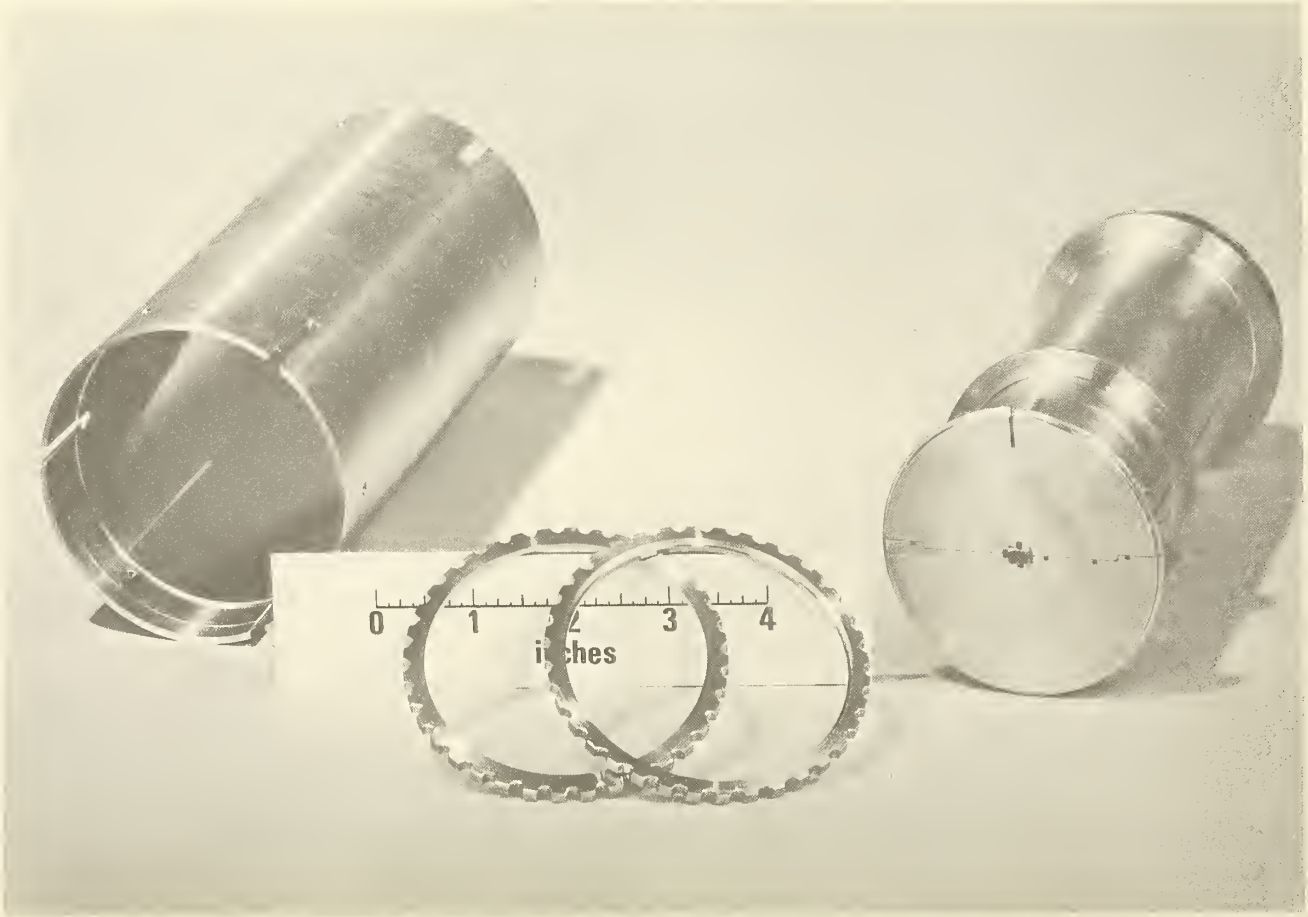

Figure 3.8. Exploded View of the Inconel Heat Distributor, Sleeve, and Locking Rings.

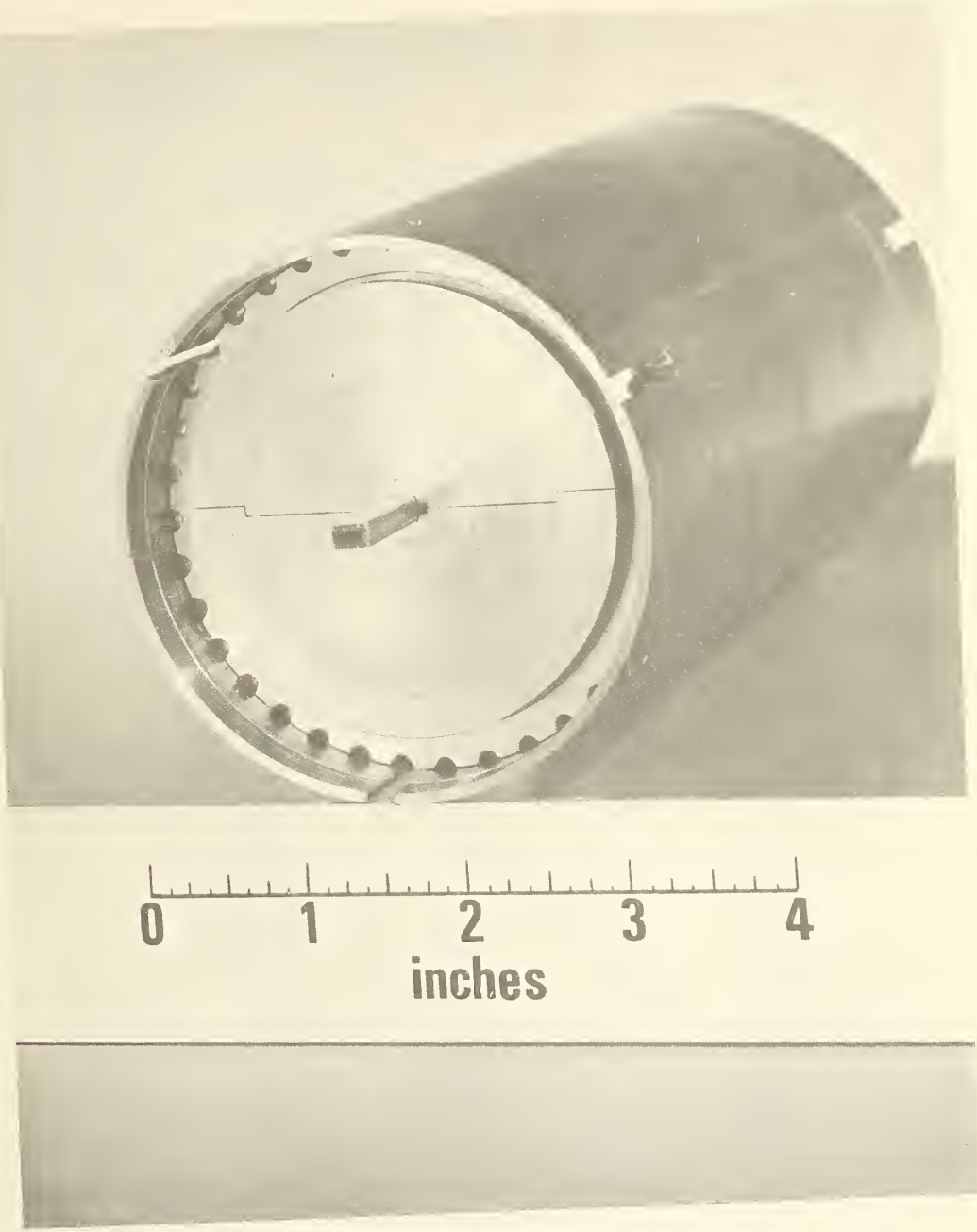

Figure 3.9. Photograph of the Heat Distributor Assembly.

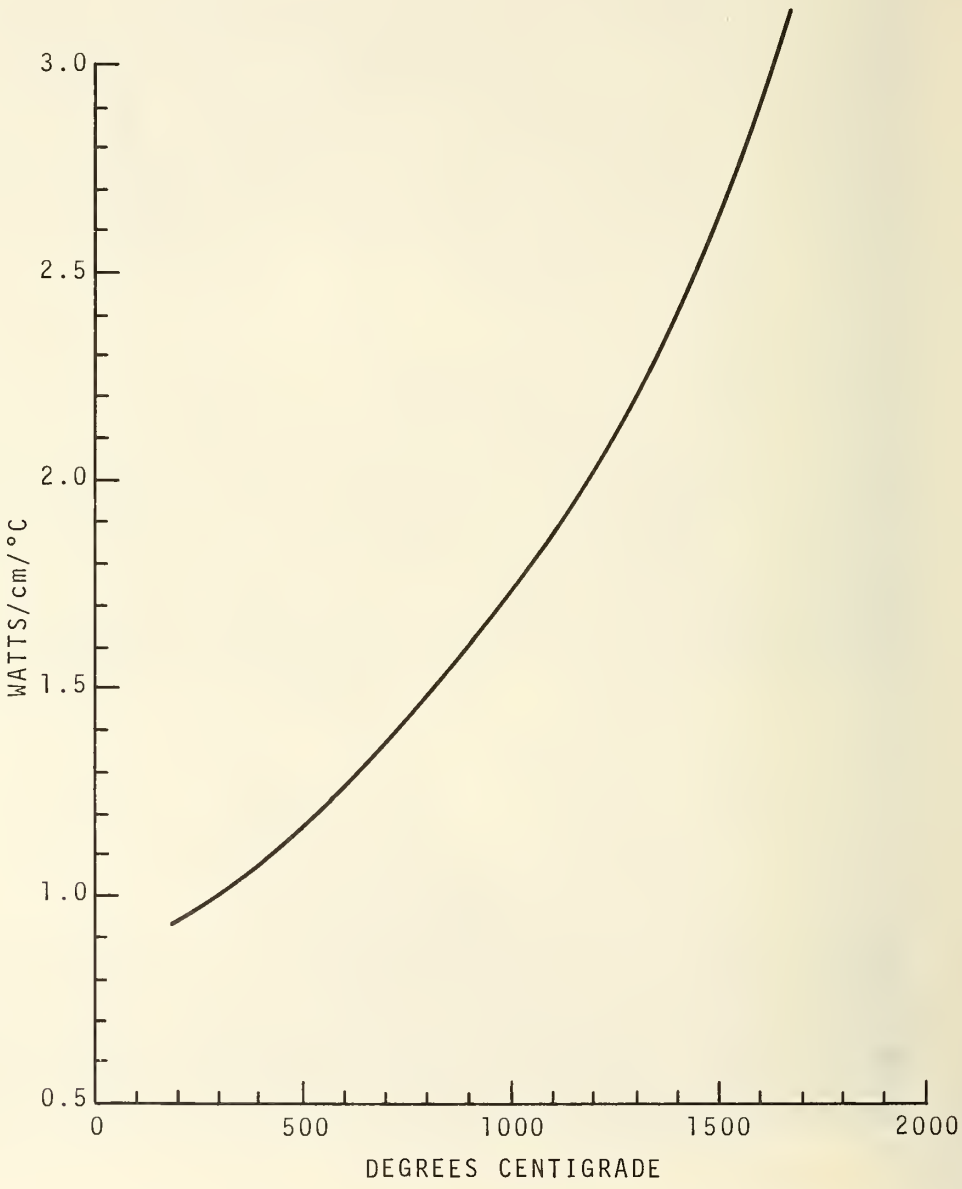

Figure 3.10. Thermal Conductivity Versus Temperature for Zirconium Oxide.

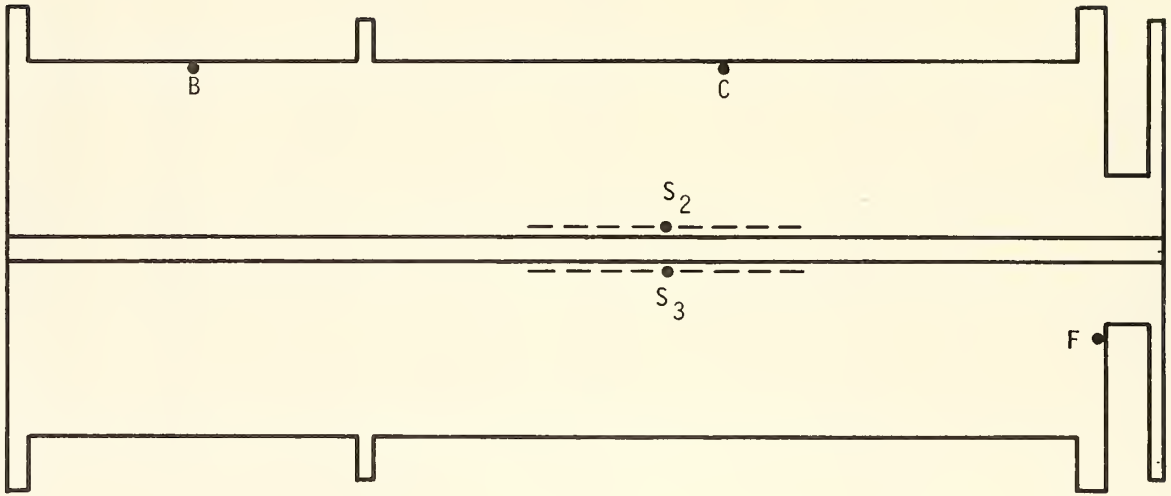

Figure 3.11. Thermocouple Junction Locations.

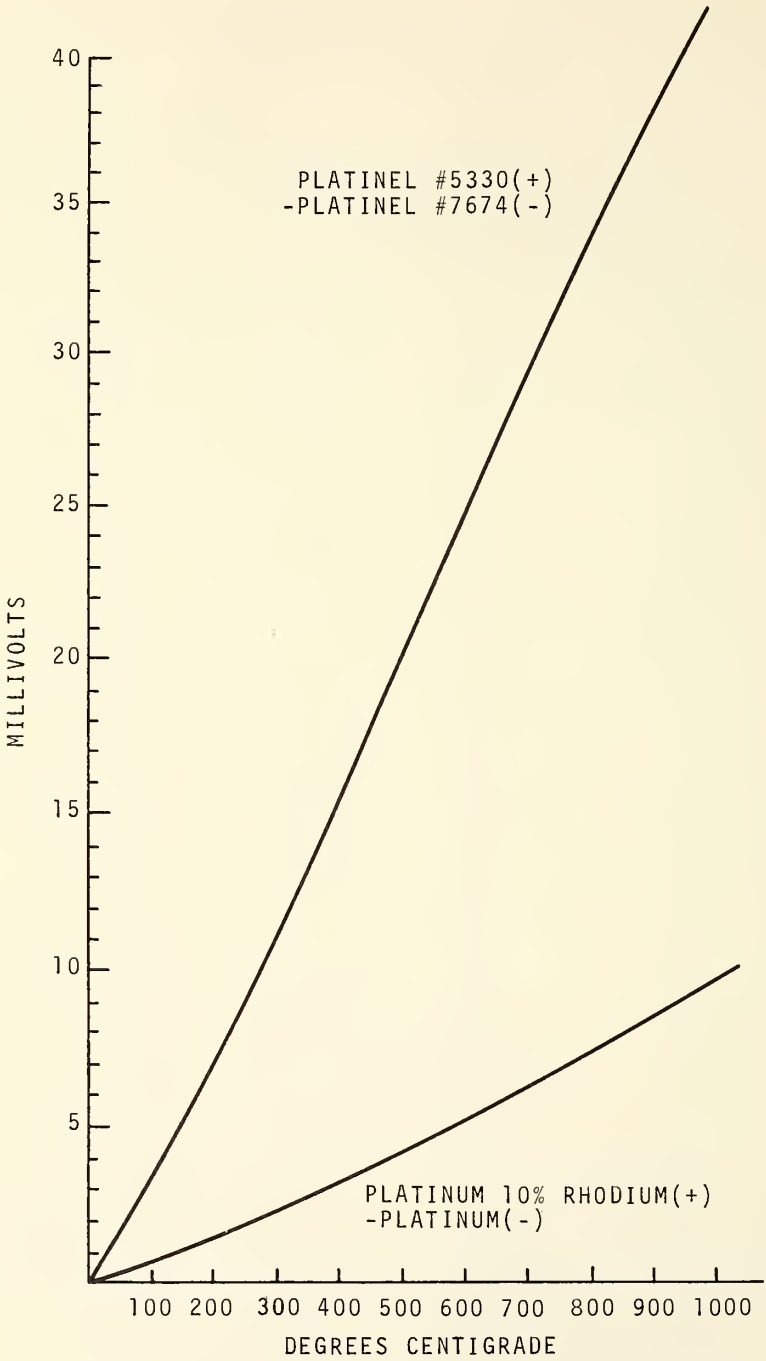

Figure 3.12. Thermal EMF Versus Temperature for Pt-Rh and Platinel Thermocouples.

FORM NBS-443
(REV. 4-11-63)

U.S. DEPARTMENT OF COMMERCE
NATIONAL BUREAU OF STANDARDS
WASHINGTON 25, D.C.

NATIONAL BUREAU OF STANDARDS

REPORT OF CALIBRATION

PLATINUM vs. PLATINUM-RHODIUM THERMOCOUPLE

Submitted by

National Bureau of Standards
Division 272, Section 60

The emf of the thermocouple was determined at 1064.43 °C (gold point), 961.93 °C (silver point), 630.74 °C, and 419.58 °C (zinc point) with the reference junctions at 0 °C. The values of emf found are given in Table 1. The uncertainties in these values are estimated not to exceed 3 microvolts.

Table 2 gives the values of the coefficients A, B, and C in the equation

$$E = A + Bt + Ct^2,$$

where E is the emf of the thermocouple in absolute microvolts and t is the temperature in degrees Celsius (IPTS-68). The equation may be used for interpolation in the range 630.74° to 1064.43 °C.

Table 3 gives values of emf from 0° to 1450 °C. The uncertainties in the values given are estimated not to exceed 5 microvolts in the range 0° to 1100 °C and then increase to not more than 30 microvolts at 1450 °C. These uncertainties are discussed in National Bureau of Standards Circular 590, Methods of Testing Thermocouples and Thermocouple Materials.

All temperatures in this report are given in degrees Celsius (IPTS-68). The International Practical Temperature Scale of 1968, IPTS-68, was adopted by the International Committee of Weights and Measures at its meeting in October, 1968, and is described in "The International Practical Temperature Scale of 1968," Metrologia, Vol. 5, No. 2, 35 (April 1969).

The calibration of a thermocouple is subject to change during use. The mangitude of the change depends upon such factors as the temperature, the length of time, and the conditions under which it is used. Factors

Work Order No.: 272-0242
Test No. : 3.1d/8432D
Completed : June 3, 1971 Page 1 of 2 pages

Figure 3.13. Sample Page from a Thermocouple Calibration Report.

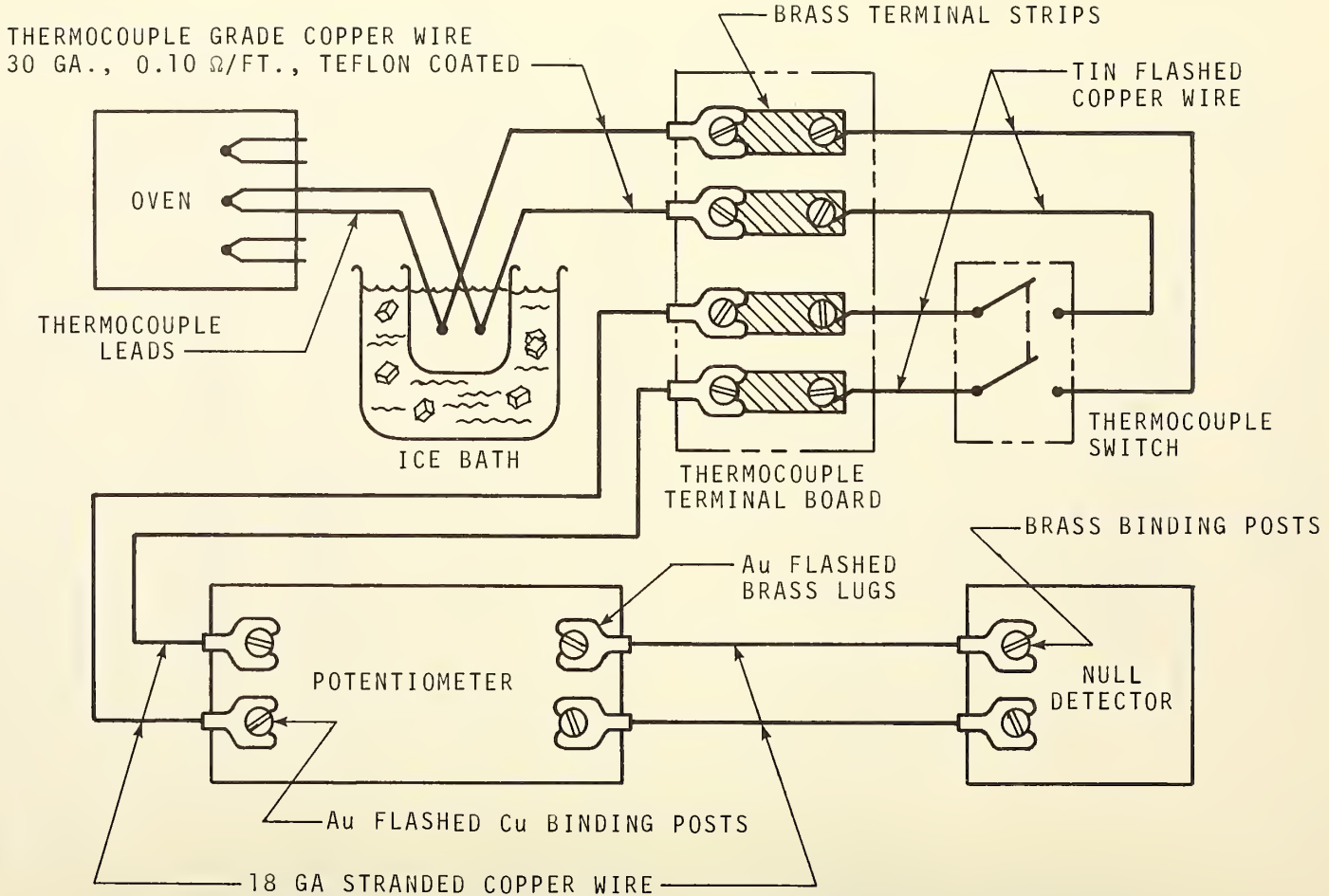

Figure 3.14. The Temperature Measurement System

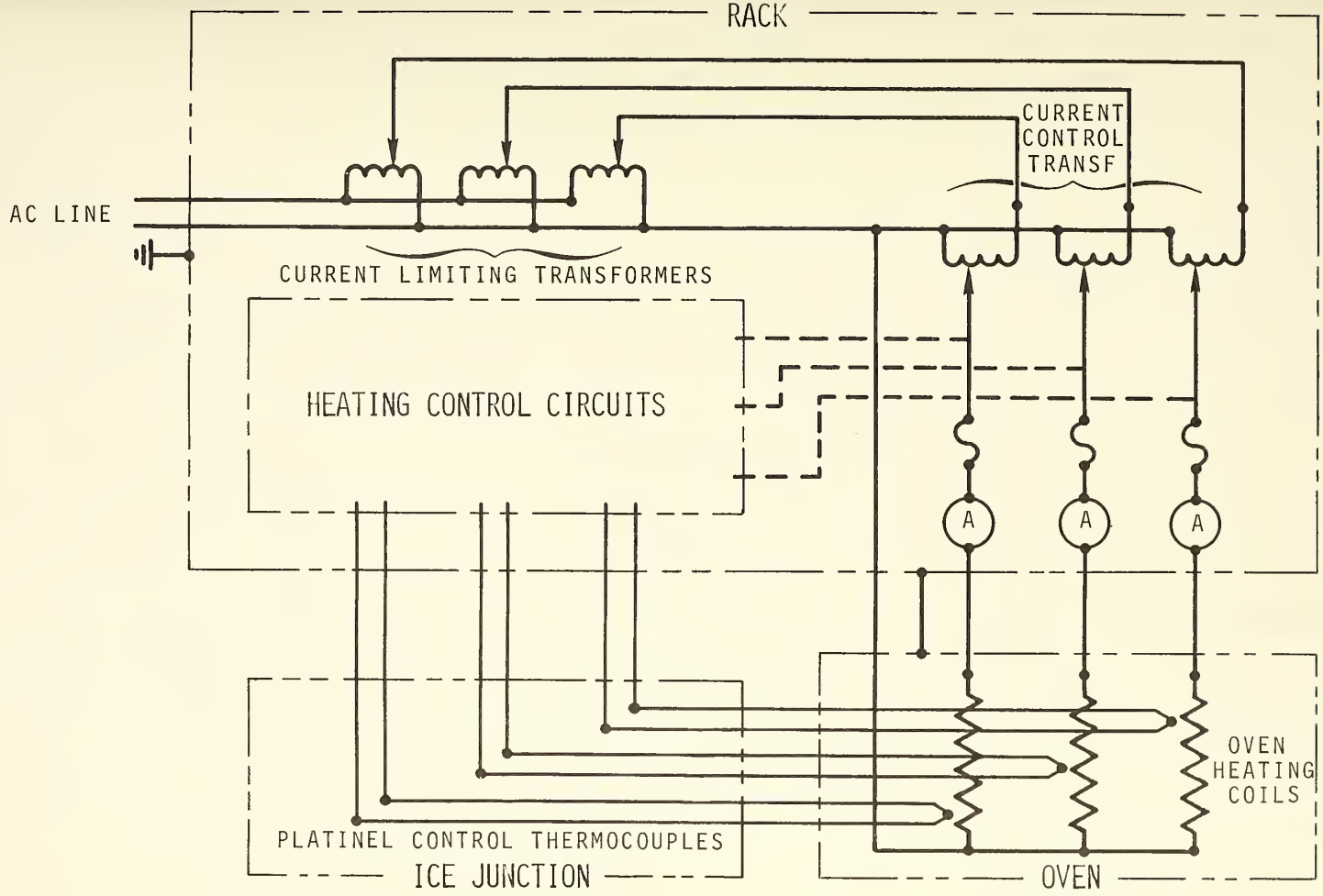

Figure 3.15. The Heating Control System.

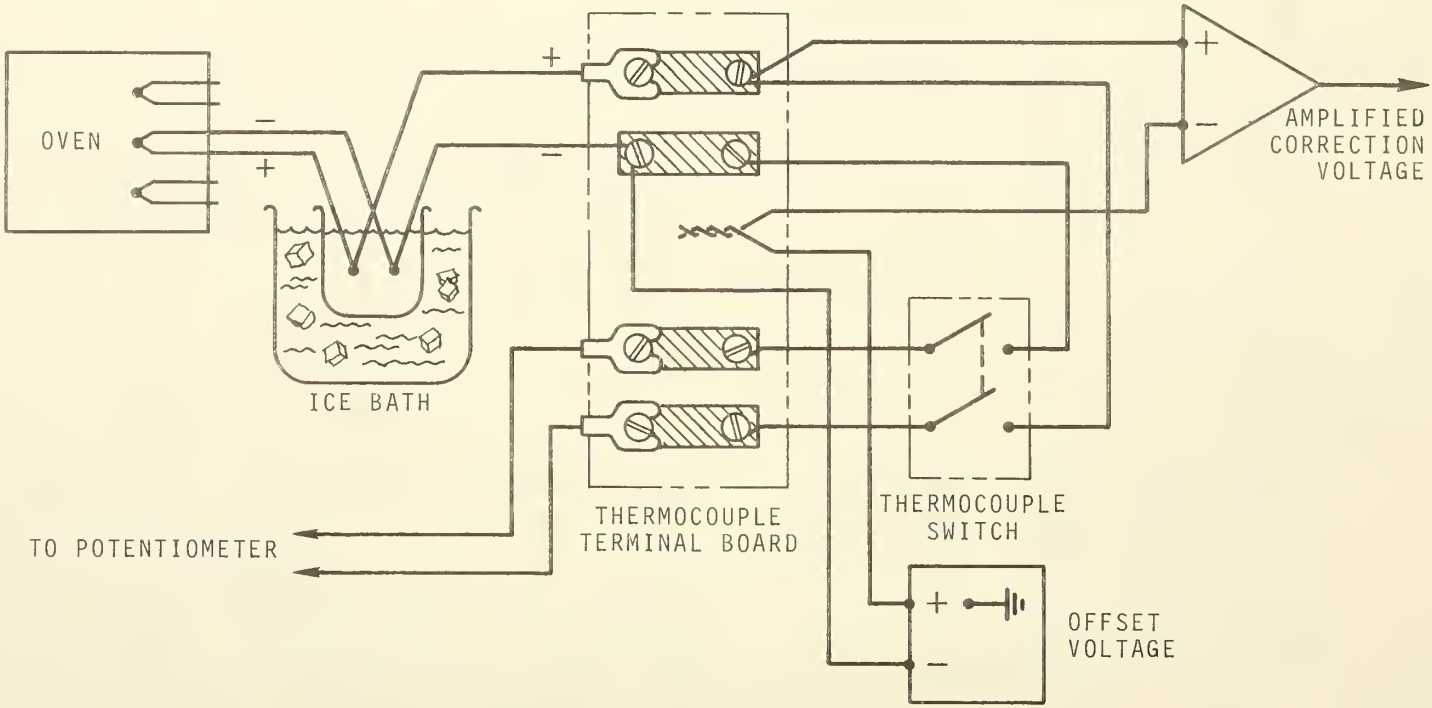

Figure 3.16. The Control Thermocouple Hookup.

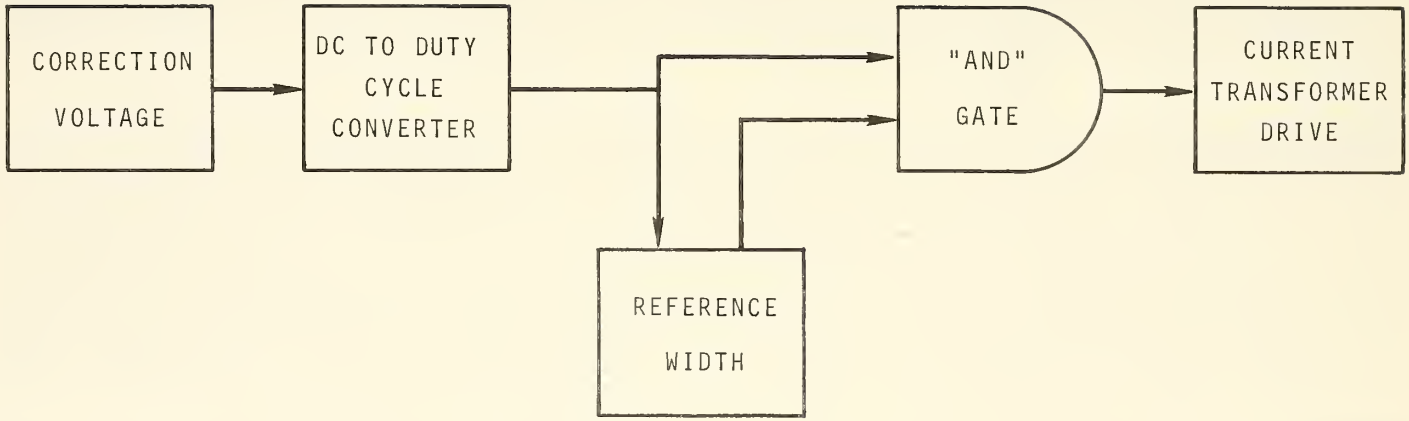

Figure 3.17. Operation of the Control Circuits.

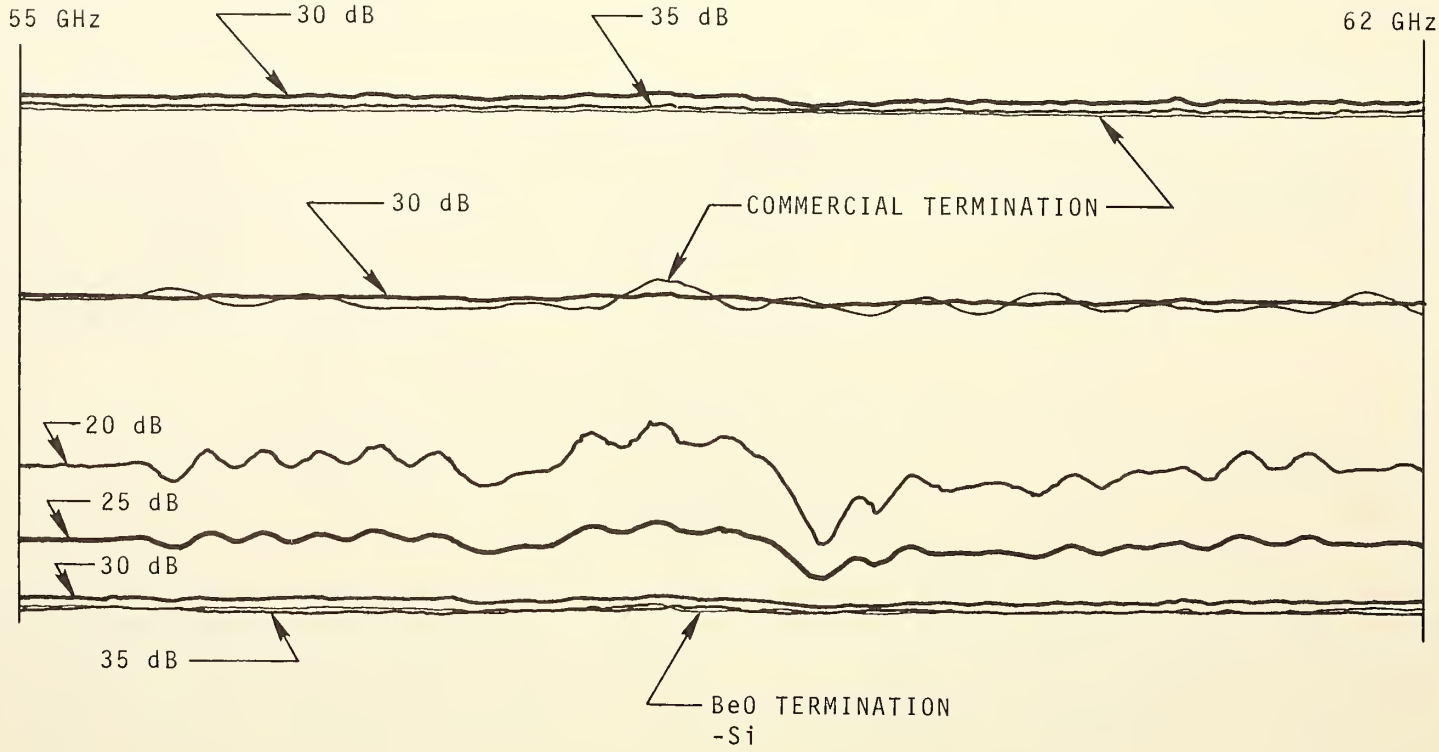

Figure 4.1. Conventional Swept Frequency Measurement of the BeO-Si Termination Reflection Coefficient.

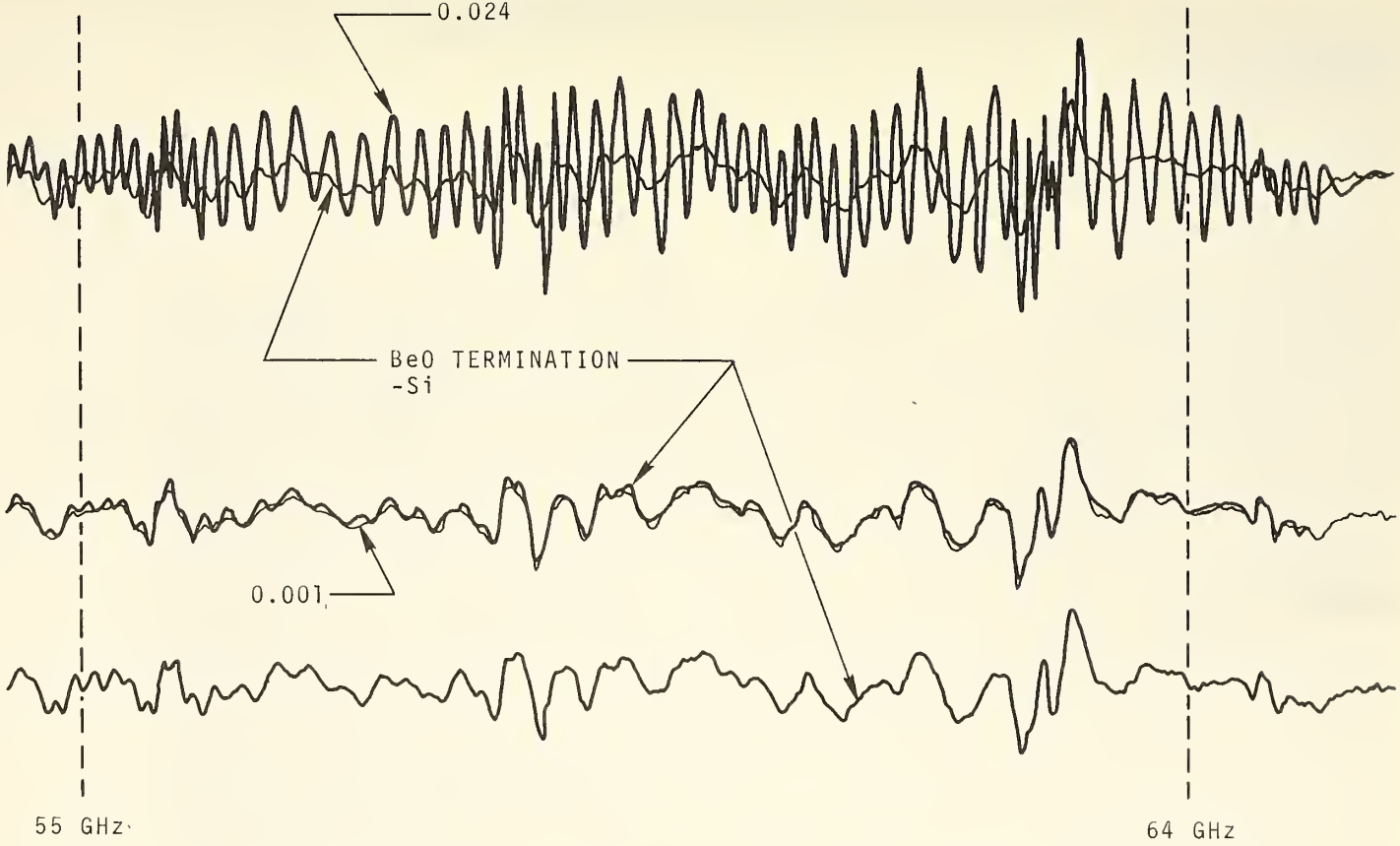

Figure 4.2. H-S Swept Frequency Measurement of the BeO-Si Termination Reflection Coefficient.

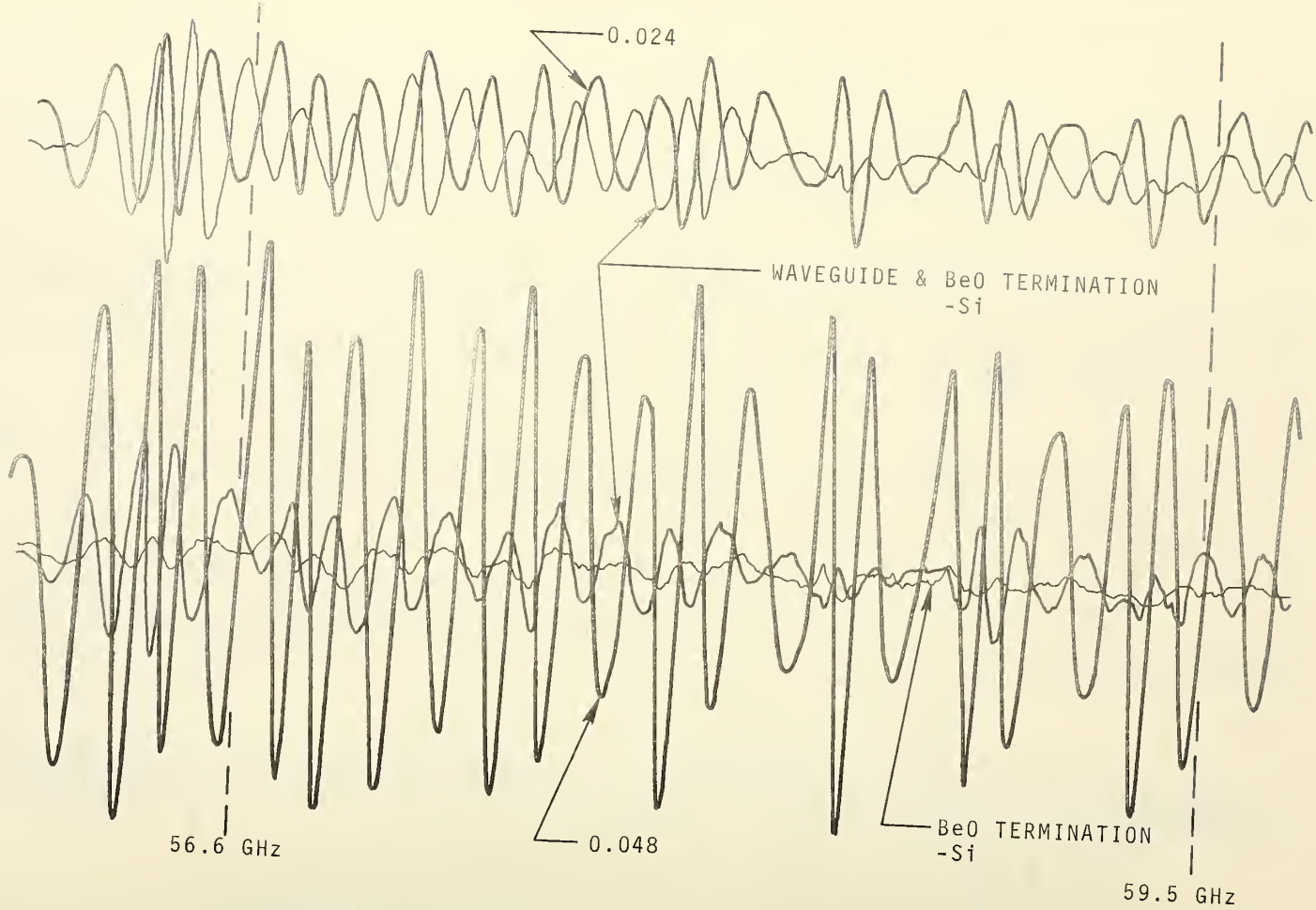

Figure 4.3. H-S Swept Frequency Measurement of the BeO-Si Termination and High-Temperature Waveguide Reflection Coefficient.

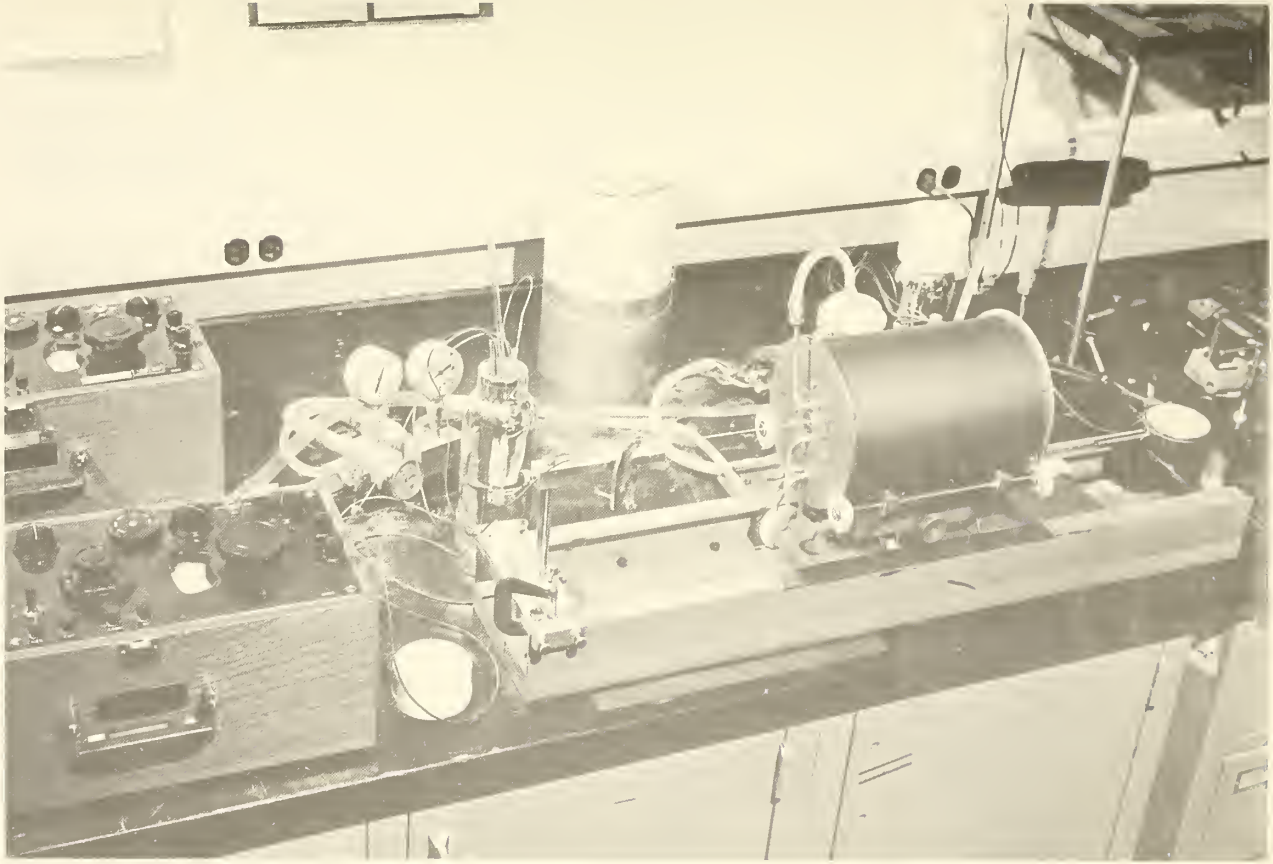

Figure 4.4. A Typical Temperature Distribution Measurement Set-up.

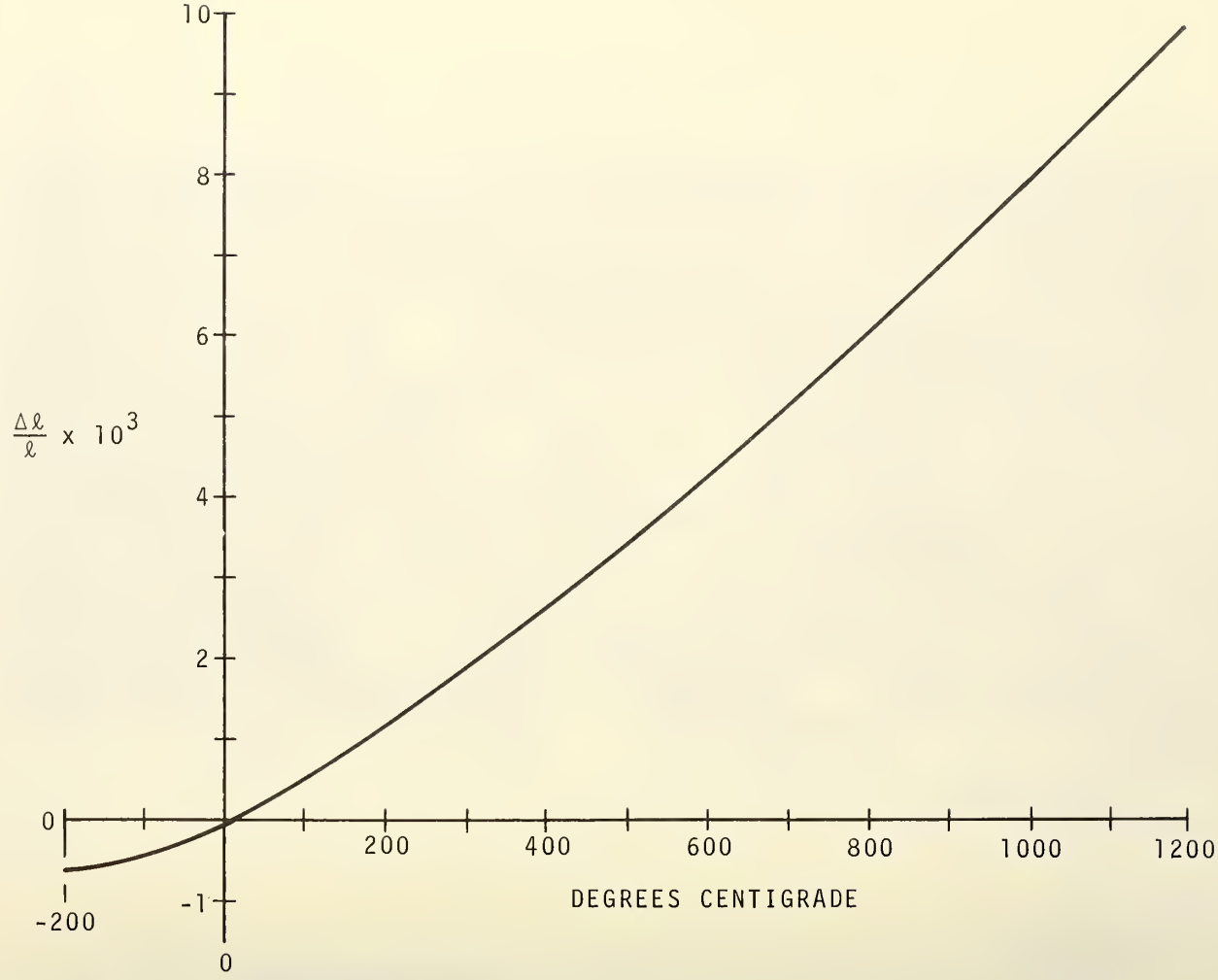

Figure 4.5. Expansion Coefficient of the Al_2O_3 Rod Versus Temperature.

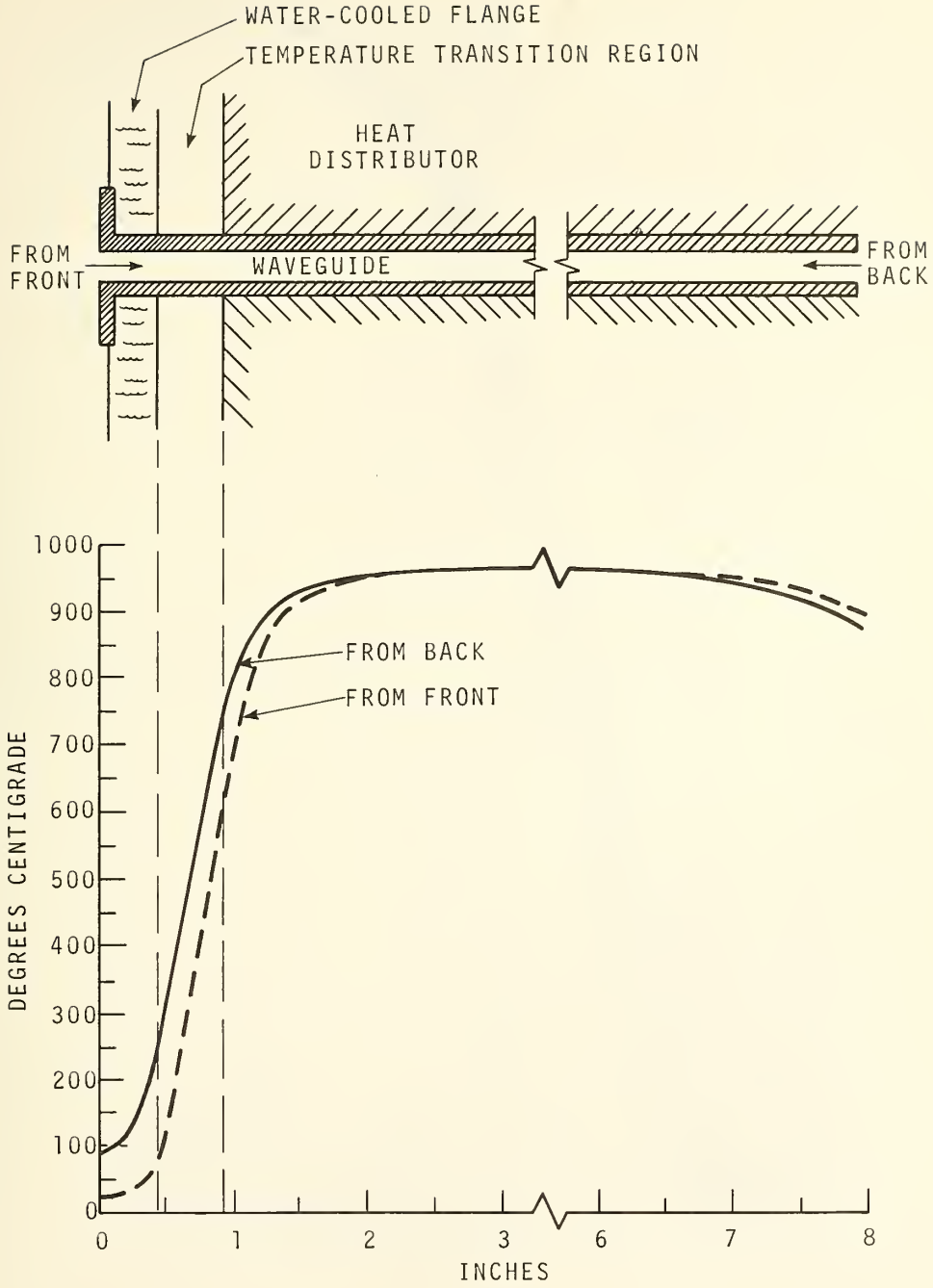

Figure 4.6. Temperature Distribution from Front and Back.

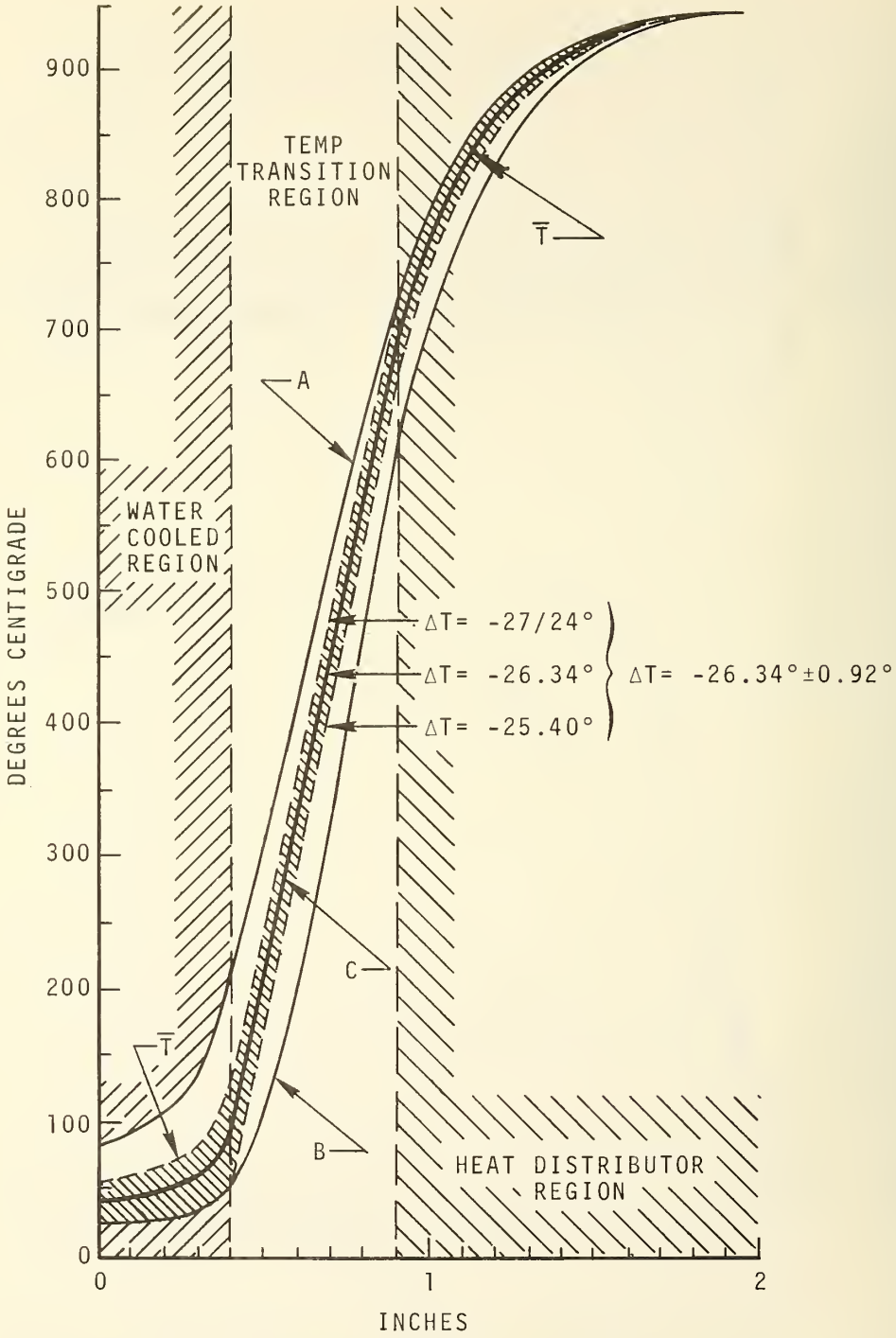

Figure 4.7. Temperature Distribution, Expanded Scale.

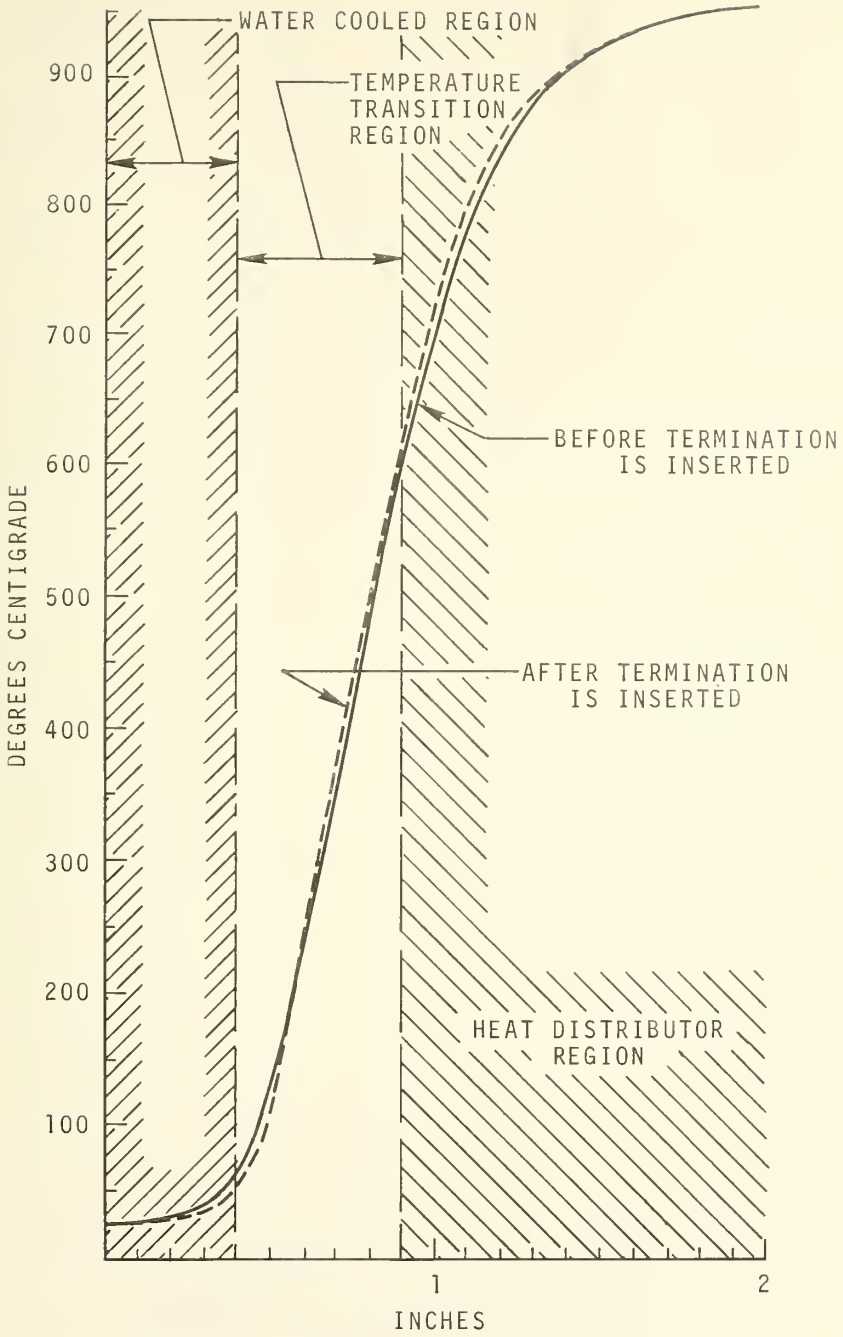

Figure 4.8. Distribution Just Before and After Termination is Inserted.

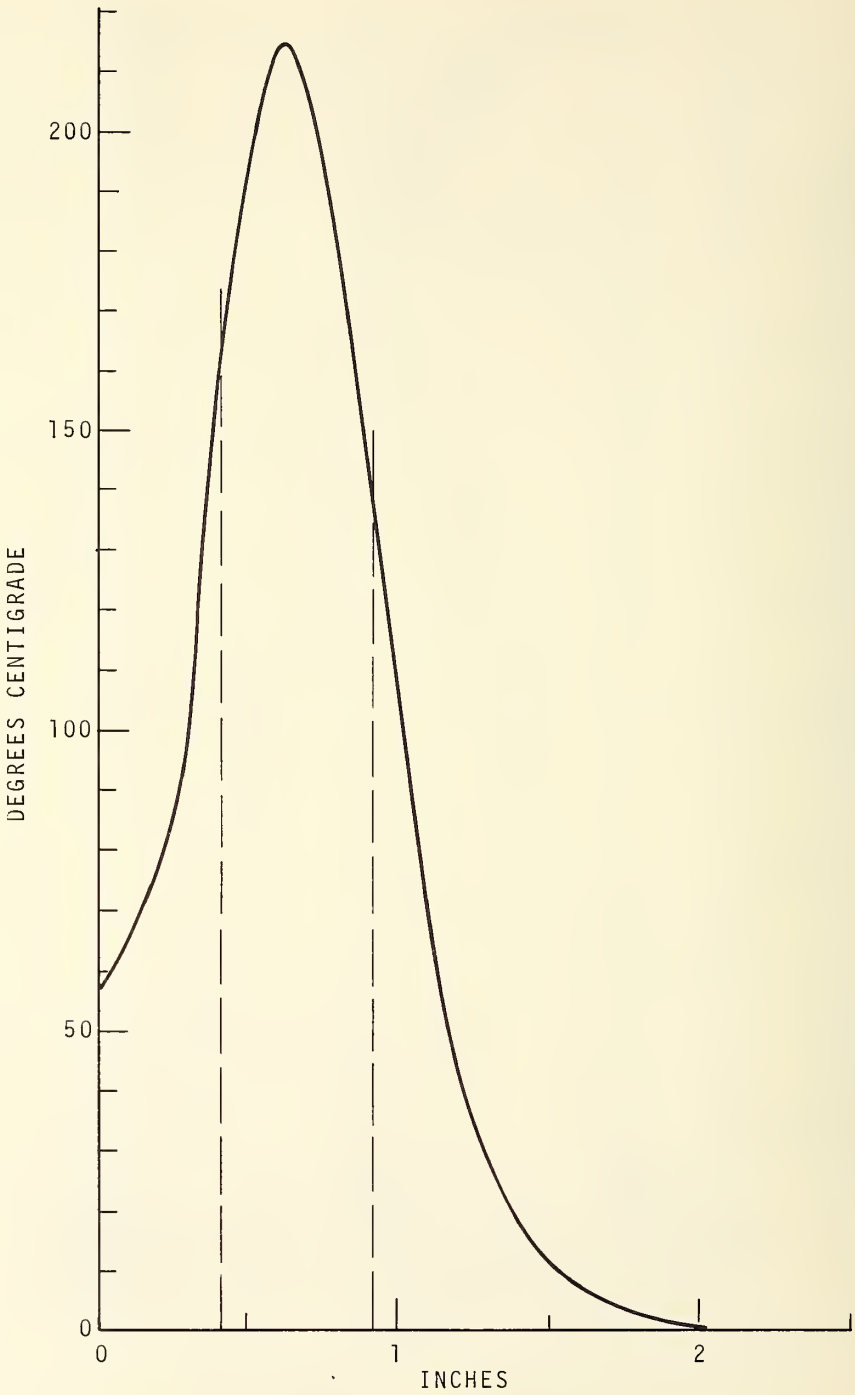

Figure 4.9. Temperature Differential Between Perturbed Distributions.

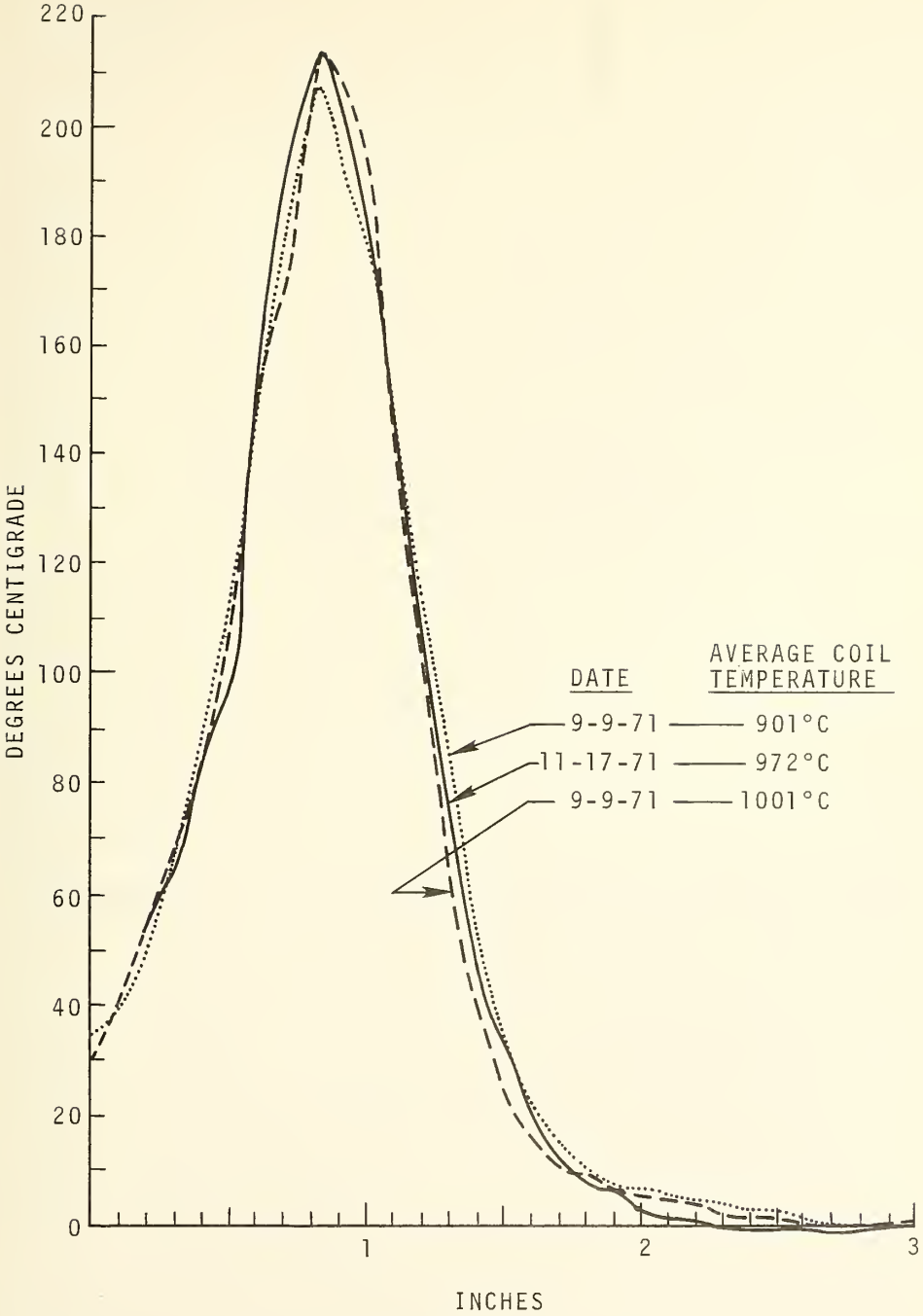

Figure 4.10. Temperature Differential at Different Coil Temperatures.

Distance in From Output Flange		
0"	0.8"	1.3"
22°C/1:29	397°C/1:34	828°C/1:41
21°C/1:50	395°C/1:57	828°C/2:03
21°C/2:07	396°C/2:14	828°C/2:19
21°C/2:25	396°C/2:36	828°C/2:45
21°C/3:52	396°C/3:03	828°C/3:13

Figure 4.11. Table of Temperature Measurement Repeatability Tests.

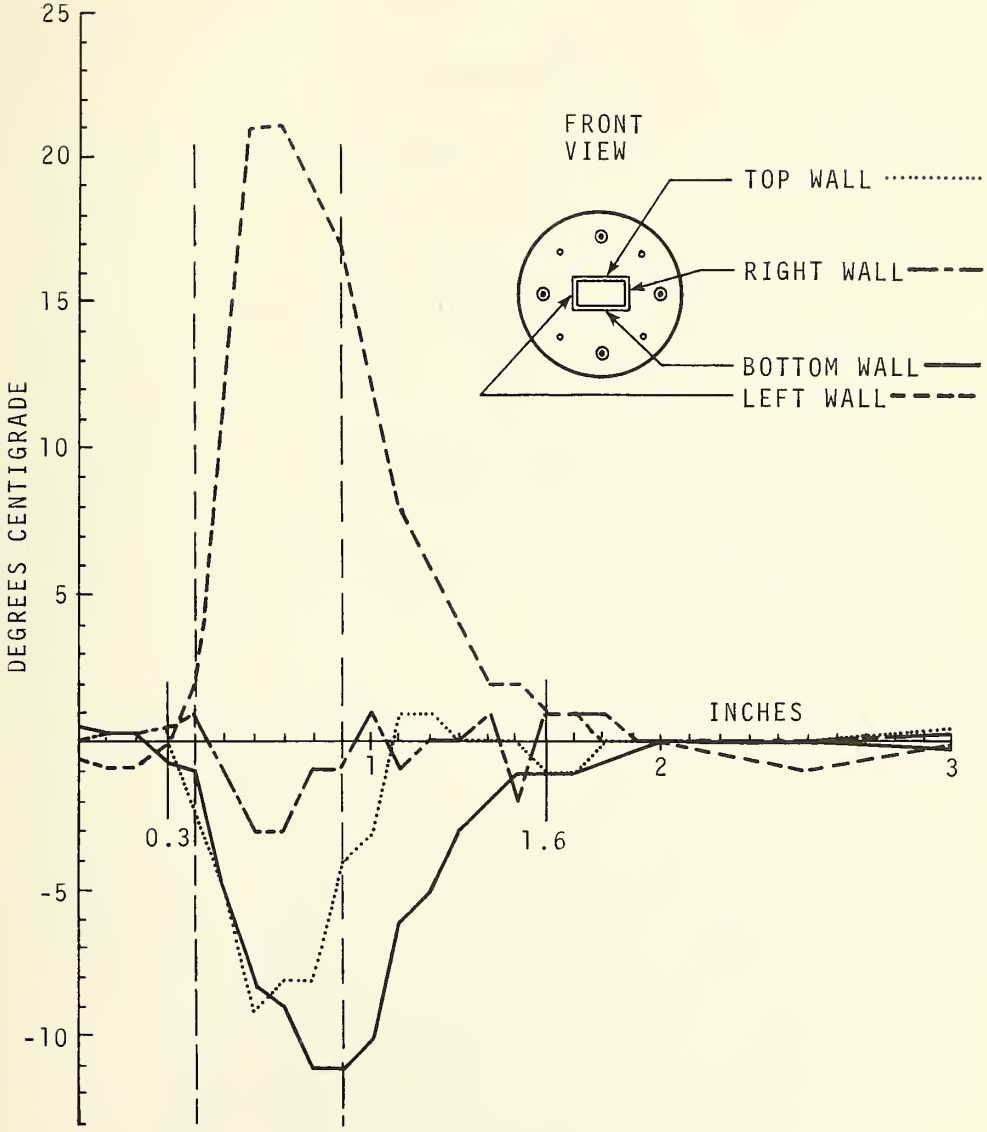

Figure 4.12. Temperature Differential Curves Along the Four Inside Waveguide Walls.

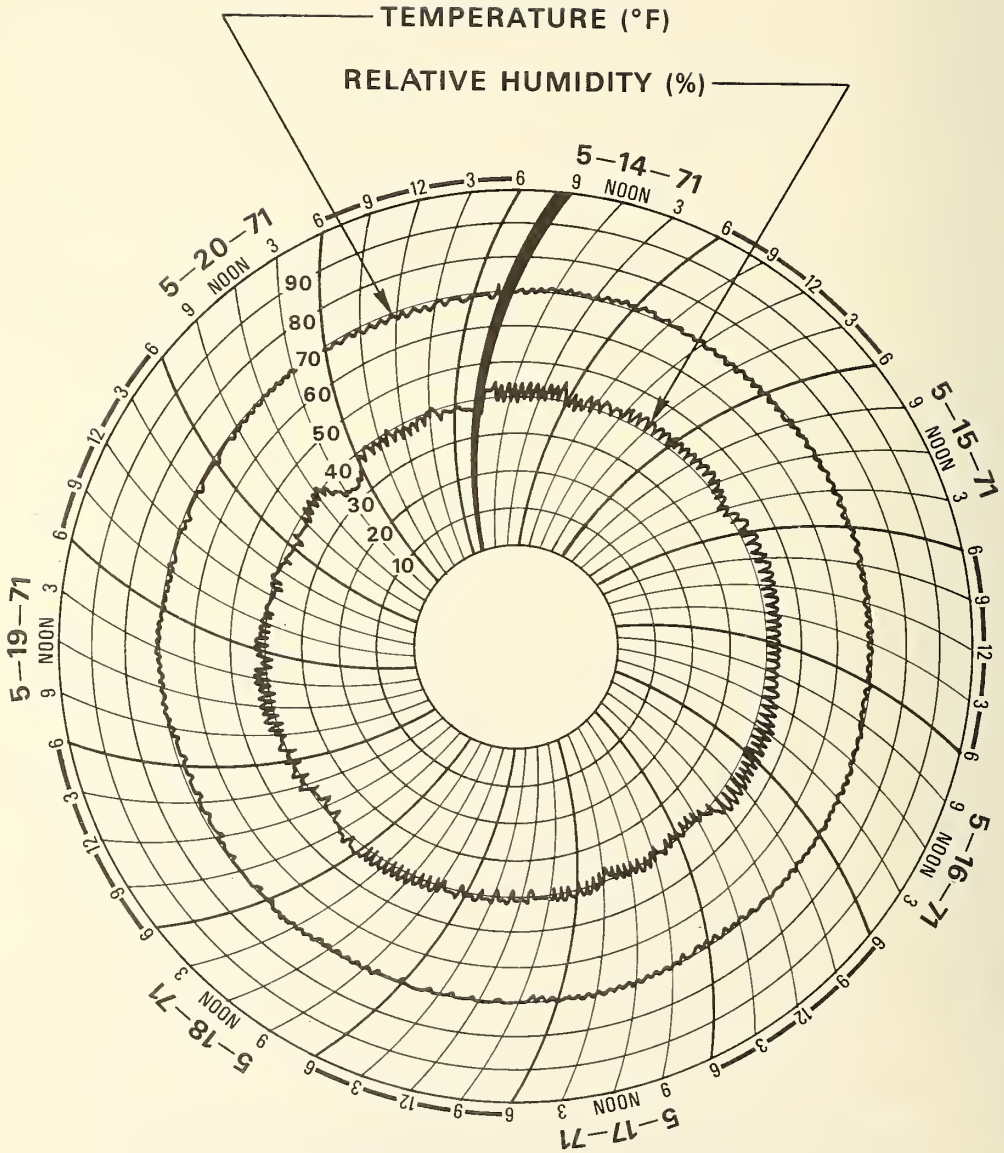

Figure 4.13. The Laboratory Environment

```
A0= 4.24485+000
A1= 3.48204-003
A2=-1.33800-006
A3= 3.22450-010

 F=  5.5000+001      A=1.4800-001      DA=1.00-003      B=7.4000-002      DB=1.00-003
 C= 3.21579-002      TM= 9.62000+002      L=  2
 AR1= 8.868-006      AR2= 1.324-009      AR3= 1.00020+000

  X          T          X          T          X          T          X          T          X          T
 0.00    9.6200+002    0.50    9.6200+002    1.00    9.5900+002    1.50    9.5100+002    1.60    9.4800+002
 1.70    9.4400+002    1.80    9.3800+002    1.90    9.3100+002    2.00    9.2200+002    2.10    9.0800+002
 2.20    8.9000+002    2.30    8.6300+002    2.40    8.2400+002    2.50    7.6600+002    2.60    6.9700+002
 2.70    5.7700+002    2.80    4.5600+002    2.90    3.3600+002    3.00    2.1500+002    3.10    9.5000+001
 3.20    6.2000+001    3.30    5.2000+001    3.40    4.5000+001    3.50    4.0000+001    0.00    0.0000+000

ATTEN= 6.7953-001          DELTA T=-2.6343+001

                  DTM        DTO        DDX        DR         DDT        DDO        DDB        DC
INPUT DATA     4.00-001   5.00-001   0.00+000   1.00-001   0.00+000   2.50-001   0.00+000   2.46-002
UNCERTAINTY    3.42-001   7.24-002   0.00+000   2.34-002   0.00+000   0.00+000   0.00+000   6.37-001

TOTAL UNCERTAINTY =  1.07+000
```

Figure D. 1. Sample Printout of the Output & Error Calculations.

INPUT TEMPERATURE DISTRIBUTION(FROM REFERENCE POSITION ON SCALE INTO OVEN)

0.000	40.0	0.100	45.0	0.200	52.0	0.300	62.0
0.400	95.0	0.500	215.0	0.600	336.0	0.700	456.0
0.800	577.0	0.900	697.0	1.000	766.0	1.100	824.0
1.200	863.0	1.300	890.0	1.400	908.0	1.500	922.0
1.600	931.0	1.700	938.0	1.800	944.0	1.900	948.0
2.000	951.0	2.500	959.0	3.000	962.0	3.500	962.0

DISTANCE IN VS. THERMOCOUPLE DISTANCE IN

0.000	0.000	0.100	0.104	0.200	0.207	0.300	0.311
0.400	0.412	0.500	0.513	0.600	0.613	0.700	0.714
0.800	0.815	0.900	0.915	1.000	1.016	1.100	1.117
1.200	1.217	1.300	1.318	1.400	1.419	1.500	1.519
1.600	1.619	1.700	1.720	1.800	1.820	1.900	1.920
2.000	2.020	2.500	2.520	3.000	3.020	3.500	3.520

Figure E.1. Sample Output from Program "TEX 998."

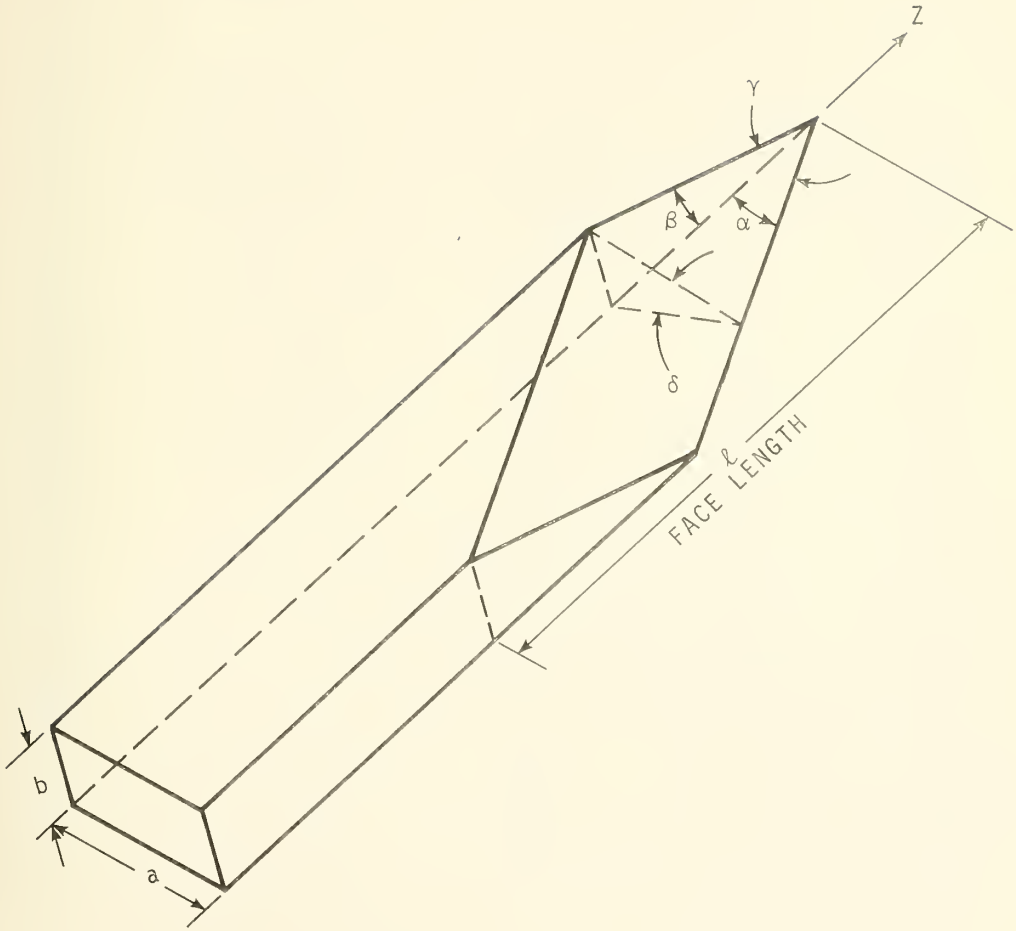

Figure F.1. The Waveguide Termination Geometry.

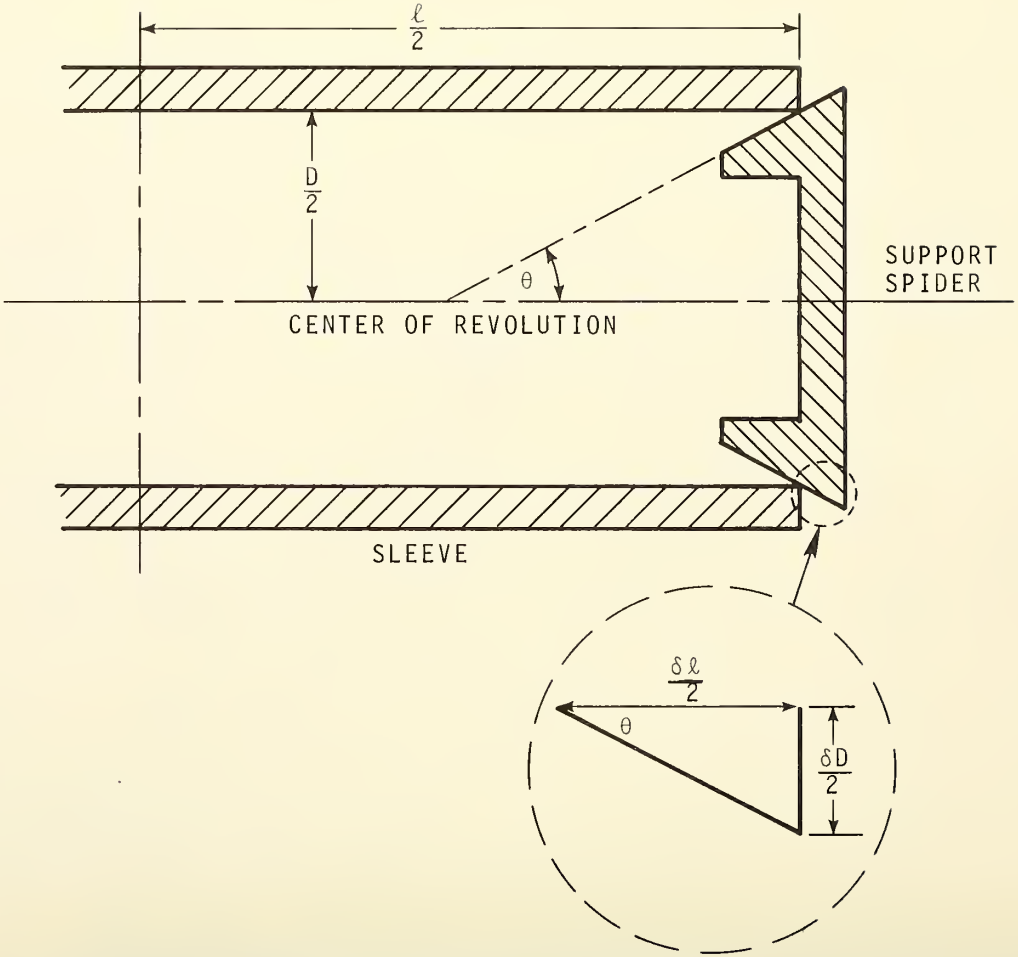

Figure J.1. The Support Spider.

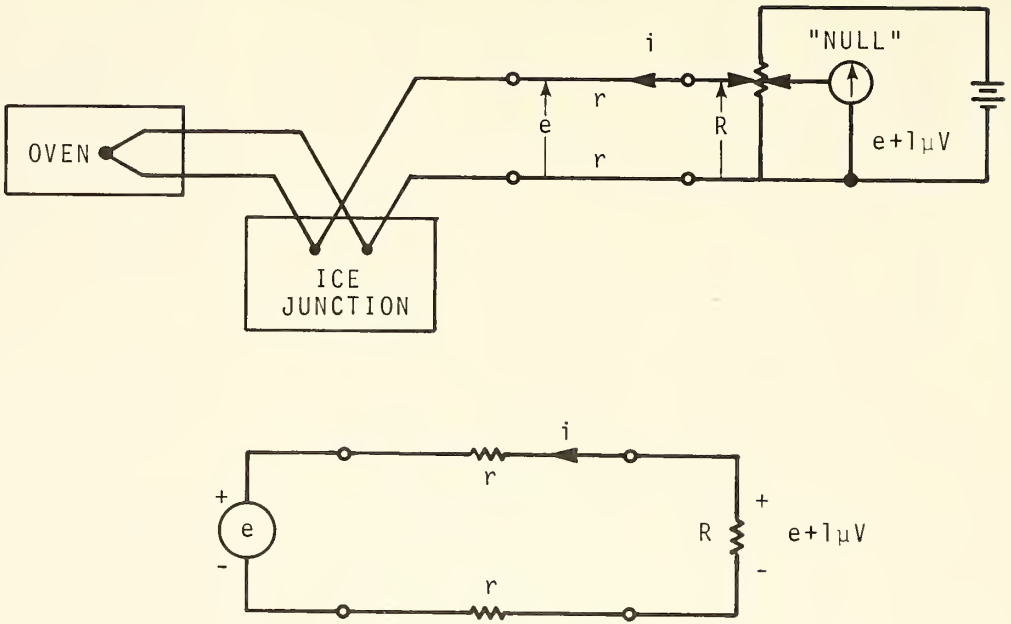

Figure L.1. Schematic for Lead Error Calculation.

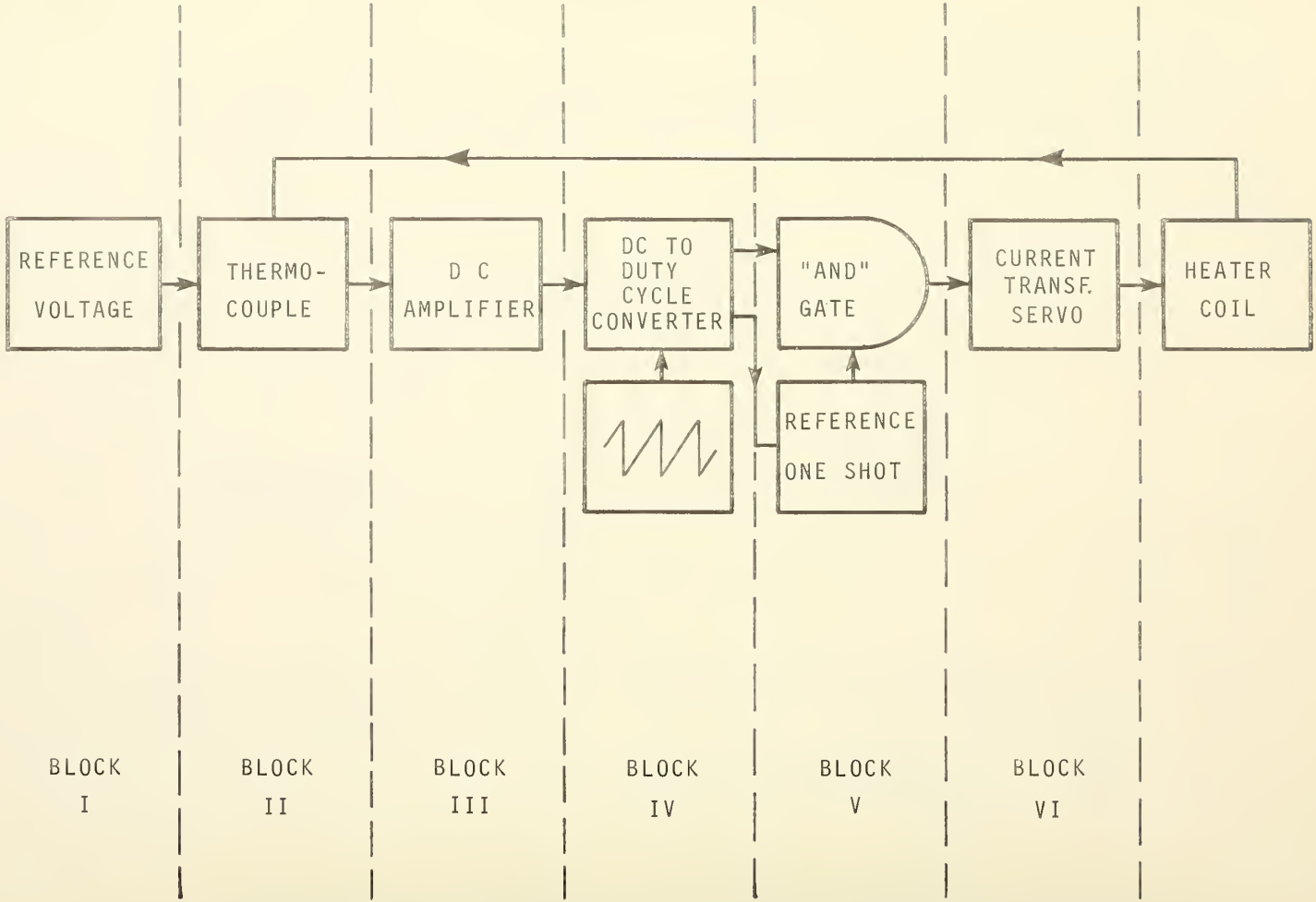

Figure M.1. Block Diagram of the Temperature Control System.

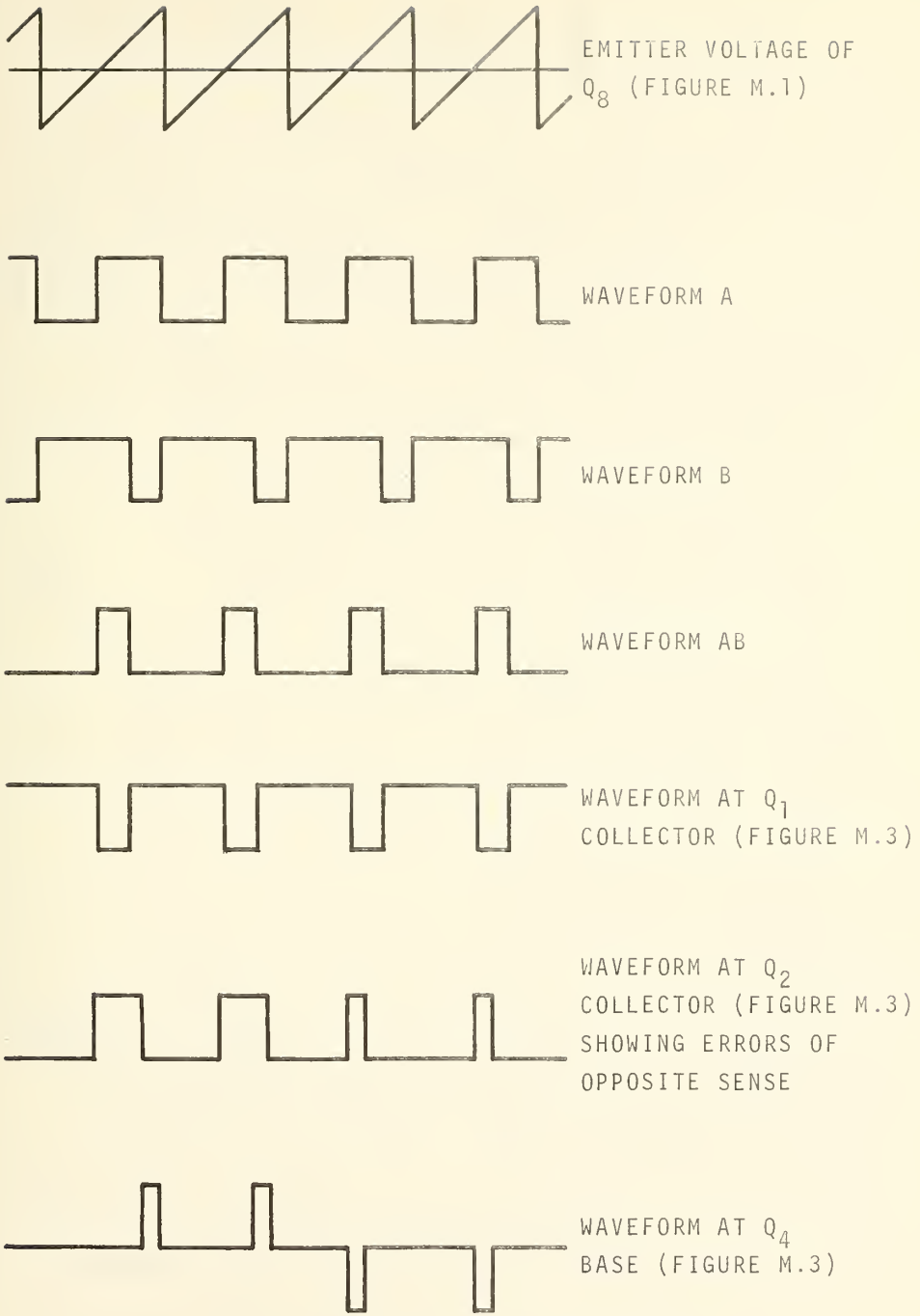

Figure M.2. Circuit Waveforms.

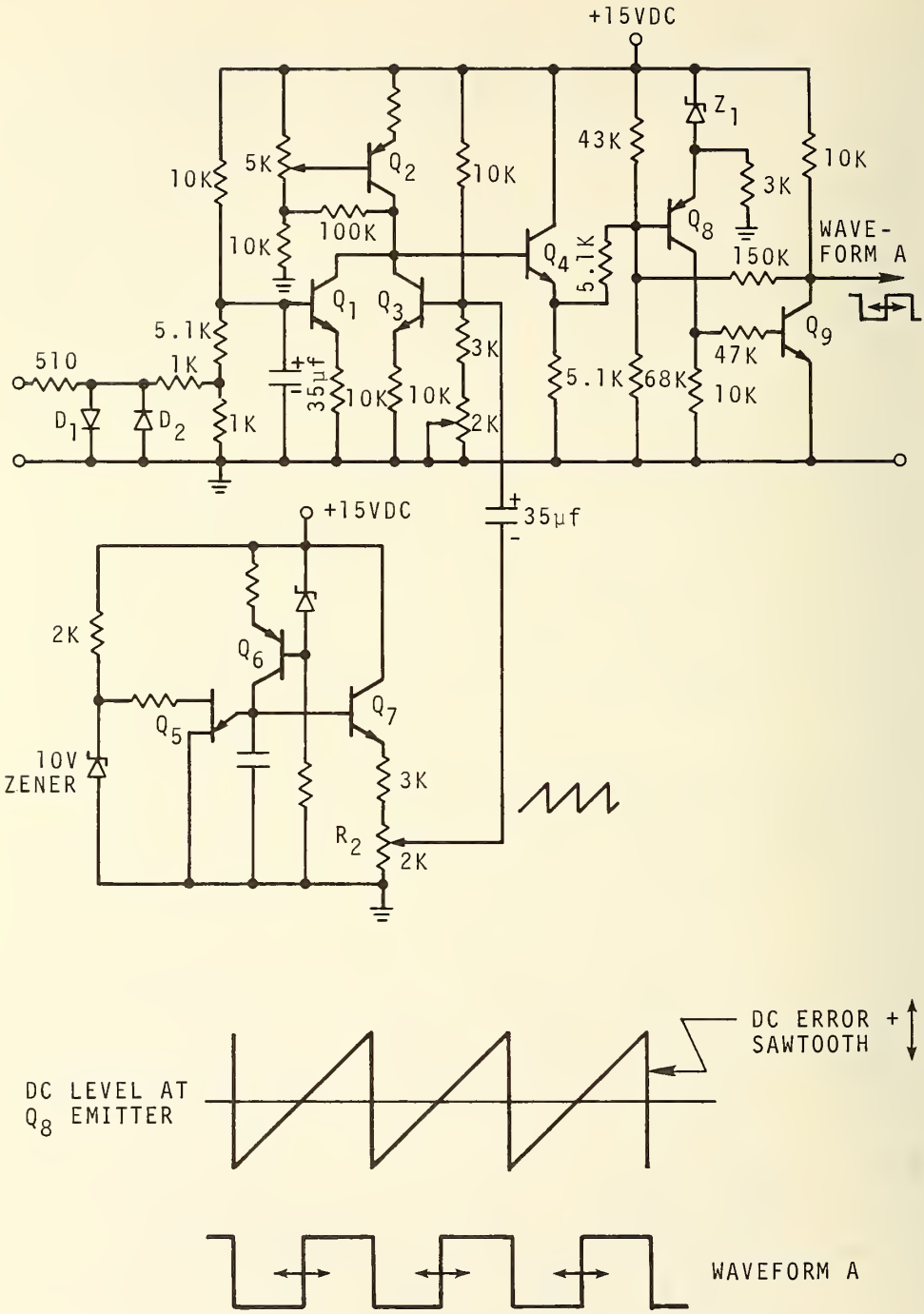

Figure M. 3. Circuit Diagram for Block IV.

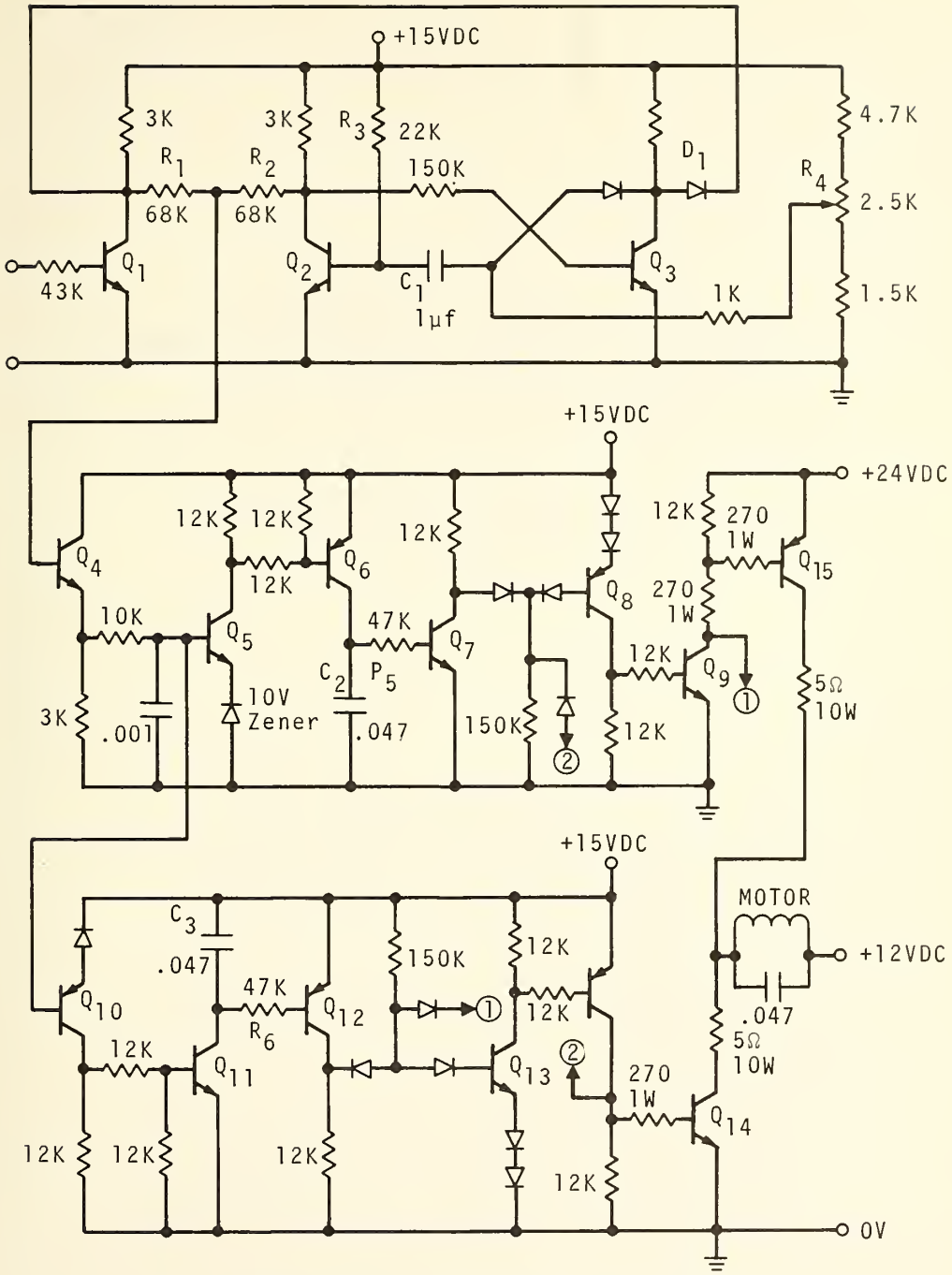

Figure M.4. Circuit Diagram for Block VI.

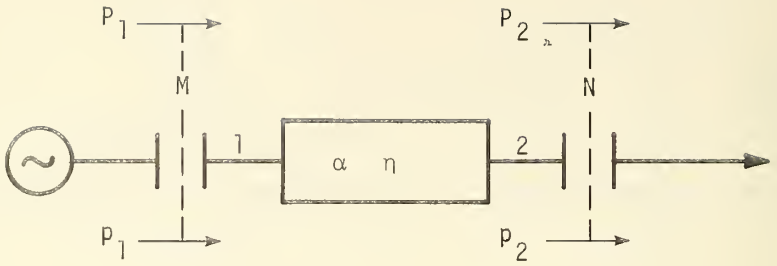

Figure N.1. Generator attached to a Two-Port Transducer.

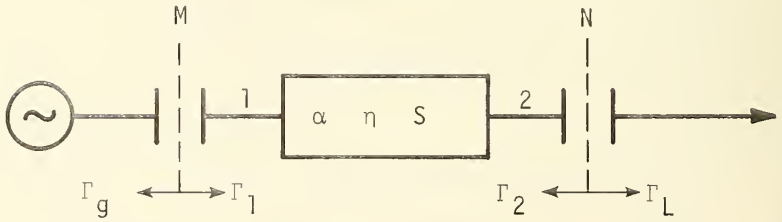

Figure N.2. Scattering Parameter Description.

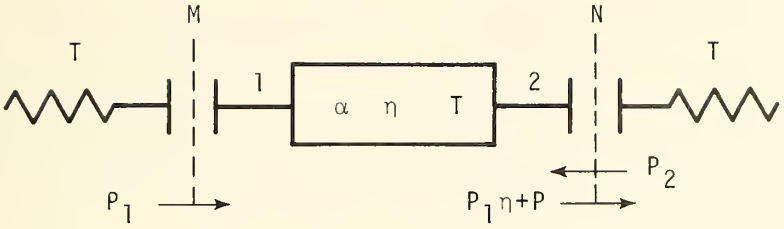

Figure N. 3. A Noisy Two-Port.

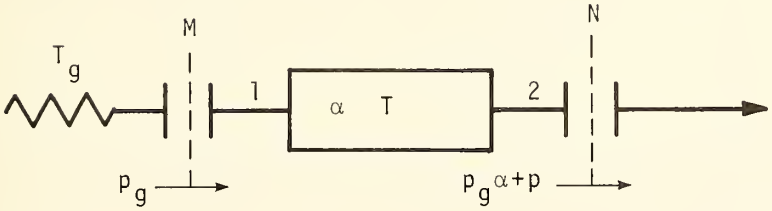

Figure N. 4. Illustration for (N. 1).

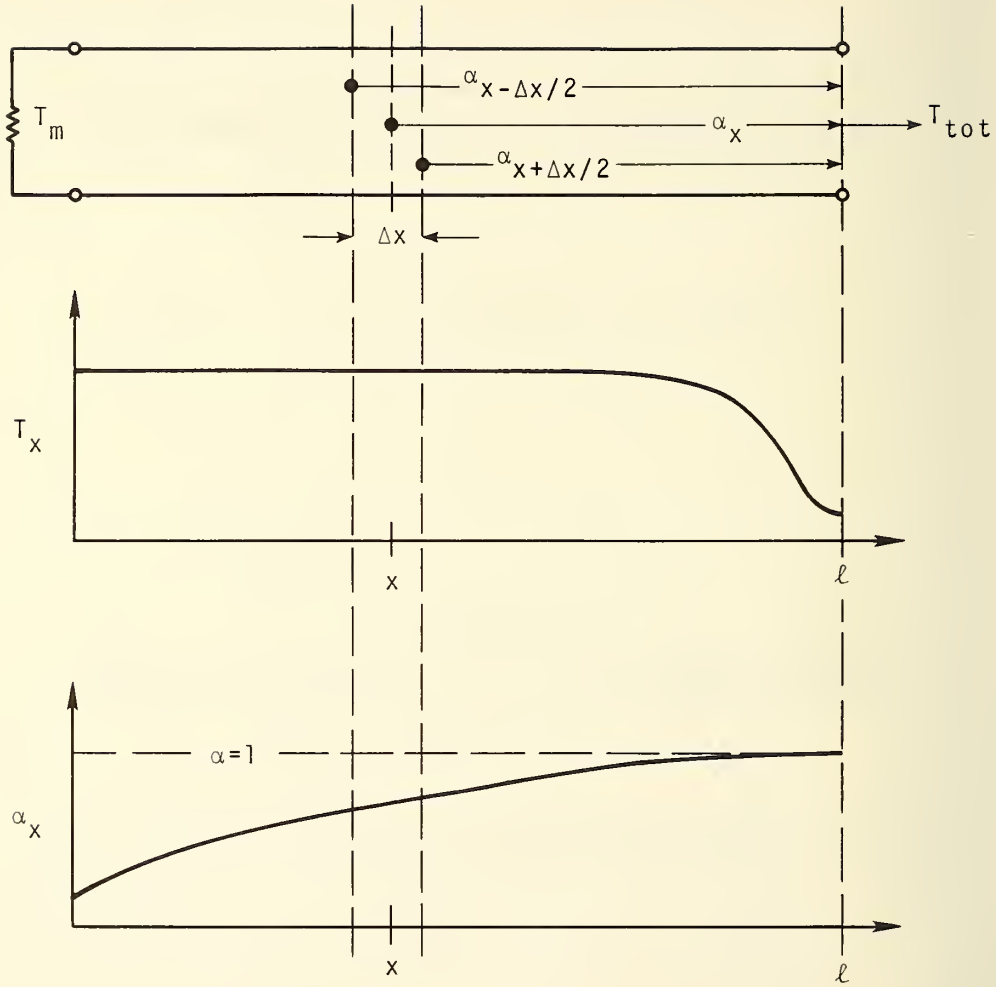

Figure N.5. A Thermal Noise Source.

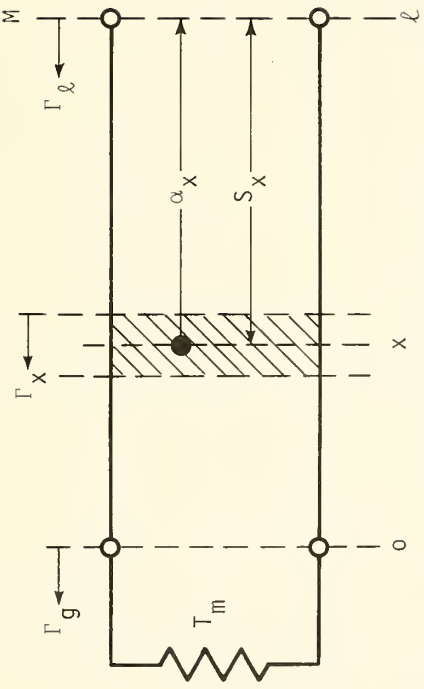

Figure N.6. A Uniform, Reflectionless Line.

8. DRAWINGS

1. Oven Assembly
2. High Temperature Resistive Termination
3. Oven Details (Iconel Heat Distributor)

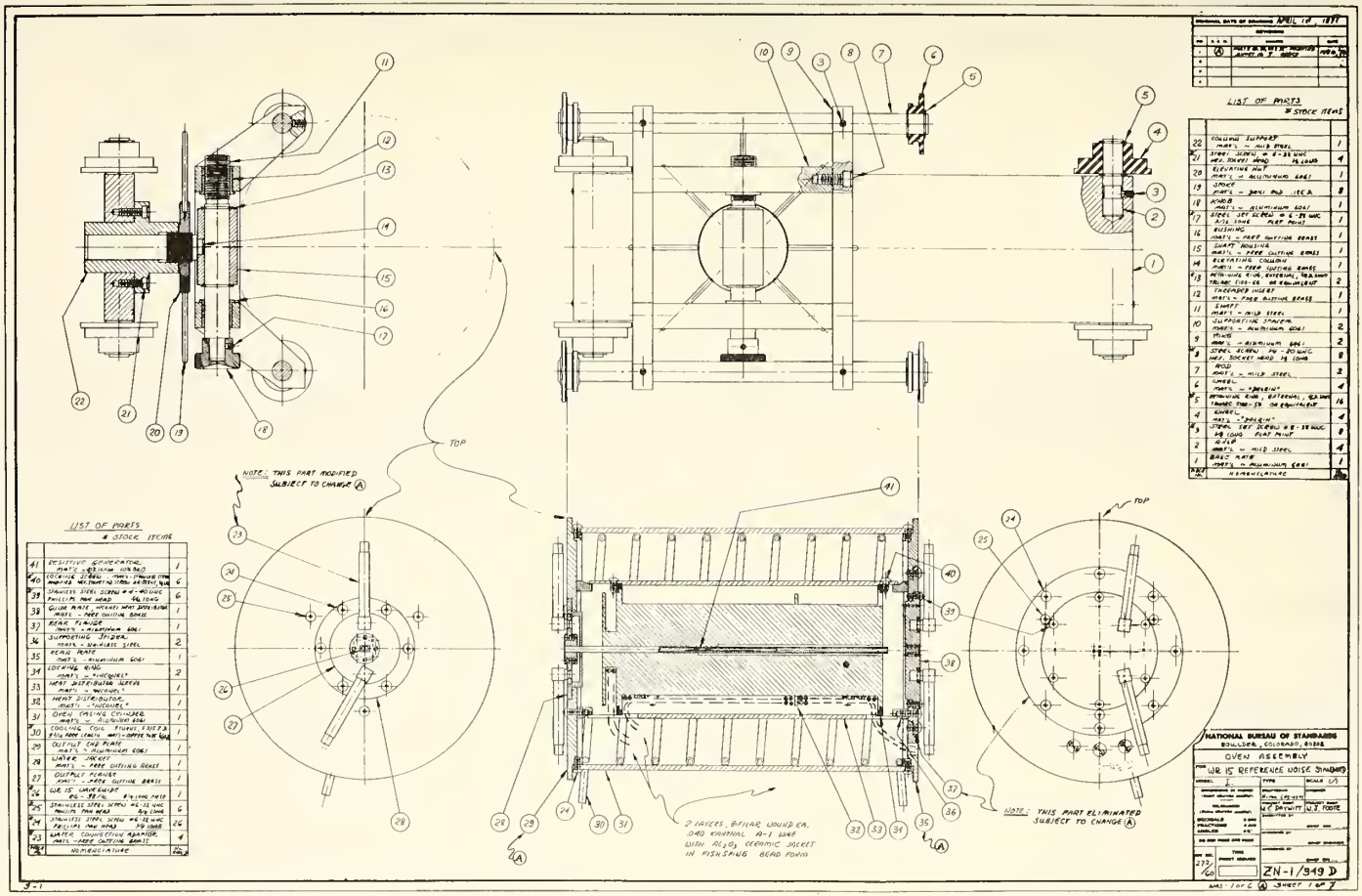

Drawing No. 1. Oven Assembly

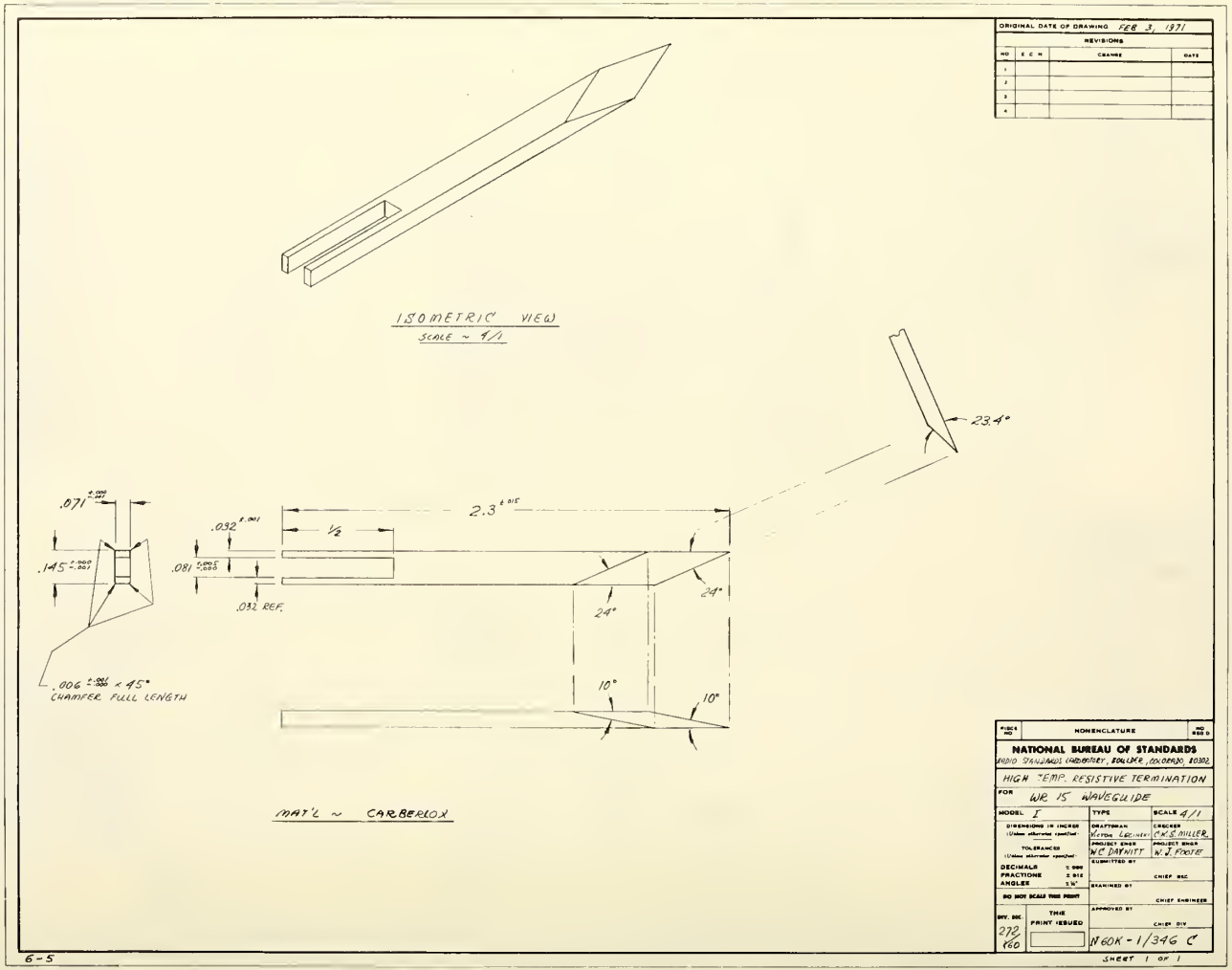

Drawing No. 2. High Temperature Resistive Termination.

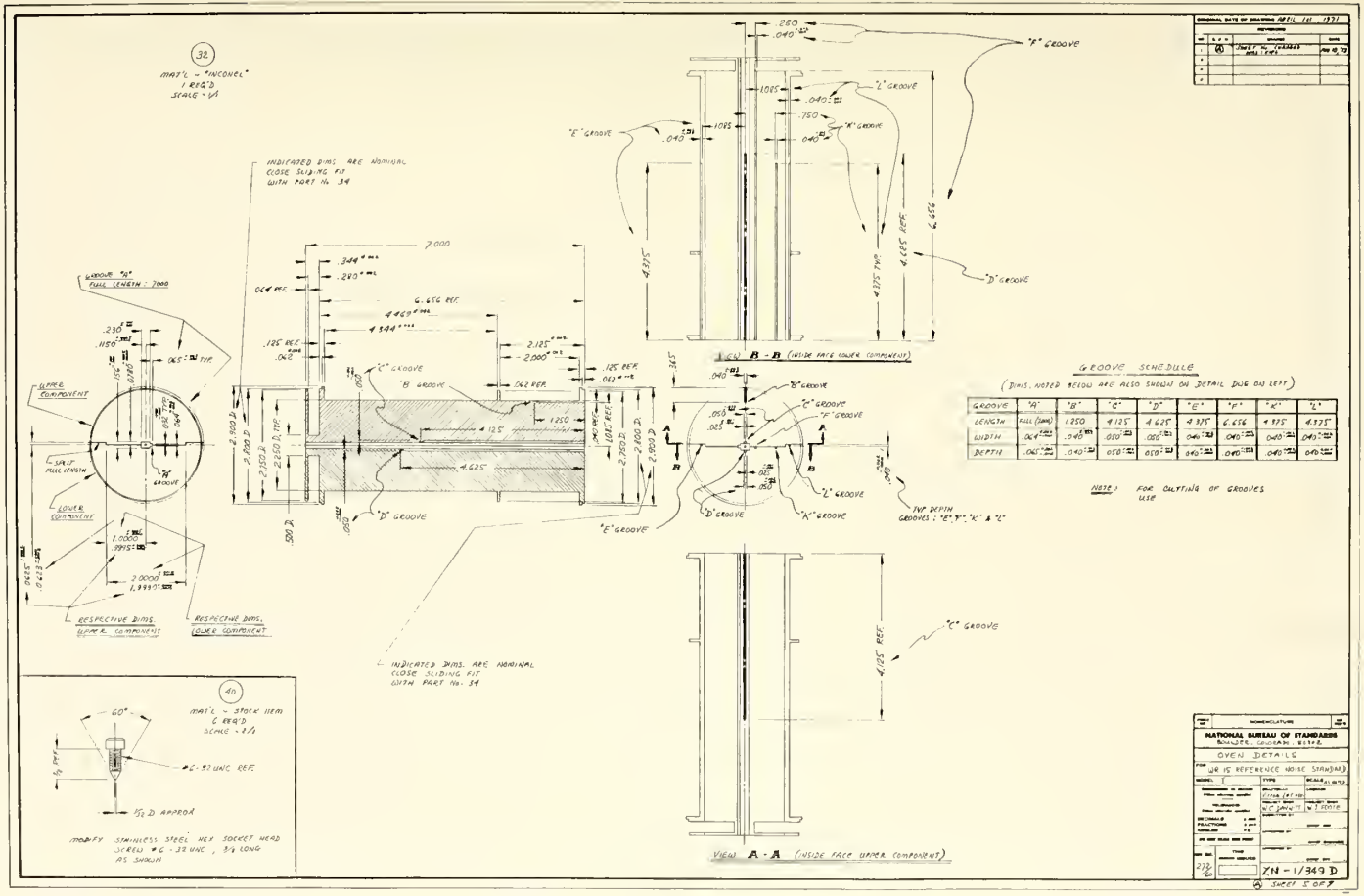

Drawing No. 3. Oven Details (Iconel Heat Distributor).

Appendix A -- The Output Equation

The output equation for the noise temperature of a noise power standard is (ap N)

$$T = T_m + \Delta T \tag{A.1}$$

where T_m is the termination temperature,

$$\Delta T = (T_o - T_m)(1-\alpha_o) + \int_o^{\ell} T_x'(1-\alpha_x)dx \tag{A.2}$$

$$\alpha_x = 10^{-A_x/10} - \frac{2|\Gamma_\ell|^2}{1 - |\Gamma_\ell|^2} \operatorname{Sinh}(A_x/10 \log e) \tag{A.3}$$

and

$$A_x = \int_x^{\ell} a_z \, dz. \tag{A.4}$$

Referring to figure 2.2,

T_x = the temperature at point x on the transmission line (e.g. $T_o \equiv T_{x=0}$)

T_x' = the derivative of T_x with respect to x at point x

α_x = the available power ratio from point x on the line to the end of the line at $x = \ell$

A_x = the attenuation in decibels of the line from x to $x = \ell$

a_x = the decibel attenuation per unit length at point x on the line

Γ_ℓ = the reflection coefficient of the termination and transmission line.

The scattering matrix for the length of line from x to $x = \ell$ is

$$S_x = \begin{bmatrix} 0 & S_{12} \\ S_{21} & 0 \end{bmatrix}$$

giving an attenuation [11] for this length of line equal to (ap N)

$$A_x \equiv -10 \log|S_{21}|^2 = \int_x^{\ell} a_z \, dz. \tag{A.5}$$

For a uniform transmission line with little loss, a_z can be approximated by

$$a_z = c\rho_z^{\frac{1}{2}} \tag{A.6}$$

where c is a constant dependent upon the frequency, f, and the transmission line geometry. ρ_z is the line resistivity. For a rectangular waveguide [2]

$$a_z = \frac{C_1(f^2 + C_2)}{f^{\frac{1}{2}}(f^2 - C_3)^{\frac{1}{2}}} \tag{A.7}$$

where

$$C_1 \equiv \frac{20 \cdot \pi^{\frac{1}{2}} \log e}{bC\mu_o^{\frac{1}{2}}},$$

$$C_2 \equiv \frac{bC^2}{2a^3},$$

$$C_3 \equiv \frac{C^2}{4a^2},$$

$$C \equiv 2.99792 \times 10^{8} \text{ meter/sec},$$

$$\mu_o \equiv 4\pi \times 10^{-7} \text{ henry/meter},$$

and

$$\log e \doteq 0.434294.$$

With the frequency expressed in gigahertz, ρ in microhm centimeters, a and b in inches, and a_z in decibel per inch,

$$C_1 = \frac{1.44865 \times 10^{-4}}{b}$$

$$C_2 = \frac{69.6533\ b}{a^3}$$

$$C_3 = \frac{34.8266}{a^2}.$$

The second term in (A.3) shows that the noise temperature of the standard is dependent upon the standard's reflection coefficient. The error in ΔT caused by dropping this term can be estimated from

$$\delta\Delta T \sim 2(\overline{T}-T_m)\ |\Gamma_\ell|^2\ 0.23\ \Delta \qquad \text{(A.8)}$$

where $\overline{T}$ is the average temperature of the transition region of the waveguide temperature gradient, and Δ is the average decibel attenuation over this same region. Using the resistivity curve given in figure 2.3 and temperature curve C in figure 4.7 to calculate Δ results in

$$\delta\Delta T < 0.01 \text{ K}.$$

A maximum value of 0.01 (SS 4.1.3) has been chosen for the reflection coefficient of the line and termination. Therefore for the WR15 standard, the second term in (A.3) can be dropped with negligible error.

Appendix B -- Quantum Correction

As the ratio hf/kT becomes significant, (A.1) should be replaced by

$$kT = W(T_m,f) + [W(T_o,f) - W(T_m,f)](1-\alpha_o) + \int_o^{\ell} W'(T_x,f)(1-\alpha_x)dx \qquad (B.1)$$

where

$$W(T,f) \equiv \frac{hf}{e^{2u} - 1}$$

and

$$u \equiv \frac{hf}{2kT}.$$

Here, h is Planck's Constant, k is Boltzmann's Constant, f is the frequency, and T is the absolute temperature. The significance of this correction can be determined by expanding (B.1) to second order in u and comparing the result to (A.1).

$$T \doteq T_m(1-u_m+u_m^2/3) + (T_o-T_m)(1-\alpha_o)(1-u_o u_m/3) + \int_o^{\ell} T_x'(1-u_x^2/3)(1-\alpha_x)dx. \qquad (B.2)$$

For T_m equal to 1200 K in the 55 to 65 GHz frequency range, the second order terms in (B.2) are found to be quite negligible. The linear term $T_m u_m$ is found to be 1.6 K at

65 GHz and is independent of the absolute temperature of the thermal noise source. The manner in which this linear term is treated depends on the application to which the standard is put. For example, in the comparison of noise sources this term drops out, but the correction must be considered when making a highly accurate noise factor measurement.

Appendix C -- Error Calculation

The maximum error δT in the calculated output (SS 2.1) T of the noise standard can be obtained from (A.1) and expressed as

$$\delta T = \delta T_m + \delta \Delta T$$

$$= (\delta T)_{T_m} + (\delta T)_{T_o} + (\delta T)_o + (\delta T)_\ell$$

$$+ (\delta T)_\rho + (\delta T)_c + (\delta T)_g + (\delta T)_1 + (\delta T)_w + (\delta T)_a \quad \text{(C.1)}$$

where the terms correspond to uncertainties in T caused by uncertainties in T_m, T_o, the location of $x = 0$, the location of $x = \ell$, ρ, c, T_x', neglecting second term in (A.3) (SS. 2.2), differing wall distributions (SS 4.4.4), and air attenuation (SS 2.2) respectively. These terms are calculated from (see ap A for definitions)

$$(\delta T)_{T_m} = (1-\alpha_o)\delta T_m \quad \text{(C.2)}$$

$$(\delta T)_{T_o} = (1-\alpha_o)\delta T_o \quad \text{(C.3)}$$

$$(\delta T)_o = |0.23\, c\alpha_o (T_o - T_m)\rho_o^{\frac{1}{2}} + (1-\alpha_o)T_o'|\ \delta(x=0) \quad \text{(C.4)}$$

$$(\delta T)_\ell = 0.23\, c\rho_\ell^{\frac{1}{2}}\ |T_\ell - T_m - \Delta T|\ \delta(x=\ell) \quad \text{(C.5)}$$

$$(\delta T)_\rho = 0.23\ \left|\alpha_o (T_o - T_m)A_o + \int_o^\ell \alpha_x A_x dx\right| \frac{\delta \rho^{\frac{1}{2}}}{\rho^{\frac{1}{2}}} \quad \text{(C.6)}$$

$$(\delta T)_c = 0.23\ \left|(T_o - T_m)A_o\alpha_o + \int_o^\ell T_x' A_x \alpha_x dx\right| \frac{\delta c}{c} \quad \text{(C.7)}$$

$$\frac{\delta c}{c} = \left| \frac{3C_2}{f^2 + C_2} + \frac{C_3}{f^2 - C_3} \right| \frac{\delta a}{a} + \left| 1 - \frac{C_2}{f^2 + C_2} \right| \frac{\delta b}{b}$$

$$+ \left| \frac{2f^2}{f^2 + C_2} - \frac{f^2}{f^2 - C_3} - \frac{1}{2} \right| \frac{\delta f}{f} \qquad \text{(C.8)}$$

and

$$(\delta T)_g = \int_0^{\ell} (1-\alpha_x)(\delta T_x')\,dx. \qquad \text{(C.9)}$$

In the WR15 standard the output flange is taken as the reference position, making $\delta(x=\ell)$ and $(\delta T)_\ell$ vanish.

The last term, (C.9), can be treated by one of two methods. The gradient uncertainty $\delta T_x'$ can be broken down into its two separate components Δt and Δx with each handled separately; or it can be estimated by calculating the output T for each of the possible gradients allowed by the temperature measurement uncertainties and taking one-half the resulting range in T as the uncertainty. The first method is the more convenient but places a much larger upper bound on δT than the second method. The second method is used in the present case.

$(\delta T)_w$ is obtained from the four temperature distributions used to generate figure 4.12 (SS 4.4.4). One-half the range in the four resulting T's calculated from these four distributions is 0.29 K. The distribution giving

T_x closest (0.07 K off) to the center of this range was the right-wall distribution (fig. 4.12). Therefore, with the right-wall distribution being used as the waveguide temperature distribution, the uncertainty incurred is no greater than 0.36 K (0.29 + 0.07 K).

Appendix D -- Computer Calculation of ΔT and $\delta\Delta T$

The computer program written to calculate ΔT and $\delta\Delta T$ (SS 2.1 and 2.2) is called "Delta T," a printout of which is shown in figure D.1. The input data fed into the computer consists of:

1. The coefficients (A0, ..., A3) of the least squares fit to the curve of $\rho^{\frac{1}{2}}$ as a function of centigrade temperature;
2. the frequency F in gigahertz;
3. the broad and narrow waveguide dimensions A and B, and their corresponding uncertainties DA and DB;
4. the termination temperature T_m in centigrade;
5. the coefficients (AR1, ..., AR3) for the waveguide expansion as a function of centigrade temperature according to the law [4]
   $\ell = \ell_o(1 + AR1 * t + AR2 * t^2)/AR3$;
6. the temperature distribution (x,T) along the right wall of the waveguide with x = 0 at the termination;
7. the input uncertainties DTM, DTO, DDX, DR, DDT, DDO, DDB, and DC, corresponding to the uncertainties in the termination temperature, the temperature of the waveguide at the termination, the length difference measurements, the square root of the resistivity, the temperature difference measurements, the position of x = 0 and x = ℓ, and the c constant.

The computer processes this data to an accuracy of 0.1% in the calculation of T.

The output results consist of:

1. the c constant;
2. the value of L showing how many times the computer must subdivide the temperature distribution data (x,T) to achieve the 0.1% calculational accuracy;
3. an approximate value ($\sim$ 10%) for the total decibel attenuation of the waveguide;
4. ΔT in kelvins;
5. the separate uncertainties in ΔT caused by DTM, ..., DC; and
6. the error in ΔT which is the sum of the separate uncertainties appearing in 5.

The data under the DDX and DDT headings are zero since the uncertainty given by (C.9) is calculated by the second method discussed in ap C.

Appendix E -- The Thermocouple Rod Expansion Program

As a thermocouple is inserted into the heated waveguide, the apparent distance the thermocouple bead enters the waveguide should be corrected for the expansion of the thermocouple rod. For any given temperature distribution, this correction can be calculated by program "TEX998" for the 99.8% alumina rods used in the thermocouples. Figure E.1 shows a sample output of the program using the distribution shown in figure 2.5. The lengths shown are measured in inches assuming the thermocouple to be inserted into the waveguide from the front of the oven.

Appendix F -- Termination Formula

Figure F.1 shows a portion of the termination, where a and b are the broad and narrow dimensions. Given a, b, and the angles α and β, the face angle γ, the cutting angle δ, and the longitudinal face length ℓ are given by:

$$\gamma = \cos^{-1}(\cos \alpha \cos \beta)$$

$$\delta = \tan^{-1}\left(\frac{\tan \beta}{\sin \alpha}\right)$$

and

$$\ell = \frac{a}{\tan \alpha} + \frac{b}{\tan \beta}$$

For the WR15 termination with $\alpha = 24°$ and $\beta = 10°$,

$$\gamma = 25.9°$$

$$\delta = 23.4°$$

and

$$\ell = 0.75''.$$

Appendix G -- The Minimum Termination Length

The minimum length of the termination is determined by two factors: 1) the amount of taper needed to produce a low VSWR; and 2) the amount of material needed to completely terminate the waveguide. Experience has shown that an effective taper geometry that produces a low VSWR and good thermal contact between the termination and the waveguide is achieved by the model shown in figure F.1 for small values of α and β. The length required to effect the first factor was determined in ap F. The length required for the second factor and the radiation length (the length of material behind the taper from which most of the thermal radiation leaving the termination originates) are determined in this appendix.

Terminating Length

An estimate of the length of material behind the taper that is required to completely terminate the waveguide can be made in the following way. Consider a length ℓ of material which is characterized by a scattering matrix S, and which is heated to a uniform temperature T_m. The reflection coefficient of the material is given by

$$\Gamma = S_{11} + \frac{S_{12}S_{21}\Gamma_L}{1 - S_{22}\Gamma_L}$$

where Γ_L is the reflection coefficient behind the material. If the length is great enough, the power delivered (in units of kB) P_d into a matched load by the material is

$$P_d = T_m(1 - |\Gamma|^2).$$

If Γ_L changes to Γ_L', then Γ changes by an amount

$$\delta\Gamma = \frac{S_{12}S_{21}(\Gamma_L - \Gamma_L')}{(1 - S_{22}\Gamma_L)(1 - S_{22}\Gamma_L')}$$

and P_d by an amount

$$\delta P_d = T_m \delta|\Gamma|^2 \leq T_m|\delta\Gamma|^2.$$

The largest change in Γ is obtained from $\Gamma_L' = 0$ and $\Gamma_L = e^{i\theta}$, giving

$$|\delta\Gamma|^2_{max} = \frac{|S_{12}S_{21}|^2}{1 - |S_{22}|^2}$$

and

$$\delta T_{max} \equiv (\delta P_d)_{max} = \frac{T_m|S_{12}S_{21}|^2}{1 - |S_{22}|^2}.$$

In the present case

$$|S_{12}|^2 = |S_{21}|^2 = 10^{-a\ell/10}$$

where a is the decibel attenuation per unit length of the material. Then

$$\delta T_{max} = \frac{T_m\ 10^{-2a\ell/10}}{1 - |S_{22}|^2}. \qquad (G.1)$$

Or to achieve a change of δT_{max} or less

$$\ell \geq \frac{5}{a} \log\left(\frac{T_m}{(1 - |S_{22}|^2)\delta T_{max}}\right). \qquad (G.2)$$

For a = 92 dB/inch (SS 3.1.1), $|S_{22}| = 0.5$, $T_m = 1200$ K, and $\delta T_{max} = 0.01$ K; $\ell \geq 0.28$". That is, if the termination (minus taper) is greater than 0.28" in length, then a maximum VSWR change behind the termination can cause no greater than 0.01 K change in the noise power delivered by the termination to the waveguide.

Radiation Length

A termination of infinite length with a temperature distribution T_x has a noise temperature T given by

$$T = \int_0^\infty T_x(0.23\ a_x dx)10^{-A_x/10} \qquad (G.3)$$

where a_x is the decibel attenuation per unit length of the termination material, and A_x is the decibel attenuation of the material from x = 0 to x.

$$A_x \equiv \int_0^x a_z dz.$$

Suppose that only the taper and the first ℓ inches of the termination could be maintained at a uniform temperature T_m. Then

$$T = 0.23\ T_m \int_0^\ell a_x 10^{-A_x/10} + 0.23 \int_\ell^\infty T_x a_x 10^{-A_x/10} dx. \qquad (G.4)$$

The length ℓ can be increased to the point where the second term in (G.4) is negligible. Taking $T_x \doteq T_o$, and $a_x \doteq a$, the ratio R of the second to first term in (G.4) becomes

$$R = \frac{T_o \, 10^{-a\ell/10}}{T_m(1 - 10^{-a\ell/10})}. \qquad \text{(G.5)}$$

This ratio is insignificant if ℓ is greater than some radiation length ℓ_R given by

$$\ell \geq \ell_R \equiv \frac{10}{a} \log\left(\frac{1 + T_m R/T_o}{T_m R/T_o}\right). \qquad \text{(G.6)}$$

For a = 92 dB/inch, T_m = 1200 K, T_o = 300 K, and R = 0.01/1200; $\ell_R \doteq 0.2$".

Appendix H -- Waveguide Reflections

Broad and Narrow Dimensions

A rectangular waveguide whose broad and narrow dimensions are in error by δa and δb respectively will produce a reflection coefficient (with respect to a perfect waveguide of dimensions a and b) whose magnitude is given by [12]

$$\Delta\Gamma = \left(\frac{\lambda_g}{\lambda_c}\right)^2 \frac{\delta a}{2a} + \frac{2\sigma}{(1+\sigma)^2}\frac{\delta b}{b} \qquad \text{(H.1)}$$

where λ_g is the waveguide wavelength, λ_c is the cutoff wavelength, and σ is the VSWR corresponding to Γ. For WR15 ($\lambda_c = 0.296"$) at 55 GHz ($\lambda_g = 0.3115"$) and a small reflection ($\sigma \doteq 1$),

$$\Delta\Gamma = 3.7\ \delta a + 6.8\ \delta b. \qquad \text{(H.2)}$$

For $\delta a = \delta b = 0.001"$, $\Delta\Gamma = 0.010$.

Corner Bend Radii

Non-vanishing corner bend radii inside an otherwise perfect rectangular waveguide will cause a reflection whose magnitude is given by [13]

$$\Delta\Gamma = \left(\frac{\lambda_g R}{a}\right)^2 \left(\frac{4-\pi}{8ab}\right) \qquad \text{(H.3)}$$

where R is the radius of the corner bend.

For WR15 waveguide at 55 GHz with $R = 0.006"$, $\Delta\Gamma = 0.002$.

Appendix I -- Atmospheric Attenuation

The maximum change in the output noise temperature of the standard δT due to the attenuation by the column of air in the waveguide between the termination and the output flange can be approximated by

$$\delta T = (T_a - T_m)(1 - \alpha) \qquad (I.1)$$

where T_a is the average temperature of the air column, T_m is the termination temperature, and α is the average attenuation of the column. With T_a = 300 K, T_m = 1200 K, and α = 0.00025 dB/inch (60 GHz in figure 3.4); ΔT = 0.05 K.

Appendix J -- Support Spider

The inconel sleeve (drawings 1 and 3) is suspended inside the oven by a support spider (which is kept near room temperature by the end plate) on each end plate. The spider is so designed that as the sleeve expands on heating its center line remains fixed. This is accomplished by choosing the angle for the support spider shown in figure J.1 so that as the sleeve length ℓ and diameter D increase, the sleeve ends climb smoothly up the support spider. It is apparent from the figure that the proper angle θ is given by

$$\tan \theta = \frac{\delta D/2}{\delta \ell/2}. \qquad (J.1)$$

Since D and ℓ expand on heating by the same factor, (J.1) reduces to

$$\tan \theta = \frac{D}{\ell}. \qquad (J.2)$$

For ℓ = 7.75" and D = 3.25"; θ = 22.75°.

Appendix K -- Thermocouple Rod Expansion

The expansion of the thermocouple rod upon heating can be described in terms of a linear coefficient of expansion ε;

$$d\ell = dx + \varepsilon \cdot \Delta t \cdot dx \qquad (K.1)$$

where dx and $d\ell$ are elemental lengths of the rod before and after heating respectively, and Δt is the corresponding temperature change. The length of the entire rod is the sum of these elemental lengths. Thus,

$$\ell = \int_o^{\ell_o} d\ell = \ell_o + \int_o^{\ell_o} \varepsilon \cdot \Delta t \cdot dx \qquad (K.2)$$

where ℓ_o is the length of the unheated rod.

The following table [10] gives ε in 10^{-6}/degree C for a 99.8% Al_2O_3 rod:

Temperature Change	ε in 10^{-6}/degree C
-200 to 25°C	3.4
25 to 200°C	6.7
25 to 500°C	7.3
25 to 800°C	7.8
25 to 1000°C	8.0
25 to 1200°C	8.3

The coefficients of a least-square curve fitting the product $\varepsilon \cdot \Delta t$ over the 0 to 1000°C temperature range are given in the next table:

$$a_0 \qquad -1.58 \times 10^{-4}$$

$$a_1 \qquad 6.28 \times 10^{-6}$$

$$a_2 \qquad 1.72 \times 10^{-9}$$

$$a_3 \qquad 9.27 \times 10^{-13}$$

$$a_4 \qquad -9.72 \times 10^{-16}$$

where now

$$\ell = \ell_o + \int_o^{\ell_o} \alpha_x dx \qquad \text{(K.3)}$$

and

$$\alpha_x \equiv \alpha(t_x) = \sum_{n=0}^{4} a_n \, t_x^n. \qquad \text{(K.4)}$$

Appendix L -- Lead Resistance Error

The copper leads from the thermocouples (fig. L.1) to the terminal board have a resistance r. In reading the thermocouple emf an error E will be caused by this resistance if an imperfect null (e + 1 μV) is obtained on the potentiometer. Neglecting the small resistance of the thermocouple itself, the current caused by this imperfect null is

$$i = \frac{1\ \mu V}{2r + R} \qquad (L.1)$$

where R is the balancing resistance of the potentiometer. The corresponding error is

$$E = 2ri = \frac{2r/R}{1 + 2r/R}. \qquad (L.2)$$

When balancing at the silver point temperature with a platinum-rhodium thermocouple (9.127 mV), R turns out to be 170 Ω. The lead resistance is (SS 4.3.2) 1.5 ohms. Therefore E is 0.017 μV which corresponds to an error of 0.002°C at the silver point temperature.

Appendix M -- Oven Temperature Control

General Description

The operation of the control system can be understood from figure M.1 and the block summaries given below.

I. The output of the reference voltage source is a variable DC voltage adjustable from zero to 50 mV.

II. The block II output is the algebraic sum of the reference source and the thermocouple voltage. This sum is zero under normal operating conditions.

III. The DC amplifier amplifies any deviation from zero of the block II output (a calibrated meter indicates magnitude and polarity).

IV. The DC to duty cycle converter changes the fluctuating DC (error signal) to a square wave of fluctuating duty cycle. The converter output is waveform A of figure M.2.

V. Waveform A (fig. M.2) together with waveform B, a waveform of fixed duty cycle, is presented to an "and" gate to produce waveform AB (fig. M.2). The width of the positive-going portion of AB determines the position of the current transformer, which in turn, determines the amount of current

delivered to the heating coil. The temperature control servo loop is closed through the heat conduction path from the heater coil to the thermocouple.

DC to Duty Cycle Converter

The output of emitter follower Q4 (fig. M.3) is the amplified sum of the DC input of Q1 from the DC amplifier, and the sawtooth input of Q3. This Q4 output is a sawtooth waveform that translates vertically with changes in temperature (changes in the DC amplifier output). Q8 and Q9 form a bistable circuit with the Q8 emitter voltage fixed by zener diode Z. When the output of Q4 is greater than the emitter voltage of Q8, Q8 and Q9 switch off. Q8 and Q9 switch on again when the Q4 emitter voltage drops sufficiently below the Q8 emitter reference. As seen in figure M.3 the negative-going transition of the Q9 collector always coincides with the negative-going transition of the free-running sawtooth waveform. The positive-going transition of the Q9 collector occurs when the Q4 output becomes greater than the Q8 fixed emitter voltage. This circuit configuration results in an output square wave which has a duty cycle determined by the DC level from the DC amplifier. This variable-duty-cycle square wave is waveform A of figure M.2. The frequency of this square wave is determined by the free-running sawtooth generator and is not critical.

Current Transformer Servo

Q1 of figure M.4 receives a variable-duty-cycle square wave signal from the "and" gate. This signal is inverted at the collector of Q1 which is connected via D1 to a "one-shot" formed by Q2 and Q3. The incoming signal triggers the "one-shot," and the collector of Q2 goes positive for a time determined by the RC time constant of R3 C1, together with the position of pot R4. R4 is mechanically connected to the transformer shaft. Therefore the rotational position of the transformer shaft determines the width of the "one-shot" output pulse. This pulse is compared to the width of the incoming signal, and any difference in width results in an error signal at the base of Q4. The signal at the base of Q4 is a narrow positive or negative-going pulse depending on whether the Q1 input is narrower or wider than the "one-shot" output. If the error signal is positive-going, it will cause Q5 to conduct, which in turn energizes the pulse stretcher Q6 together with C2 and R5. The pulse stretcher output signal is sufficient to drive the servomotor in one direction through Q7, Q8, Q9, and Q15. The same thing happens for an error of the opposite sense via Q10 through Q14 driving the motor in the opposite direction. The servomotor will continue to drive until R4 adjusts the

"one-shot" pulse width to equal that of the incoming signal. Q8 and Q13 are "nand" gates (inverting "and" gates) that are coupled so that both drive circuits (clockwise and counter-clockwise) cannot be energized simultaneously.

Appendix N -- Derivation of the Output Equation

N.1. Introduction

A thermal noise source consists of a termination and a transmission line to convey the noise generated in the termination to an output port. The transmission line is lossy, so it both attenuates the termination noise and adds noise of its own to the output, and the line must be chosen in such a way that the output power can be accurately calculated.

The derivation begins in SS N.2 with a review of some two-port power relationships which are used in SS N.3 to find an expression for the noise output power of a lossy two-port. Finally, this output power equation is applied in SS N.4 to incremental segments of a transmission line to obtain the output noise power equation for the noise standard.

N.2. Some Basic Two-Port Equations

The work to follow requires the use of some two-port power equations. These equations will be presented in this section in a form that is most useful to SS N.3 and SS N.4. Throughout this appendix a capital 'P' will stand for net or delivered average power and a small 'p' for available average power. It is to be understood that where the

parameters are frequency dependent, the bandwidth is narrow enough to insure that these parameters are essentially constant across it.

A passive, linear, two-port transducer is shown in figure N.1 with a generator attached to its input (first) port, and a load attached to its output (second) port. M and N are the mismatch factors of port one and port two respectively, and are defined in the following equations:

$$M \equiv P_1/p_1, \quad N \equiv P_2/p_2,$$

where p_1 is the average power available from the generator, and p_2 is that portion of p_1 available at port two of the junction. P_1 is the net average power into port one from the generator and P_2 is the net average power from port two. The ratio α of available powers is defined by

$$\alpha \equiv p_2/p_1.$$

The corresponding transducer efficiency η is

$$\eta \equiv P_2/P_1.$$

The definitions for M, N, α, and η can be combined to obtain the following relationship between these four quantities:

$$M\eta \equiv N\alpha$$

Furthermore, by considering the definitions of α and η, it can be seen that if the transducer is lossless, then both α and η are unity.

These definitions are general because they apply to a transducer with any number of propagating modes. However, to have a workable expression for the noise power output calculation, one is restricted to a single propagating mode, in which case the transducer has an equivalent circuit like figure N.1. This circuit is shown in figure N.2 where scattering parameters [11] are used and where, in terms of these parameters, M, N, α, and η take the following form [11,1]:

$$M = \frac{(1-|\Gamma_g|^2)(1-|\Gamma_1|^2)}{|1-\Gamma_g\Gamma_1|^2}$$

$$N = \frac{(1-|\Gamma_L|^2)(1-|\Gamma_2|^2)}{|1-\Gamma_L\Gamma_2|^2}$$

$$\alpha = \frac{(1-|\Gamma_g|^2)|S_{21}|^2}{(1-|\Gamma_2|^2)|1-S_{11}\Gamma_g|^2}$$

$$\eta = \frac{(1-|\Gamma_L|^2)|S_{21}|^2}{(1-|\Gamma_1|^2)|1-S_{22}\Gamma_L|^2}.$$

The two-port scattering matrix is given by

$$S = \begin{pmatrix} S_{11} & S_{12} \\ S_{21} & S_{22} \end{pmatrix}.$$

The reflection coefficients of the generator, the input and output ports of the two-port, and the reflection coefficient of the load are denoted by Γ_g, Γ_1, Γ_2, and Γ_L respectively.

The input and output port reflection coefficients are related to the scattering matrix parameters and the terminal reflection coefficients through the equations [11]

$$\Gamma_1 = S_{11} + \frac{S_{12}S_{21}\Gamma_L}{1 - S_{22}\Gamma_L},$$

$$\Gamma_2 = S_{22} + \frac{S_{12}S_{21}\Gamma_g}{1 - S_{11}\Gamma_g}.$$

It can be seen from the equations for α, η, Γ_1, and Γ_2, that α is independent of the load reflection coefficient, and that η is independent of the generator reflection coefficient.

N.3. Two-Port Noise

An expression for the average thermal noise power of a lossy two-port transducer is derived in this section. The expression to be obtained can be found in at least two other sources [14,15], so the short derivation given here is not intended to be new or unique. It is presented because it is an important logical step between SS N.2 and SS N.4 and because it will help familiarize the reader with the parameters just described.

A linear, passive, two-port transducer is shown in figure N.3, terminated at both ends. Both of these terminations and the two-port are thermally isolated from their

surroundings, and have come to a uniform absolute temperature T. P_1 represents the average net power from the first termination, and P_2 that from the second. The portion of P_1 that emerges from port two is $P_1\eta$. P represents the noise power added to $P_1\eta$ by the two-port itself, and is the quantity to be found. M and N are mismatch factors, and again a capital 'P' refers to delivered or net power while small 'p' refers to the available power. For example, if p_1 and p_2 denote the available powers from port one and port two terminations respectively, then the definitions in SS N.2 lead to

$$P_1 = Mp_1 \quad \text{and} \quad P_2 = Np_2.$$

Since the entire circuit is thermally isolated from its surroundings, the temperature of the two-port and the terminations must remain equal even though there is a continual exchange of electromagnetic energy between them. This fact leads to the important conclusion that the average net powers leaving and entering port two must be equal,

$$P_1\eta + P = P_2.$$

In terms of the available powers p_1 and p_2,

$$P = Np_2 - Mp_1\eta.$$

Since both terminations are at the temperature T,

$$p_1 = p_2,$$

where both p_1 and p_2 are equal to kTB in the low frequency approximation.

Therefore

$$P = NkTB(1-\alpha)$$

where the relationship

$$M\eta = N\alpha$$

has been used to eliminate η. Representing the available power generated in the two-port by p,

$$p = P/N = kTB(1-\alpha). \qquad (N.1)$$

This equation is still general in the sense of the fourth paragraph of SS N.2, and is assumed to hold for all passive input and output terminations.

To illustrate the use of (N.1), consider figure N.4 and the total noise power available from port two that is generated in the two-port at temperature T, and the termination at temperature T_g. This total power consists of the attenuated power $p_g\alpha$ available from the termination and the available two-port power p. By using (N.1) in place of p, the total available power is given by

$$p_g\alpha + p = kT_gB\alpha + kTB(1-\alpha).$$

The net amount of this power actually delivered to the right from port two is equal to N times the total available power, or

$$N(p_g\alpha+p) = NkT_gB\alpha + NkTB(1-\alpha).$$

N.4. The Thermal Noise Source and Standard

In 1958, Sees [16] derived an expression for the average noise power output of a thermal source along the lines presented here, but without the benefit of the expressions found in SS N.3. Therefore, in this section those expressions will be applied to a lossy transmission line to find the contribution of the line to the total noise output of the source.

Figure N.5 shows a thermal noise source consisting of a termination at a temperature T_m that terminates a transmission line of length ℓ. T_x is the temperature of the transmission line at point x along its length, and α_x is the available power ratio of the section of line from x to ℓ. Plots of T_x and α_x as a function of position along the line are also shown in the figure.

For analysis the line is divided into many small segments, each of length Δx, where the particular segment at position x is shown in the figure, and (N.1) of the previous section is applied to each segment. Thus, the available power Δp_x

from the segment at x is equal to the average temperature T_x of the segment times one minus the available power ratio $\Delta\alpha_x$ for the segment,

$$\Delta p_x = kT_xB(1-\Delta\alpha_x).$$

Using

$$\alpha_{x-\Delta x/2} = \Delta\alpha_x \cdot \alpha_{x+\Delta x/2}$$

leads to

$$\Delta p_x = kT_xB\left(\frac{\alpha_{x+\Delta x/2} - \alpha_{x-\Delta x/2}}{\alpha_{x+\Delta x/2}}\right).$$

For small segments

$$\alpha_x' \equiv \frac{d\alpha_x}{dx} = \frac{\alpha_{x+\Delta x/2} - \alpha_{x-\Delta x/2}}{\Delta x},$$

and $\alpha_{x+\Delta x/2}$ can be replaced by α_x. Therefore.

$$\Delta p_x = \frac{kT_xB\alpha_x'\Delta x}{\alpha_x}.$$

The portion of this power that reaches the output port at $x = \ell$ is

$$\alpha_x\Delta p_x = kT_xB\alpha_x'\Delta x.$$

To get the total effect of the line, the effects due to each segment are added together:

$$\Sigma\ \alpha_x\Delta p_x = \Sigma\ kT_xB\alpha_x'\Delta x = kB\int_0^{\ell} T_x\alpha_x'dx.$$

The amount of termination noise available at the output is

$$kT_m B\alpha_o .$$

Therefore the total available noise power output, $kT_{tot}B$, of the thermal source is given by the sum of these last two expressions and leads to a noise temperature T_{tot} given by

$$T_{tot} = T_m\alpha_o + \int_o^{\ell} T_x\alpha_x' dx. \qquad (N.2)$$

Another form for this equation can be obtained from an integration by parts:

$$T_{tot} = T_m + \Delta T, \qquad (N.3)$$

where the correction temperature ΔT is

$$\Delta T \equiv (T_o - T_m)(1-\alpha_o) + \int_o^{\ell} T_x'(1-\alpha_x)dx. \qquad (N.4)$$

The net power delivered across the output port corresponds to

$$MT_{tot} = M(T_m + \Delta T).$$

Equations (N.3) and (N.4) are valid for any number of simultaneously propagating modes. However, to have a workable expression for α_x to be used in calculating the output of a noise standard it is necessary to select the transmission line and operating frequency so that only one mode is present. This means using a uniform, reflectionless line at a frequency below cutoff for all but the dominant mode. Figure N.6

illustrates such a condition, where now any portion of the line, for example the section from x to ℓ, can be represented electrically by a two-port. The termination reflection coefficient is represented by Γ_g, the reflection coefficient looking from point x towards the termination by Γ_x, and the entire reflection coefficient of the thermal standard by Γ_ℓ. α_x is the available power ratio from x to ℓ, and S_x is the corresponding scattering matrix.

From Kerns and Beatty [11, p.77], S_x for a uniform, reflectionless line is

$$S_x = \begin{bmatrix} 0 & e^{-\int_x^\ell \lambda_y dy} \\ e^{-\int_x^\ell \lambda_y dy} & 0 \end{bmatrix}$$

where λ_y is the propagation constant

$$\lambda_y = \varepsilon_y + i\beta$$

and ε_y is real positive and determines the wave attenuation. For example, the attenuation in decibels of the line is $8.68 \int_0^\ell \varepsilon_y dy$. This attenuation constant depends on the resistivity (which in turn is a function of the line temperature) of the material making up the line. It can be measured [17] or, with care, calculated from a perturbation expansion [18,2]. Using these scattering parameters in the expression

for α of SS N.2 leads to

$$\alpha_x = \frac{\left(1-|\Gamma_x|^2\right)\ e^{-2\int_x^{\ell} \varepsilon_y dy}}{1\ -\ |\Gamma_{\ell}|^2}$$

where $|\Gamma_x|$, $|\Gamma_{\ell}|$, and $|\Gamma_g|$ are related by the equation [11, p. 42, eq. (2.12)]

$$|\Gamma_x| = |\Gamma_g e^{-2\int_o^x \lambda_y dy}| = |\Gamma_g|\ e^{-2\int_o^x \varepsilon_y dy}$$

$$= |\Gamma_{\ell}|\ e^{2\int_x^{\ell} \varepsilon_y dy}.$$

The α_x ratio can be rewritten in the following form

$$\alpha_x = e^{-2\int_x^{\ell} \varepsilon_y dy} - \frac{2|\Gamma_{\ell}|^2}{1\ -\ |\Gamma_{\ell}|^2} \sinh\left(2\int_x^{\ell} \varepsilon_y dy\right) \qquad (N.5)$$

where the dependence on the reflection coefficient Γ_{ℓ} of the noise generator is more evident. In calculating T_{tot} this last term can usually be neglected.

N.5. Summary and Conclusions

The results of SS N.2 and SS N.3 have been applied in SS N.4 to find the noise temperature T_{tot} of a thermal noise standard:

$$T_{tot} = T_m + \Delta T \qquad (N.3)$$

in which

$$\Delta T \equiv (T_o - T_m)(1-\alpha_o) + \int_o^{\ell} T_x'(1-\alpha_x)dx \qquad (N.4)$$

and

$$\alpha_x = e^{-2\int_x^{\ell} \varepsilon_y dy} - \frac{2|\Gamma_\ell|^2}{1 - |\Gamma_\ell|^2} \sinh\left(2\int_x^{\ell} \varepsilon_y dy\right). \qquad (N.5)$$

Most output calculations neglect the second term in (N.5). Little error results, however, since most thermal standards are constructed from low-loss lines (small ε_y) and low reflection coefficient terminations (small $|\Gamma_g|$), making

$$|\Gamma_\ell| = |\Gamma_g| \, e^{-2\int_o^{\ell} \varepsilon_y dy}$$

small and the last term in (N.5) small also.

The net power delivered to a load at the output of the standard source is MT_{tot}, where M is the output mismatch factor. If Γ_L is the load reflection coefficient, then

$$M = \frac{(1-|\Gamma_L|^2)(1-|\Gamma_\ell|^2)}{|1-\Gamma_L\Gamma_\ell|^2}.$$

M and Γ_ℓ can also be written in terms of the standard and load impedances, Z_ℓ and Z_L.

$$M = \frac{4 \, \mathrm{Re}Z_\ell \, \mathrm{Re}Z_L}{|Z_\ell + Z_L|^2},$$

and

$$\Gamma_\ell = \frac{Z_\ell - Z_o}{Z_\ell + Z_o},$$

where Z_o is the characteristic line impedance [11].

FORM NBS-114A (1-71)

U.S. DEPT. OF COMM. BIBLIOGRAPHIC DATA SHEET	1. PUBLICATION OR REPORT NO.	2. Gov't Accession No.	3. Recipient's Accession No.

4. TITLE AND SUBTITLE

WR15 Thermal Noise Standard

5. Publication Date

6. Performing Organization Code

7. AUTHOR(S)

W.C. Daywitt, W. J. Foote, and E. Campbell

8. Performing Organization

9. PERFORMING ORGANIZATION NAME AND ADDRESS

NATIONAL BUREAU OF STANDARDS, Boulder Labs.
DEPARTMENT OF COMMERCE
Boulder, Colorado 80302

10. Project/Task/Work Unit No.

Project #2726203

11. Contract/Grant No.

12. Sponsoring Organization Name and Address

Same as 9.

13. Type of Report & Period Covered Final

1-71 - 1-72

14. Sponsoring Agency Code

15. SUPPLEMENTARY NOTES

16. ABSTRACT (A 200-word or less factual summary of most significant information. If document includes a significant bibliography or literature survey, mention it here.)

This note describes the design and construction of a WR15 thermal noise power standard. The standard is designed to operate around the Silver Point Temperature (963.19°C) with a noise temperature output accurate to approximately ± 2 K.

Complete details of the theory, design, construction, and performance tests are given.

17. KEY WORDS (Alphabetical order, separated by semicolons)

Error analysis; millimeter wave; Noise; Nyquist's theorem; Thermal noise standard

18. AVAILABILITY STATEMENT

[X] UNLIMITED.

[ ] FOR OFFICIAL DISTRIBUTION. DO NOT RELEASE TO NTIS.

19. SECURITY CLASS (THIS REPORT)

UNCLASSIFIED

21. NO. OF PAGES

154

20. SECURITY CLASS (THIS PAGE)

UNCLASSIFIED

22. Price

$1.25

USCOMM-DC 66244-P71

NBS TECHNICAL PUBLICATIONS

PERIODICALS

JOURNAL OF RESEARCH reports National Bureau of Standards research and development in physics, mathematics, chemistry, and engineering. Comprehensive scientific papers give complete details of the work, including laboratory data, experimental procedures, and theoretical and mathematical analyses. Illustrated with photographs, drawings, and charts.

Published in three sections, available separately:

• Physics and Chemistry

Papers of interest primarily to scientists working in these fields. This section covers a broad range of physical and chemical research, with major emphasis on standards of physical measurement, fundamental constants, and properties of matter. Issued six times a year. Annual subscription: Domestic, $9.50; $2.25 additional for foreign mailing.

• Mathematical Sciences

Studies and compilations designed mainly for the mathematician and theoretical physicist. Topics in mathematical statistics, theory of experiment design, numerical analysis, theoretical physics and chemisty, logical design and programming of computers and computer systems. Short numerical tables. Issued quarterly. Annual subscription: Domestic, $5.00; $1.25 additional for foreign mailing.

• Engineering and Instrumentation

Reporting results of interest chiefly to the engineer and the applied scientist. This section includes many of the new developments in instrumentation resulting from the Bureau's work in physical measurement, data processing, and development of test methods. It will also cover some of the work in acoustics, applied mechanics, building research, and cryogenic engineering. Issued quarterly. Annual subscription: Domestic, $5.00; $1.25 additional for foreign mailing.

TECHNICAL NEWS BULLETIN

The best single source of information concerning the Bureau's research, developmental, cooperative, and publication activities, this monthly publication is designed for the industry-oriented individual whose daily work involves intimate contact with science and technology—*for engineers, chemists, physicists, research managers, product-development managers, and company executives.* Annual subscription: Domestic, $3.00; $1.00 additional for foreign mailing.

NONPERIODICALS

Applied Mathematics Series. Mathematical tables, manuals, and studies.

Building Science Series. Research results, test methods, and performance criteria of building materials, components, systems, and structures.

Handbooks. Recommended codes of engineering and industrial practice (including safety codes) developed in cooperation with interested industries, professional organizations, and regulatory bodies.

Special Publications. Proceedings of NBS conferences, bibliographies, annual reports, wall charts, pamphlets, etc.

Monographs. Major contributions to the technical literature on various subjects related to the Bureau's scientific and technical activities.

National Standard Reference Data Series. NSRDS provides quantitative data on the physical and chemical properties of materials, compiled from the world's literature and critically evaluated.

Product Standards. Provide requirements for sizes, types, quality, and methods for testing various industrial products. These standards are developed cooperatively with interested Government and industry groups and provide the basis for common understanding of product characteristics for both buyers and sellers. Their use is voluntary.

Technical Notes. This series consists of communications and reports (covering both other agency and NBS-sponsored work) of limited or transitory interest.

Federal Information Processing Standards Publications. This series is the official publication within the Federal Government for information on standards adopted and promulgated under the Public Law 89–306, and Bureau of the Budget Circular A–86 entitled, Standardization of Data Elements and Codes in Data Systems.

Consumer Information Series. Practical information, based on NBS research and experience, covering areas of interest to the consumer. Easily understandable language and illustrations provide useful background knowledge for shopping in today's technological marketplace.

NBS Special Publication 305, Supplement 1, Publications of the NBS, 1968-1969. When ordering, include Catalog No. C13.10:305. Price $4.50; $1.25 additional for foreign mailing.

Order NBS publications from:

Superintendent of Documents
Government Printing Office
Washington, D.C. 20402

U.S. DEPARTMENT OF COMMERCE
National Bureau of Standards
Washington, D.C. 20234